

NASA/TM-2022-104606/Vol. 60



**Technical Report Series on Global Modeling and Data Assimilation,
Volume 60**

Randal D. Koster, Editor

**Soil Moisture Active Passive (SMAP) Project Assessment
Report for Version 6 of the L4_SM Data Product**

*Rolf H. Reichle, Qing Liu, Randal D. Koster, Joseph V. Ardizzone, Andreas
Colliander, Wade T. Crow, Gabrielle J. M. De Lannoy and John S. Kimball*

January 2022

NASA STI Program ... in Profile

Since its founding, NASA has been dedicated to the advancement of aeronautics and space science. The NASA scientific and technical information (STI) program plays a key part in helping NASA maintain this important role.

The NASA STI program operates under the auspices of the Agency Chief Information Officer. It collects, organizes, provides for archiving, and disseminates NASA's STI. The NASA STI program provides access to the NTRS Registered and its public interface, the NASA Technical Reports Server, thus providing one of the largest collections of aeronautical and space science STI in the world. Results are published in both non-NASA channels and by NASA in the NASA STI Report Series, which includes the following report types:

- **TECHNICAL PUBLICATION.** Reports of completed research or a major significant phase of research that present the results of NASA Programs and include extensive data or theoretical analysis. Includes compilations of significant scientific and technical data and information deemed to be of continuing reference value. NASA counterpart of peer-reviewed formal professional papers but has less stringent limitations on manuscript length and extent of graphic presentations.
- **TECHNICAL MEMORANDUM.** Scientific and technical findings that are preliminary or of specialized interest, e.g., quick release reports, working papers, and bibliographies that contain minimal annotation. Does not contain extensive analysis.
- **CONTRACTOR REPORT.** Scientific and technical findings by NASA-sponsored contractors and grantees.
- **CONFERENCE PUBLICATION.** Collected papers from scientific and technical conferences, symposia, seminars, or other meetings sponsored or co-sponsored by NASA.
- **SPECIAL PUBLICATION.** Scientific, technical, or historical information from NASA programs, projects, and missions, often concerned with subjects having substantial public interest.
- **TECHNICAL TRANSLATION.** English-language translations of foreign scientific and technical material pertinent to NASA's mission.

Specialized services also include organizing and publishing research results, distributing specialized research announcements and feeds, providing information desk and personal search support, and enabling data exchange services.

For more information about the NASA STI program, see the following:

- Access the NASA STI program home page at <http://www.sti.nasa.gov>
- E-mail your question to help@sti.nasa.gov
- Phone the NASA STI Information Desk at 757-864-9658
- Write to:
NASA STI Information Desk
Mail Stop 148
NASA Langley Research Center
Hampton, VA 23681-2199

NASA/TM-2022-104606/Vol. 60



**Technical Report Series on Global Modeling and Data Assimilation,
Volume 60**

Randal D. Koster, Editor

**Soil Moisture Active Passive (SMAP) Project Assessment
Report for Version 6 of the L4_SM Data Product**

Rolf H. Reichle

Global Modeling and Assimilation Office, NASA Goddard Space Flight Center, Greenbelt, MD

Qing Liu

Science Systems and Applications Inc., Lanham, MD

Randal D. Koster

Global Modeling and Assimilation Office, NASA Goddard Space Flight Center, Greenbelt, MD

Joseph V. Ardizzone

Science Systems and Applications Inc., Lanham, MD

Andreas Colliander

Jet Propulsion Laboratory, Caltech, Pasadena, CA

Wade T. Crow

U.S. Department of Agriculture, Agricultural Research Service, Beltsville, MD

Gabrielle J. M. De Lannoy

KULeuven, Leuven, Belgium

John S. Kimball

University of Montana, Missoula, MT

National Aeronautics and
Space Administration

Goddard Space Flight Center
Greenbelt, Maryland 20771

January 2022

Trade names and trademarks are used in this report for identification only. Their usage does not constitute an official endorsement, either expressed or implied, by the National Aeronautics and Space Administration.

Level of Review: This material has been technically reviewed by technical management.

Available from

NASA STI Program
Mail Stop 148
NASA's Langley Research
Center Hampton, VA
23681-2199

National Technical Information
Service 5285 Port Royal Road
Springfield, VA 22161
703-605-6000

TABLE OF CONTENTS

EXECUTIVE SUMMARY	3
1 INTRODUCTION	5
2 SMAP CALIBRATION AND VALIDATION OBJECTIVES.....	6
3 L4_SM CALIBRATION AND VALIDATION APPROACH	8
4 L4_SM ACCURACY REQUIREMENT.....	9
5 L4_SM VERSION 6 RELEASE	10
5.1 Process and Criteria.....	10
5.2 Processing and Science ID Version.....	10
5.3 Summary of Changes from Previous Version	11
6 L4_SM DATA PRODUCT ASSESSMENT.....	13
6.1 Global Patterns and Features	13
6.2 Core Validation Sites	18
6.2.1 Method	18
6.2.2 Results.....	22
6.3 Sparse Networks.....	25
6.3.1 Method	25
6.3.2 Results.....	27
6.4 Satellite Soil Moisture Retrievals.....	28
6.5 Data Assimilation Diagnostics.....	31
6.5.1 Observation-Minus-Forecast Residuals	31
6.5.2 Increments.....	36
6.5.3 Uncertainty Estimates	38
7 LIMITATIONS AND PLAN FOR FUTURE IMPROVEMENTS	40
7.1 L4_SM Algorithm Calibration and Temporal Homogeneity.....	40
7.2 Impact of Ensemble Perturbations.....	40
7.3 Precipitation Data	41
7.4 Peatland and Permafrost Modeling.....	41
8 SUMMARY AND CONCLUSIONS.....	42
ACKNOWLEDGEMENTS	45
APPENDIX	46
Performance Metrics at Core Validation Site Reference Pixels.....	46
REFERENCES.....	56

This page intentionally left blank.

EXECUTIVE SUMMARY

This report closely examines Version 6 of the NASA Soil Moisture Active Passive (SMAP) Level 4 Surface and Root Zone Soil Moisture (L4_SM) product, which was first released on 8 December 2021. The assessment includes comparisons of L4_SM soil moisture estimates with in situ measurements from SMAP core validation sites and sparse networks. Also provided is a quasi-global evaluation of the product's anomaly correlation skill relative to the previous version and a model-only version, based on independent satellite radar soil moisture retrievals and an Instrumental Variable approach. The assessment further provides a global evaluation of the internal diagnostics from the ensemble-based data assimilation system that is used to generate the L4_SM product, including observation-minus-forecast (O-F) brightness temperature (T_b) residuals and soil moisture analysis increments. The core validation site comparisons, the assessment of the anomaly correlation skill using independent radar soil moisture retrievals, and the statistics of the assimilation diagnostics are considered primary validation methodologies for the L4_SM product. Comparisons against in situ measurements from regional-scale sparse networks are considered a secondary validation methodology because such in situ measurements are subject to upscaling errors from their native point-scale to the grid-cell scale of the data product. The validation period is April 2015 to March 2021.

The precipitation forcing data of earlier L4_SM versions was derived primarily through temporal and spatial downscaling of the NOAA Climate Prediction Center Unified (CPCU) gauge product using background data from the Goddard Earth Observing System (GEOS) Forward Processing (FP) weather analysis. Validation of the earlier L4_SM versions, however, revealed serious deficiencies in the CPCU product. To address the shortcomings in the CPCU product, Version 6 of the L4_SM algorithm primarily uses satellite-gauge and satellite-only products provided by the NASA Global Precipitation Measurement (GPM) mission. First, the reference precipitation climatology for the Version 6 L4_SM algorithm is based on the NASA Integrated Multi-satellitE Retrievals for GPM (IMERG) Final (Version 06B) product. Where the IMERG climatology is not available (in much of the high latitudes north of 60°N), the climatology of the Global Precipitation Climatology Project (GPCP) v2.3 product is used as reference. Second, outside of North America, the precipitation forcing in the Version 6 L4_SM algorithm is corrected to match the daily totals from the IMERG (Version 06B) product. The IMERG-Final product, which is informed by satellite observations and monthly totals from precipitation gauges, was used during L4_SM reprocessing through 29 June 2021. Owing to the ~3.5-month latency of the IMERG-Final product, the satellite-only IMERG-Late product, which is available with ~14-hour latency, is used from 30 June 2021 to present. This switch from IMERG-Final to IMERG-Late inputs is reflected in a change in the L4_SM Science Version ID from Vv6032 to Vv6030. In North America, daily precipitation corrections in the Version 6 L4_SM algorithm are based on CPCU data, as in all previous L4_SM versions. Consequently, the mean latency of the Version 6 L4_SM product is still driven by that of the CPCU product and remains at ~2.5 days.

An analysis of the time-average surface and root zone soil moisture shows that the global pattern of arid and humid regions is well captured by the Version 6 L4_SM estimates. Compared to Version 5, the Version 6 surface and root-zone soil moisture is wetter in much of South America and Australia and drier in most of Africa, owing primarily to the revised precipitation climatology. These changes are also reflected in the surface turbulent fluxes and the surface and soil temperatures. Because of these climatological differences, the Version 5 and Version 6 products should *not* be combined into a single dataset for use in applications outside of the continental United States.

Results from the core validation site comparisons indicate that the Version 6 L4_SM product meets its accuracy requirement, which is formulated in terms of the root-mean square (RMS) error after removal of the long-term mean error, i.e., $ubRMSE \leq 0.04 \text{ m}^3 \text{ m}^{-3}$, where the error is vs. the unknown true soil moisture. Computed directly against core site in situ measurements at the 9 km scale, the average unbiased RMS difference (ubRMSD) of the 3-hourly Version 6 L4_SM data is $0.040 \text{ m}^3 \text{ m}^{-3}$ for surface soil moisture and

0.027 m³ m⁻³ for root zone soil moisture. When factoring in the measurement error of the in situ data, the L4_SM product clearly meets the 0.04 m³ m⁻³ ubRMSE requirement.

The ubRMSD values of the Version 6 soil moisture are essentially unchanged from those of Version 5. There is a small increase in the correlation and anomaly correlation skill of the Version 6 surface soil moisture. On the other hand, the mean differences of the Version 6 surface and root-zone soil moisture from the corresponding in situ measurements are slightly larger in Version 6 than in Version 5. Since most of the in situ measurement sites are in North America, where both product versions use CPCU data for the daily precipitation corrections, it is not surprising that the skill of the Version 5 and 6 products is very similar.

The L4_SM estimates are an improvement compared to estimates from a model-only Open Loop (OL6000) simulation, which demonstrates the beneficial impact of the SMAP Tb data. Overall, L4_SM surface and root zone soil moisture estimates are more skillful than OL6000 estimates, with statistically significant improvements for surface soil moisture R and anomaly R values (based on 95% confidence intervals). The correlation and anomaly correlation skill differences between the L4_SM product and the Open Loop are slightly smaller in Version 6 than in Version 5. This is because the Open Loop baseline skill is somewhat larger in Version 6 than in Version 5, which leaves less room for improvement associated with the assimilation of the SMAP Tb observations.

Results from comparisons of the L4_SM product to in situ measurements from more than 400 sparse network sites corroborate the core validation site results.

The evaluation of the anomaly correlation skill based on the independent radar soil moisture retrievals reveals that the improvements in the Version 6 surface soil moisture (relative to Version 5) are concentrated in South America, Africa, Australia, and parts of East Asia. In these regions, the Version 5 system used either the uncorrected (simulated) GEOS FP precipitation (throughout Africa) or CPCU-corrected precipitation, albeit with the CPCU data relying on sparse or faulty regional gauge networks (including parts of South America, central Australia, and Myanmar). Using IMERG data for the daily precipitation corrections in the Version 6 algorithm considerably improves the surface soil moisture anomaly correlation in these regions.

The instantaneous soil moisture analysis increments lie within a reasonable range and result in spatially smooth soil moisture analyses. The long-term mean soil moisture analysis increments make up only a small fraction of the water budget. The O-F Tb residuals exhibit only a small regional bias (less than 3 K) between the (rescaled) SMAP Tb observations and the L4_SM model forecast, which indicates that the assimilation system is reasonably unbiased. The globally averaged time series standard deviation of the O-F Tb residuals is 5.1 K, which represents a reduction of ~0.4 K from that of the Version 5 product. This considerable improvement in the Tb simulation skill is concentrated in the same regions where the anomaly correlation skill is most improved based on the independent satellite radar soil moisture retrievals (that is, in parts of South America and Africa, central Australia, and Myanmar). Regionally, the time series standard deviation of the normalized O-F Tb residuals deviates considerably from unity, which indicates that regionally the L4_SM assimilation algorithm over- or underestimates the total (model and observation) error present in the system, although the consistency is somewhat improved in Version 6 compared to Version 5. The globally averaged time series standard deviation is 3.3 K for the observation-minus-analysis Tb residuals, reflecting the impact of the SMAP observations on the L4_SM system.

In summary, Version 6 of the L4_SM product is sufficiently mature and of adequate quality for distribution to, and use by, the larger science and application communities.

1 INTRODUCTION

The NASA Soil Moisture Active Passive (SMAP) mission provides space-borne global measurements of the Earth’s L-band (1.4 GHz) brightness temperature (Tb) emission from a 685-km, near-polar, sun-synchronous orbit. These observations are primarily sensitive to soil moisture and temperature in the top few centimeters of the soil. SMAP data can therefore be used to enhance our understanding of processes that link the terrestrial water, energy, and carbon cycles, and to potentially extend the capabilities of weather and climate prediction models (Entekhabi et al. 2014).

The suite of SMAP science data products includes the Level 4 Surface and Root Zone Soil Moisture (L4_SM) product, which provides deeper-layer soil moisture estimates that are not available in the Level 2-3 retrieval products. The L4_SM product is based on the assimilation of SMAP Tb observations into the NASA Catchment land surface model (Koster et al. 2000) using a customized version of the Goddard Earth Observing System (GEOS) land data assimilation system (Figure 1; Reichle et al. 2014a, 2017a,b, 2019). This system, which is based on the ensemble Kalman filter (EnKF), accounts for model and observational uncertainty through perturbations of select Catchment model forcing and soil moisture prognostic variables, propagates the surface information from the SMAP instrument to the deeper soil, and ultimately provides global, 3-hourly estimates of soil moisture and other land surface fields without gaps in coverage. The mean publication latency of the L4_SM product is ~2.5 days. This latency is driven by the availability of gauge-based precipitation data used to force the land surface model (Reichle and Liu 2014; Reichle et al. 2014b, 2017a,b, 2021a,b).

The L4_SM product provides surface and root zone soil moisture (along with other geophysical fields) as 3-hourly, time-average fields on the global, cylindrical, 9 km Equal-Area Scalable Earth, version 2 (EASEv2; Brodzik et al. 2012) grid in the “geophysical” (or “gph”) output Collection (Reichle et al. 2018a). Moreover, instantaneous soil moisture and soil temperature fields before and after the assimilation update are provided every three hours on the same grid in the “analysis update” (or “aup”) output Collection, along with other assimilation diagnostics and error estimates. Time-invariant land model parameters, such as soil porosity, wilting point, and microwave radiative transfer model parameters, are provided in the “land-model-constants” (or “lmc”) Collection (Reichle et al. 2018a).

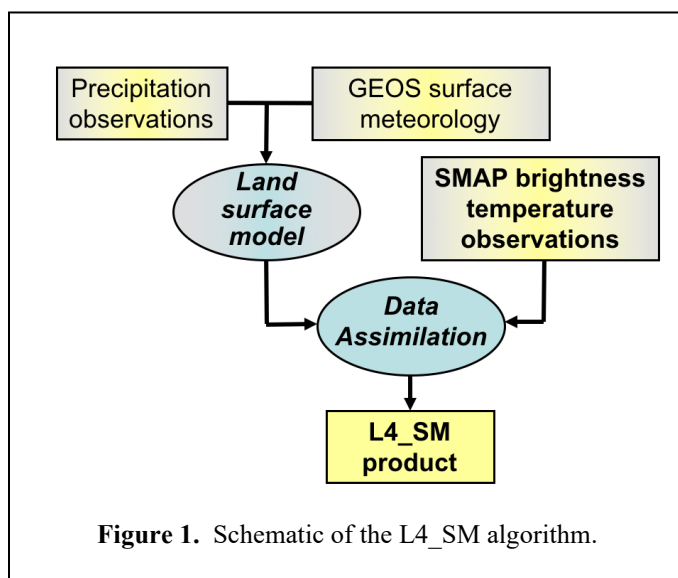


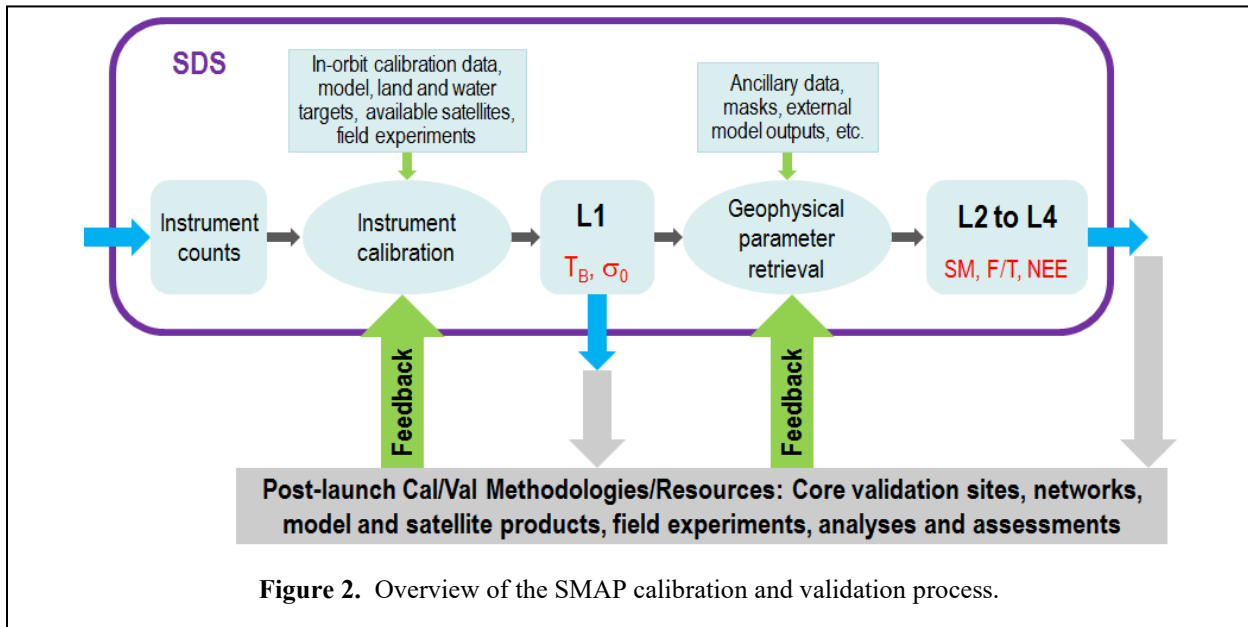
Figure 1. Schematic of the L4_SM algorithm.

For geophysical data products that are based on the assimilation of satellite observations into numerical process models, validation is critical and must be based on quantitative estimates of uncertainty. Direct comparison with independent observations, including ground-based measurements, is a key part of validation. This assessment report provides a detailed description of the status of the L4_SM data quality for the Version 6 release of the L4_SM data product. The L4_SM validation process and data quality of previous versions are discussed by Reichle et al. (2015, 2016, 2017a,b, 2018b, 2019, 2021a,b) and Colliander et al. (2021).

2 SMAP CALIBRATION AND VALIDATION OBJECTIVES

During the post-launch SMAP calibration and validation (Cal/Val) phase each science product team pursues two objectives:

1. Calibrate, verify, and improve the performance of the science algorithm.
2. Validate the accuracy of the science data product as specified in the science requirements and according to the Cal/Val schedule.



The overall SMAP Cal/Val process is illustrated in Figure 2. This process was first formalized in the SMAP Science Data Cal/Val Plan (Jackson et al. 2014) and the SMAP L2-L4 Data Products Cal/Val Plan (Colliander et al. 2014). Recently, many pioneering aspects of the SMAP Cal/Val process were incorporated into community standards for soil moisture product validation and good practices (Gruber et al. 2020; Montzka et al. 2020). Moreover, Colliander et al. (2021) provide a comprehensive and up-to-date overview of the SMAP project's approach to soil moisture validation. The present assessment report describes how the L4_SM team addressed the Cal/Val objectives for the Version 6 release. The validation approach and procedures that apply specifically to the L4_SM product are further detailed in the Algorithm Theoretical Basis Document for the L4_SM data product (Reichle et al. 2014b).

SMAP established unified definitions to address the mission requirements. These are documented in the SMAP Handbook (Entekhabi et al. 2014), where calibration and validation are defined as follows:

- *Calibration*: The set of operations that establish, under specified conditions, the relationship between sets of values or quantities indicated by a measuring instrument or measuring system and the corresponding values realized by standards.
- *Validation*: The process of assessing by independent means the quality of the data products derived from the system outputs.

To ensure the public's timely access to SMAP data, the mission was required to release validated data products within one year of the beginning of mission science operations. The objectives and maturity of the SMAP validated release products follow the guidance provided by the Committee on Earth Observation

Satellites (CEOS) Working Group on Calibration and Validation (CEOS 2015), which can be summarized as follows (Colliander et al. 2021, their Appendix A):

- Stage 1 Validation: Product accuracy is assessed from a small (typically < 30) set of locations and time periods by comparison with in-situ or other suitable reference data.
- Stage 2 Validation: Product accuracy is estimated over a significant (typically > 30) set of locations and time periods by comparison with reference in situ or other suitable reference data. Spatial and temporal consistency of the product, and its consistency with similar products, has been evaluated over globally representative locations and time periods. Results are published in the peer-reviewed literature.
- Stage 3 Validation: Uncertainties in the product and its associated structure are well quantified over a significant (typically > 30) set of locations and time periods representing global conditions by comparison with reference in situ or other suitable reference data. Validation procedures follow community-agreed-upon good practices. Spatial and temporal consistency of the product, and its consistency with similar products, has been evaluated over globally representative locations and time periods. Results are published in the peer-reviewed literature.
- Stage 4 Validation: Validation results for Stage 3 are systematically updated when new product versions are released and as the interannual time-series expands. When appropriate for the product, uncertainties in the product are quantified using fiducial reference measurements over a global network of sites and time periods (if available).

For the Version 6 release, the L4_SM team has completed all of the above validation stages, including repeated publication of the latest validation results in the peer-reviewed literature (Reichle et al. 2017a,b, 2019, 2021a; Colliander et al. 2021). Consequently, Version 6 of the L4_SM product replaces Version 5. The Cal/Val program will continue over the SMAP mission life span. Incremental improvements are ongoing as more measurements become available from the SMAP observatory. Version 6 data will be replaced in the archive when upgraded product versions become available.

3 L4_SM CALIBRATION AND VALIDATION APPROACH

During the mission definition and development phase, the SMAP Science Team and Cal/Val Working Group identified the metrics and methodologies that would be used for L2-L4 product assessment. These metrics and methodologies were vetted in community Cal/Val Workshops and tested in SMAP pre-launch Cal/Val rehearsal campaigns. The following validation methodologies and their general roles in the SMAP Cal/Val process were identified:

- *Core Validation Sites:* Accurate estimates at matching scales for a limited set of conditions.
- *Sparse Networks:* One point in the grid cell for a wide range of conditions.
- *Satellite Products:* Estimates over a very wide range of conditions at matching scales.
- *Model Products:* Estimates over a very wide range of conditions at matching scales.
- *Field Campaigns:* Detailed estimates for a very limited set of conditions.

The assessment of the L4_SM data product includes comparisons of SMAP L4_SM soil moisture estimates with in situ soil moisture observations from core validation sites and sparse networks. Moreover, independent soil moisture retrievals from satellite radar observations are used to measure the contribution of the SMAP analysis to the anomaly time series correlation skill of the L4_SM product across much of the global land surface. Finally, the assessment includes a global evaluation of the internal diagnostics from the ensemble-based data assimilation system that is used to generate the L4_SM product. This evaluation focuses on the statistics of the observation-minus-forecast (O-F) Tb residuals and the analysis increments.

The core site comparisons, the assessment of the anomaly correlation skill using independent radar soil moisture retrievals, and the statistics of the assimilation diagnostics are considered primary validation methodologies for the L4_SM product. Comparisons against in situ measurements from regional-scale sparse networks are considered a secondary validation methodology because such in situ measurements are subject to upscaling errors from the point-scale to the grid-cell scale of the data product.

Due to their very limited spatial and temporal extent, data from field campaigns play only a tertiary role in the validation of the L4_SM data product. Note, however, that field campaigns are instrumental tools in the provision of high-quality, automated observations from the core validation sites and thus play an important indirect role in the validation of the L4_SM data product.

4 L4_SM ACCURACY REQUIREMENT

There is no formal Level 1 mission requirement for the validation of the L4_SM product, but the L4_SM team self-imposed an accuracy requirement mirroring the one applied to the Level 2 Radar/Radiometer soil moisture (L2_SM_AP) product. Specifically, the L4_SM surface and root zone soil moisture estimates are required to meet the following criterion:

$\text{ubRMSE} \leq 0.04 \text{ m}^3 \text{ m}^{-3}$ within the data masks specified in the *SMAP Level 2 Science Requirements* (that is, excluding regions of snow and ice, frozen ground, mountainous topography, open water, urban areas, and vegetation with (above-ground) water content greater than 5 kg m^{-2}),

where ubRMSE is the “unbiased” root-mean square (RMS) error, that is, the RMS error computed after removing long-term mean bias from the data (Entekhabi et al. 2010; Reichle et al. 2015, their Appendix A). (The ubRMSE is the same as the standard deviation of the error.) This criterion applies to the L4_SM instantaneous surface and root zone soil moisture estimates at the 9 km grid-cell scale from the “aup” Collection. It is verified by comparing the L4_SM product to the grid-cell scale in situ measurements from the core validation sites (section 6.2), resulting in the unbiased RMS difference (ubRMSD) metric. The criterion applies to the site-average ubRMSE, which is estimated by averaging across the ubRMSD values for all 9 km core site reference pixels that provide suitable in situ measurements (Reichle et al. 2015). It is important to note that even the high-quality SMAP core site measurements are subject to error. Consequently, the ubRMSD generally overestimates the ubRMSE and therefore is a conservative estimate of the performance of the data product (Chen et al. 2019).

L4_SM output fields other than instantaneous surface and root zone soil moisture are provided as research products (including surface meteorological forcing variables, soil temperature, evaporative fraction, net radiation, etc.) and will be evaluated against in situ observations to the extent possible given available resources.

As part of the validation process, additional metrics, including the mean difference (MD), the time series correlation coefficient (R), and anomaly R values, are also computed for the L4_SM output. This includes computation of the metrics outside of the limited geographic area for which the $\text{ubRMSE} \leq 0.04 \text{ m}^3 \text{ m}^{-3}$ validation criterion applies.

For the computation of the *anomaly* R metric, climatological values of soil moisture from a given dataset (i.e., the L4_SM product or the in situ measurements) at a given location are computed for each day of the year using a 31-day smoothing window, thereby generating a local climatological seasonal cycle for that dataset. Anomaly time series are then computed by subtracting this climatological seasonal cycle from the corresponding raw data. The anomaly R metric is derived by computing the correlation coefficient between the L4_SM and the in situ anomaly time series (Reichle et al. 2015).

The validation includes additional metrics that are based on the statistics of the O-F Tb residuals and other data assimilation diagnostics (section 6.5). Reichle et al. (2015) provide detailed definitions of all the validation metrics and confidence intervals used here.

5 L4_SM VERSION 6 RELEASE

5.1 Process and Criteria

Since the beginning of the SMAP science data flow on 31 March 2015, the L4_SM team has been conducting frequent assessments of the L4_SM data product and will continue to evaluate the product throughout the life of the SMAP mission. These assessments are based on core validation sites, sparse networks, independent satellite soil moisture retrievals, and assimilation diagnostics, and they capture a wide range of geophysical conditions. The present report summarizes the status of this process for the Version 6 L4_SM product.

The validation of the Version 6 L4_SM product includes comparisons against output from two model-only simulations that are based on the same land surface model and forcing data as the Version 6 L4_SM estimates but are not informed by SMAP Tb observations (Table 1). Any accuracy in these model-only estimates is derived from the imposed meteorological forcing and land model structure and parameter information. The first model-only simulation, the ensemble “Open Loop” (OL6000), employs 24 ensemble members and applies the same forcing and model prognostics perturbations that are also used in the Version 6 L4_SM algorithm, whereas the second model-only simulation, the “Nature Run,” version 9.1 (NRv9.1), is a single-member land model simulation without perturbations (Table 1). The OL6000 estimates were prepared for the SMAP period (31 March 2015 to present) and are the primary reference for the model-only skill. The NRv9.1 estimates were generated for the period 1 January 2000 to present and provide the simulated climatological information required by the L4_SM assimilation algorithm (Reichle et al. 2014b). The NRv9.1 estimates are also used to determine any bias in the ensemble simulations relative to the unperturbed NRv9.1 simulation.

Table 1. Overview of L4_SM products and model-only simulations.

	No. Ensemble Members	Perturbations	SMAP Assimilation	Version 6	Version 5
L4_SM Product	24	Yes	Yes	Vv6032 (thru 29 Jun 2021) Vv6030 (from 30 Jun 2021)	Vv5030
Ensemble Open Loop	24	Yes	No	OL6000	OL5030
Nature Run	1	No	No	NRv9.1	NRv8.3

5.2 Processing and Science ID Version

To date, the Version 6 L4_SM product (Reichle et al. 2021c,d,e) has been generated under Science Version ID Vv6032 for 31 March 2015 through 29 June 2021 and Vv6030 thereafter (Table 1), with the minor version change indicating a change in the precipitation inputs (section 5.3).

The Version 6 L4_SM algorithm assimilates operational data from the Version 5 SMAP Tb observations provided in the Level 1C Radiometer Half-Orbit 36 km Brightness Temperature (L1C_TB)

product (Chan et al. 2020). The assimilated Version 5 L1C_TB data were generated under several Composite Release IDs (CRIDs), which all produce scientifically equivalent brightness temperature data. Specifically, the L4_SM Vv6032 algorithm used L1C_TB data with CRID R17000 through 22 April 2021 and CRID R17030 from 23 April 2021 through 29 June 2021; the Vv6030 algorithm used L1C_TB data with CRID 17030 from 30 June 2021 through 27 October 2021 and CRID R18240 thereafter. Some L1C_TB half-orbit granules assimilated into the Version 6 algorithm differ in their minor processing version from those assimilated into Version 5 (Vv5030). These minor differences do not represent science changes and are caused by late-arriving L1C_TB granules that were generated as part of the effort to correct antenna scan angle errors in early Version 5 L1C_TB processing (Reichle et al. 2021b, their section 5.2). Neither Version 5 nor Version 6 of L4_SM used L1C_TB data with known antenna scan angle errors.

The assessment period for this report is defined as the 6-year period from **1 April 2015, 0z to 1 April 2021, 0z**. The start date matches the first full day when the radiometer was operating under sufficiently stable conditions following instrument start-up operations. The end date was selected to include the maximum possible number of full years available at the time when the present report was prepared. Consequently, only L4_SM data with Science Version ID **Vv6032** were used to prepare this assessment report.

For illustrating select changes from the previous L4_SM product versions, this report also used published Version 5 L4_SM data (Science Version ID Vv5030; Reichle et al. 2020a,b,c), along with the corresponding Nature Run (NRv8.3) and ensemble Open Loop (OL5030) simulations (Table 1).

Like all previous versions, Version 6 of the L4_SM algorithm ingests only the SMAP L1C_TB radiometer Tb observations, contrary to the originally planned use of downscaled Tb observations from the L2_SM_AP product and landscape freeze-thaw state retrievals from the SMAP Level 2 Radar Half-Orbit 3 km Soil Moisture (L2_SM_A) product. The latter two products are based on SMAP radar observations and are only available for the 10-week period from 13 April to 7 July 2015 because of the failure of the SMAP radar instrument. The decision to again use only radiometer (L1C_TB) inputs for the Version 6 release was made to ensure homogeneity in the longer-term L4_SM data record.

5.3 Summary of Changes from Previous Version

This section provides a summary of algorithm changes between the previous (Version 5) L4_SM algorithm and the current Version 6 assessed here. **The key change in Version 6 of the L4_SM algorithm is the improved precipitation forcing that is applied in the Catchment land surface model.** In addition to the gauge-only NOAA Climate Prediction Center Unified (CPCU) product used in all previous versions, the Version 6 L4_SM algorithm uses data provided by the NASA Global Precipitation Measurement (GPM) mission. Specifically, the Integrated Multi-satellitE Retrievals for GPM (IMERG) suite of products is used as follows:

- 1.) In Version 6, the climatology to which all L4_SM precipitation forcing inputs are rescaled is based on the climatology of the NASA IMERG-Final (Version 06B) product¹. Where the IMERG climatology is not available (primarily poleward of 60°N latitude), L4_SM precipitation inputs are rescaled to the climatology of the Global Precipitation Climatology Project (GPCP) v2.3 product. The revised precipitation reference climatology results in a change in the Version 6 soil moisture climatology across the global land surface compared to Version 5 (section 6.1).
- 2.) In Version 6, the precipitation forcing outside of North America and the high latitudes is corrected to match the daily totals from the NASA IMERG (Version 06B) product. As in Version 5, precipitation corrections based on CPCU data are used in North America. In Version 6, the latitude band for the linear tapering of the daily precipitation corrections was changed to 50-60°N/S (from 42.5-62.5°N/S in all previous versions) to give more weight to the observations in the mid-latitudes and because the full coverage of IMERG is limited to 60°N-60°S. The IMERG-Final product, which is informed by satellite observations and monthly totals from precipitation gauges and has a ~3.5-month latency, was used during the bulk of L4_SM reprocessing. The satellite-only IMERG-Late product, which is not informed by precipitation gauges and has a ~14-hour latency, is used for forward-processing. A change in the L4_SM Science Version ID from Vv6032 to Vv6030 on data-day 30 June 2021 indicates the switch from IMERG-Final to IMERG-Late inputs. Since CPCU data are still used for daily precipitation corrections in North America, the mean publication latency of the Version 6 L4_SM product remains at ~2.5 days from the time of the SMAP observations.

Reichle and Liu (2021) provide a comprehensive discussion of the revised precipitation climatology, corrections approach, and input datasets.

Additionally, the following minor changes impact the L4_SM Tb analysis:

- 3.) In Version 6, the standard-normal deviates generated for the multiplicative perturbations of the precipitation and downward shortwave forcing are truncated at ± 3 . (In earlier versions, the limit was ± 2.5 for all perturbations. In Version 6, the limit for additive perturbations remains at ± 2.5 .)
- 4.) In Version 6, the Tb scaling parameters are based on six years of SMAP Tb observations (April 2015 – March 2021).

Finally, the Version 6 L4_SM algorithm includes improved file compression:

- 5.) In Version 6, a lossy compression (“bit shaving”) is applied to reduce the volume of the Geophysical Data (“gph”) and Analysis Update (“aup”) hdf-5 granules. Specifically, this lossy compression retains only the 12 most important bits (out of 24) that make up the mantissa of each science data value. The 12 least important bits, which generally do not contain meaningful science information, are modified to enhance compressibility. The same lossy compression had been applied to “gph” output only in Versions 1-4 of L4_SM. In Version 5, only lossless compression was applied.

¹ IMERG-Final data are an optimal combination of satellite observations with monthly gauge data from the Global Precipitation Climatology Centre (GPCC). As a result, the IMERG-Final climatology is not identical to that of the underlying gauge data. Moreover, IMERG-Final uses a more recent version of the GPCC gauge product than does the GPCPv2.2 product, which provided the reference climatology in the Version 5 L4_SM algorithm.

6 L4_SM DATA PRODUCT ASSESSMENT

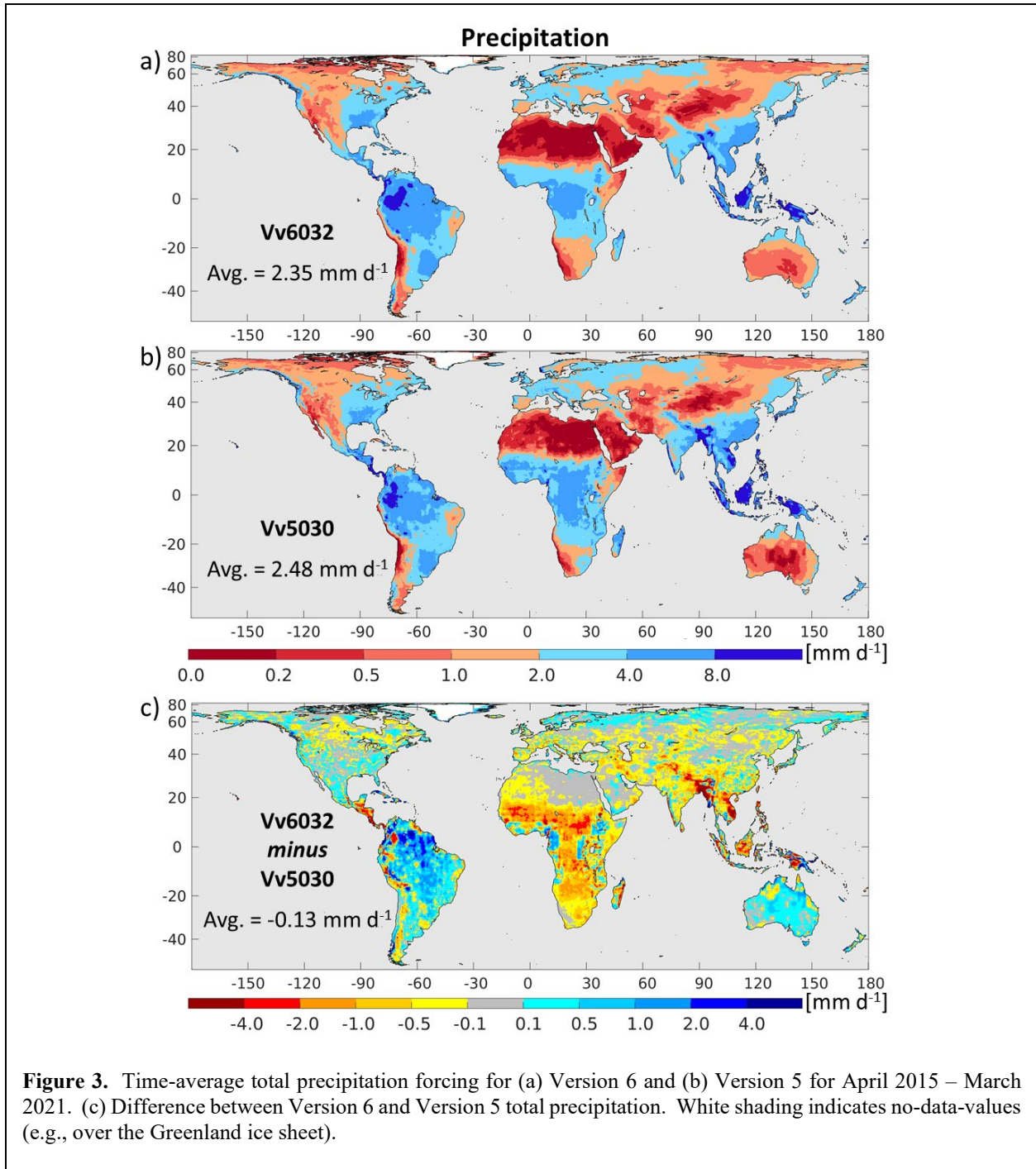
This section provides a detailed assessment of the Version 6 L4_SM data product. First, global patterns and features are discussed, with a focus on the changes in the precipitation and soil moisture climatology of Version 6 (section 6.1). Next, we briefly present comparisons and metrics versus in situ measurements from core validation sites (section 6.2) and sparse networks (section 6.3), followed by a discussion of the assessment versus satellite retrievals (section 6.4). Thereafter, we evaluate the assimilation diagnostics (section 6.5) through an analysis of the O-F Tb residuals, the soil moisture increments, and the data product uncertainty estimates.

6.1 Global Patterns and Features

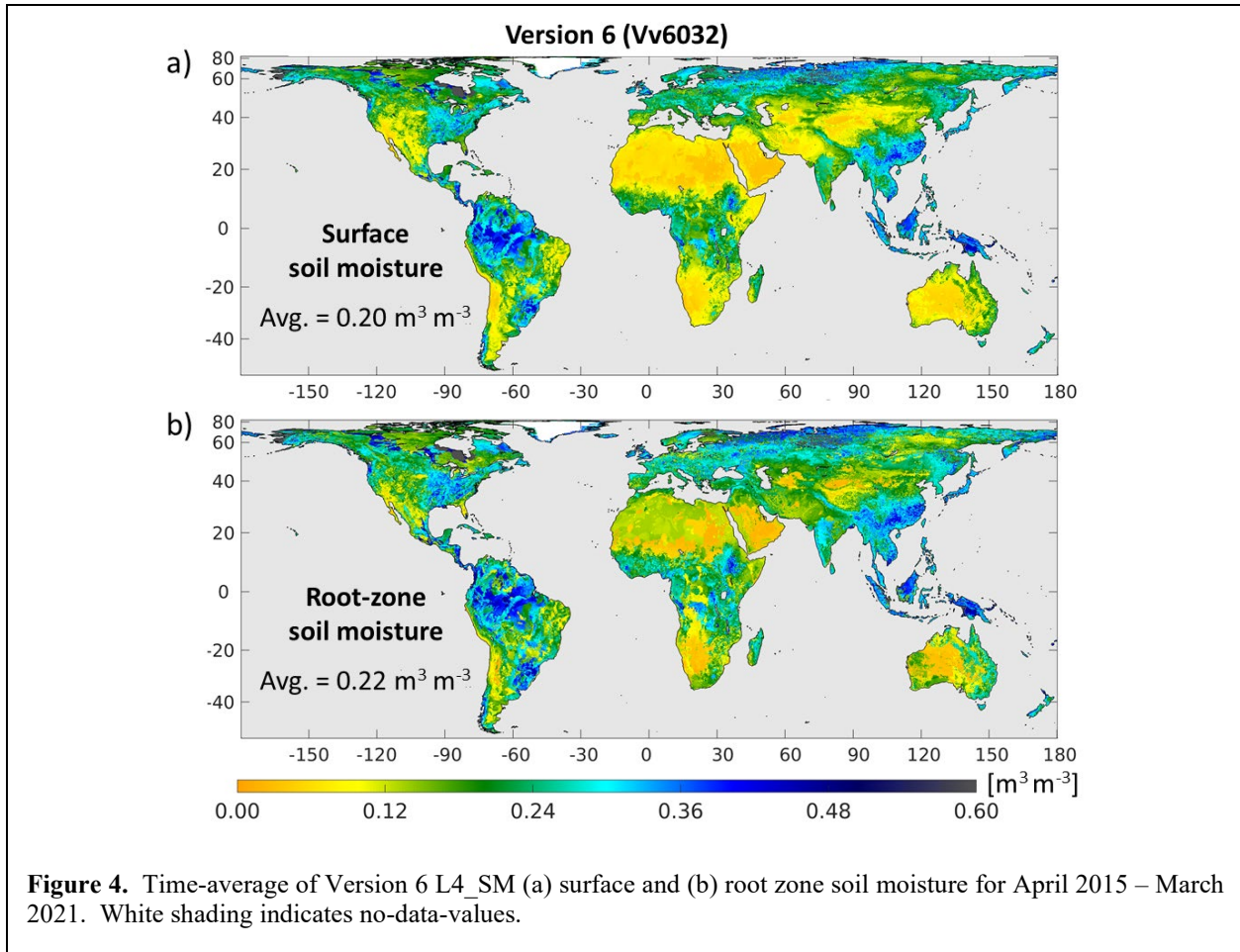
Figure 3a shows the time-averaged total precipitation forcing in Version 6 for the validation period (April 2015 – March 2021). Figure 4 shows the time-averages for surface and root-zone soil moisture. The global patterns are as expected – arid regions such as the southwestern US, the Sahara Desert, the Arabian Peninsula, the Middle East, southern Africa, and central Australia exhibit little precipitation and generally dry surface and root zone soil moisture conditions, whereas the tropics (Amazon, central Africa, and Indonesia) and high-latitude regions show wetter conditions. The global patterns of soil moisture are further impacted by soil texture, which is noticeable, for example, in the coarse-scale pattern of root-zone soil moisture in the Sahara Desert, where little is known about the spatial distribution of mineral soil fractions. Areas with highly organic peat soil include, for example, the region along the southern edge of Hudson Bay and portions of Alaska. In the land model, the soils in this region are assigned a high porosity value and show persistently wetter conditions than seen in other areas.

The time-average precipitation of Version 6 (Figure 3a) exhibits generally smoother spatial patterns than that of Version 5, which exhibits unrealistically heterogeneous patterns and occasionally blocky structures, particularly in tropical South America and Africa, the Sahel, and Southeast Asia (Figure 3b). The latter are an artefact of the much coarser (2.5-degree) GPCPv2.2 climatology used in Version 5 compared to the higher-resolution IMERG-Final data and climatology used in Version 6; see (Reichle and Liu 2021) for details. In the global average, the time-average precipitation decreases slightly from 2.48 mm d⁻¹ in Version 5 to 2.35 mm d⁻¹ in Version 6.

The difference between the time-averaged precipitation of Version 6 and Version 5 is shown in Figure 3c. Generally, Version 6 has more precipitation in most of South America and Australia and less precipitation in most of Africa and Southeast Asia. The climatological differences are particularly large in the northern Amazon and in Myanmar and Vietnam. Minor climatological differences can also be seen in the continental United States (CONUS), especially in the western mountains and in California. The difference in the time-averaged precipitation is imprinted on the differences in the time-averaged surface and root-zone soil moisture (Figure 5), which can reach several volumetric percent in the regions where the differences in the time-average precipitation are largest. In CONUS, time-average soil moisture changes are typically within 0.01 m³ m⁻³. Across the globe, the soil moisture differences balance out and the global average of the climatological surface or root-zone soil moisture in Version 6 remains unchanged from that in Version 5. Because of the regional differences in the long-term average soil moisture (Figure 5), however, the Version 5 and Version 6 products should *not* be combined into a single dataset for use in applications outside of CONUS.

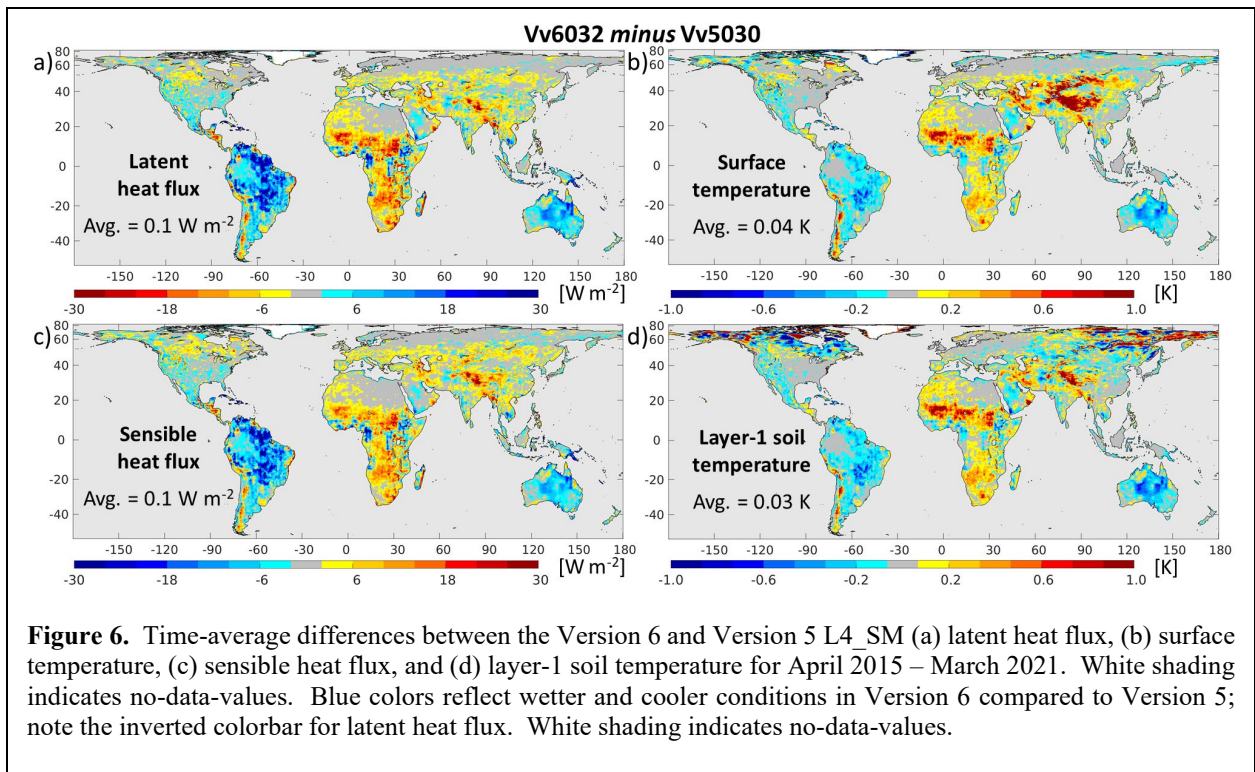
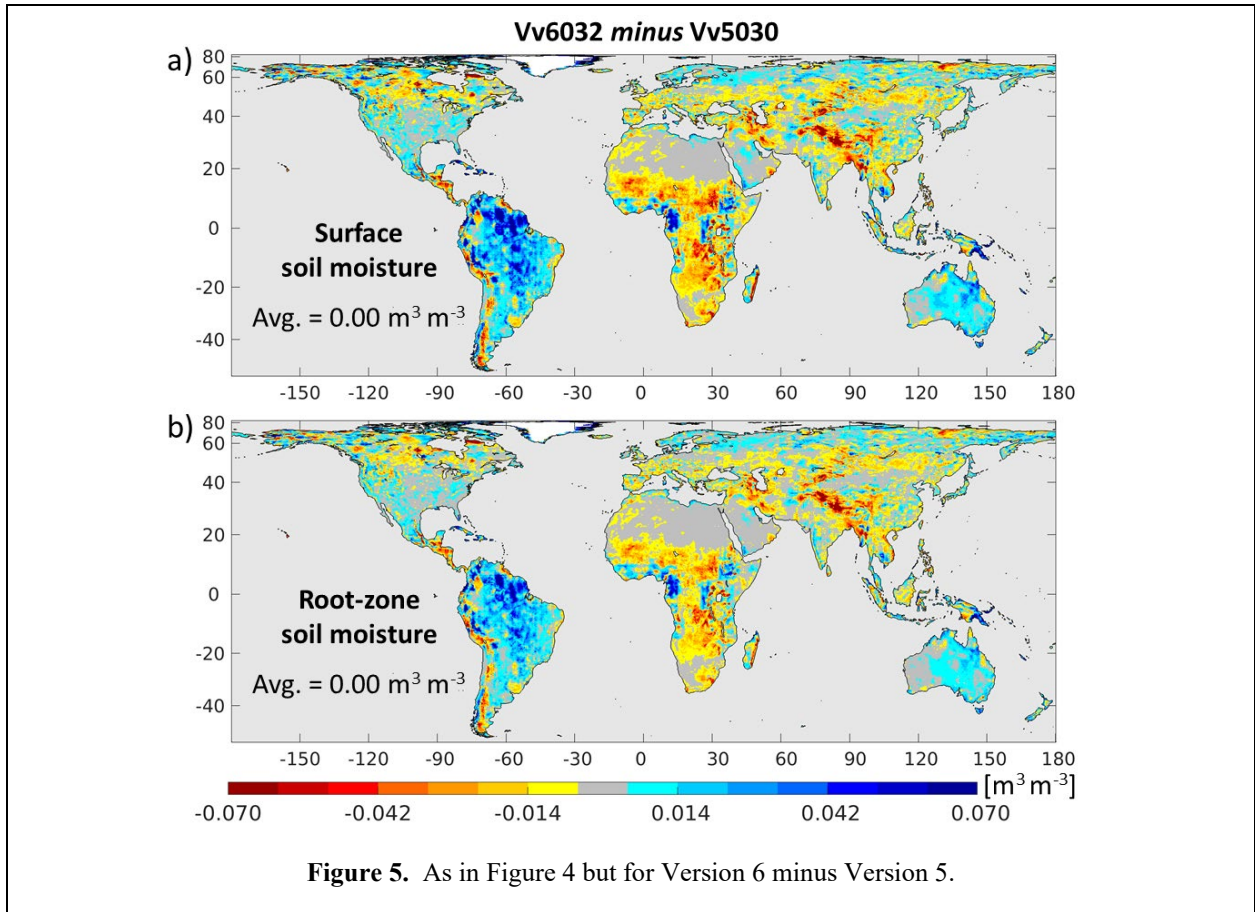


The changes in precipitation and soil moisture are also reflected in the latent and sensible heat fluxes and the surface and soil temperatures (Figure 6). Generally, regions that are wetter in Version 6 exhibit increased latent heat fluxes, decreased sensible heat fluxes, and cooler temperatures compared to Version 5. Conversely, regions that are drier in Version 6 exhibit lower latent and higher sensible heat fluxes along with higher temperatures compared to Version 5. Changes range from -30 to 30 W m⁻² in the turbulent fluxes and from -1 to 1 K in the surface and soil temperatures. Note that these “research” output fields are not subject to formal validation requirements.

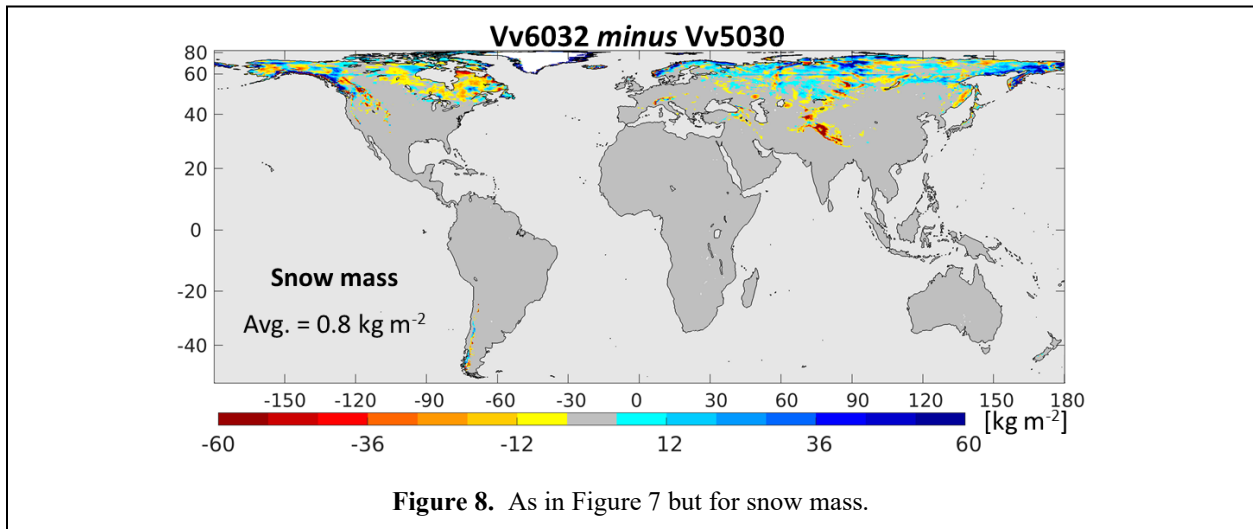
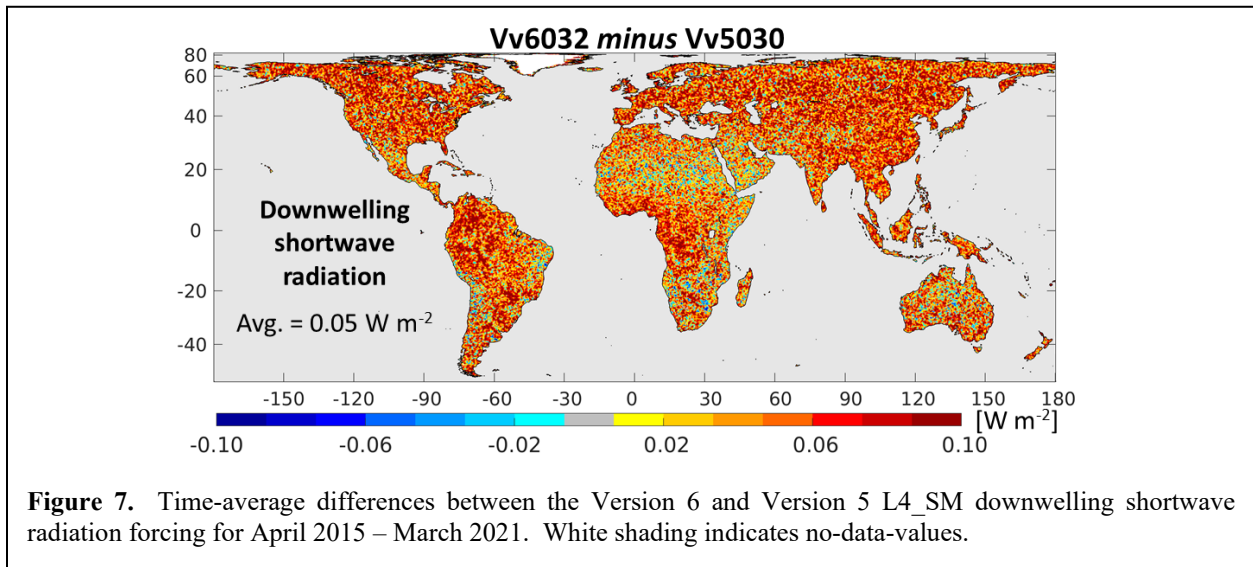


The standard-normal deviates for the lognormal, multiplicative perturbations of the precipitation and downward shortwave forcing are truncated at ± 3 in Version 6 and at ± 2.5 times in Version 5. This change was motivated by the small bias of -1.4 W m^{-2} in the ensemble-mean of the perturbed forcing with respect to the unperturbed forcing seen in Version 5 (Reichle et al. 2021b, their Figure 7b). The bias was indeed reduced through the increase in the maximum allowed multiplicative perturbations in Version 6 and the associated increase in downwelling shortwave radiation in Version 6, but only marginally by $\sim 0.05 \text{ W m}^{-2}$ (Figure 7). This suggests that the bias in the perturbed shortwave forcing is mainly caused by other nonlinear effects in the perturbations scheme.

Finally, Figure 8 shows the differences in time-average snow mass between Version 6 and Version 5, which range from -60 to 60 kg m^{-2} (or mm of snow water equivalent). These differences reflect the changes in the precipitation climatology (Figure 3c). Owing to the insulating properties of snow, the snow mass differences imprint themselves on the soil temperature (Figure 6d), with deeper snowpacks generally resulting in warmer soil temperatures.



Unfortunately, a line feature is visible in the snow mass differences along 60°N latitude in Eurasia and northwestern Canada (Figure 8). This artefact is noticeable even in a global map of the Version 6 time-average snow mass and snow depth (not shown). It can be traced back to a corresponding linear feature in the snowfall forcing (not shown), which is likely caused by the stitching of the IMERG-Final climatology with that of GPCPv2.3 along this latitude. The artefact imprints itself on the Version 6 time-average surface temperature and soil temperature along 60°N latitude; the temperatures just north and south of this latitude can differ by up to ~0.2 and ~0.5 K, respectively, as can be inferred from the Version 6 minus Version 5 temperature difference plots (Figure 6b and d). Further impacts are seen in net shortwave radiation (up to 1 W m⁻²) and runoff (up to 0.5 mm d⁻¹; not shown). The line is *not* noticeable in the time-average soil moisture or any other output field, nor in the corresponding Version 6 minus Version 5 difference plots. Further investigation is necessary to understand how this artefact can be removed in future L4_SM versions.



6.2 Core Validation Sites

This section provides an assessment of the L4_SM soil moisture estimates using data from SMAP core validation sites, which provide estimates of soil moisture and soil temperature at the scale of 9 km and 33 km grid cells based on locally dense networks of in situ sensors (Colliander et al. 2017a,b, 2021).

6.2.1 Method

The core site in situ measurements used here are identical to those used in the Version 5 assessment report (Reichle et al. 2021b). This subsection is a lightly edited version of the corresponding section 6.2.1 of Reichle et al. (2021b); the only notable difference is that the present subsection corrects a minor error in the average number of sensors reported in Table 3 of Reichle et al. (2021b).

Like the assessments for Version 4 and 5 of L4_SM (Reichle et al. 2018b, 2019, 2021b), the present report uses reference pixel data on the 33 km EASEv2 grid (defined through suitable aggregation of the 3 km EASEv2 grid), instead of the 36 km reference pixels used in earlier assessments (Reichle et al. 2015, 2016, 2017a). Additional details about the processing of the data and the validation methodology can be found in Reichle et al. (2015, their section 6.2.1).

The status of the core validation sites is reviewed periodically. The set of core sites that provide data for this assessment of the L4_SM product are listed in Table 2, with details of the 9 km and 33 km reference pixels that are used here shown in Table 3. The validation is based on a total of 48 reference pixels from 19 different core validation sites. Surface soil moisture measurements are available for all 48 reference pixels, which include 18 reference pixels at the 33 km scale from 18 different sites and 30 reference pixels at the 9 km scale from 18 different sites. For root zone soil moisture, measurements are available for only 20 reference pixels from 8 different core sites, including 8 reference pixels at the 33 km scale from 8 different sites and 12 reference pixels at the 9 km scale from 7 different sites. The 9 km reference pixels for root zone soil moisture belong to the core validation sites of Little Washita (Oklahoma), Fort Cobb (Oklahoma), Little River (Georgia), South Fork (Iowa), Tonzi Ranch (California), Kenaston (Saskatchewan), and TxSON (Texas). The same 7 sites plus Yanco (Australia) provide root zone soil moisture data at the 33 km scale. This very limited set obviously lacks the diversity to be fully representative of global conditions, but we are not aware of any other comparable datasets. Finally, note that Table 2 lists the land cover at Yanco as grassland (Colliander et al. 2021), which is more appropriate than the cropland/natural mosaic classification reported in earlier L4_SM assessment reports.

The metrics at a given site are computed from 3-hourly data, provided at least 480 measurements, or about 2 months of data, are available for the site after quality control. The computation of the anomaly R value (section 4) further requires estimates of the 6-year mean seasonal cycle, for which we required a minimum of at least 240 measurements for a given 31-day smoothing window across the 6-year validation period. This requirement implies that the anomaly R metric is available for surface (root zone) soil moisture at only 17 (7) reference pixels at the 33 km scale. At the 9 km scale, the anomaly R metric is available whenever the other metrics are also available.

Table 3 also lists the depths of the deepest sensors that contribute to the in situ root zone soil moisture measurements. The measurements from the individual sensors are vertically averaged with weights that are proportional to the spacing of the depth of the sensors within the 0-100 cm layer depth of the L4_SM root zone soil moisture estimates. At all reference pixels except Little River and Yanco, the deepest sensors are at 40-50 cm depth. At Little River and Yanco, the deepest sensors are at 30 cm and 75 cm, respectively, with Yanco's second-deepest sensors being installed at 45 cm depth. In all cases, the deepest sensors are therefore weighted most strongly in the computation of the vertical average. To compute the vertically

averaged root zone soil moisture at a given time from a given sensor profile, all sensors within the profile must provide measurements that pass the automated quality control.

Table 2. Soil moisture core validation sites used in the present assessment.

<i>Site Name</i>	<i>Country</i>	<i>Climate Regime</i>	<i>Land Cover</i>	<i>Number of 9-km (33-km) Reference Pixels</i>		<i>Reference</i>
				<i>Surface Soil Moisture</i>	<i>Root-zone Soil Moisture</i>	
REMEDHUS	Spain	Temperate	Croplands	2 (1)	- (-)	Sanchez et al. 2012; Gonzalez-Zamora et al. 2015
Reynolds Creek	USA (Idaho)	Arid	Grasslands	2 (1)	- (-)	Seyfried et al. 2001
Yanco	Australia (New South Wales)	Arid	Grasslands	2 (1)	- (1)	Pancieria et al. 2014
Carman	Canada (Manitoba)	Cold	Croplands	1 (1)	- (-)	McNairn et al. 2015
Ngari	Tibet	Cold	Barren / sparse	- (1)	- (-)	Wen et al. 2014
Walnut Gulch	USA (Arizona)	Arid	Shrub open	3 (1)	- (-)	Keefer et al. 2008
Little Washita	USA (Oklahoma)	Temperate	Grasslands	3 (1)	2 (1)	Cosh et al. 2006
Fort Cobb	USA (Oklahoma)	Temperate	Grasslands	2 (1)	2 (1)	Cosh et al. 2014
Little River	USA (Georgia)	Temperate	Cropland / natural mosaic	1 (1)	1 (1)	Bosch et al. 2007
St Josephs	USA (Indiana)	Temperate	Croplands	1 (1)	- (-)	Heathman et al. 2012
South Fork	USA (Iowa)	Cold	Croplands	3 (1)	3 (1)	Coopersmith et al. 2015
Monte Buey	Argentina	Temperate	Croplands	1 (1)	- (-)	Thibeault et al. 2015
Tonzi Ranch	USA (California)	Temperate	Savannas woody	1 (1)	1 (1)	Clewley et al. 2017; Moghaddam et al. 2016
Kenaston	Canada (Saskatchewan)	Cold	Croplands	2 (1)	1 (1)	Rowlandson et al. 2015; Tetlock et al. 2019
Valencia	Spain	Cold	Savannas woody	1 (-)	- (-)	Juglea et al. 2010; Khodayar et al. 2019
Niger	Niger	Arid	Grassland	1 (1)	- (-)	Galle et al. 2018
Benin	Benin	Tropical	Savannas	1 (1)	- (-)	Galle et al. 2018
TxSON	USA (Texas)	Temperate	Grasslands	2 (1)	2 (1)	Caldwell et al. 2018
HOBE	Denmark	Temperate	Croplands	1 (1)	- (-)	Bircher et al. 2012; Jensen and Refsgaard 2018
All Sites				30 (18)	12 (8)	

Table 3. Soil moisture core validation site reference pixels used in the present assessment. The 33 km reference pixels are shown in boldface. See Table 2 for core validation site characteristics.

Site Name (Abbreviation)	Reference Pixel										
	ID	Latitude [degree]	Longitude [degree]	Horizont al Scale [km]	Depth of Deepest Sensor [m]	Number of Sensors (Surface Soil Moisture)			Number of Sensors (Root Zone Profiles)		
						Min.	Mean	Max.	Min.	Mean	Max.
REMEDHUS (RM)	03013302	41.29	-5.46	33	0.05	8	12.1	15	n/a	n/a	n/a
	03010903	41.42	-5.37	9	0.05	4	4.0	4	n/a	n/a	n/a
	03010908	41.32	-5.27	9	0.05	4	4.0	4	n/a	n/a	n/a
Reynolds Creek (RC)	04013302	43.19	-116.75	33	0.05	7	7.0	7	n/a	n/a	n/a
	04010907	43.19	-116.72	9	0.05	4	4.0	4	n/a	n/a	n/a
	04010910	43.09	-116.81	9	0.05	4	4.0	4	n/a	n/a	n/a
Yanco (YC)	07013301	-34.86	146.16	33	0.75	8	19.0	23	7	15.6	23
	07010902	-34.72	146.13	9	0.05	8	8.5	9	n/a	n/a	n/a
	07010916	-34.98	146.31	9	0.05	8	10.0	11	n/a	n/a	n/a
Carman (CR)	09013301	49.60	-97.98	33	0.05	8	17.9	20	n/a	n/a	n/a
	09010906	49.67	-97.98	9	0.05	8	9.9	11	n/a	n/a	n/a
Ngari (NG)	12033301	32.50	79.96	33	0.05	6	6.0	6	n/a	n/a	n/a
Walnut Gulch (WG)	16013302	31.75	-110.03	33	0.05	8	14.9	18	n/a	n/a	n/a
	16010906	31.72	-110.09	9	0.05	8	9.1	11	n/a	n/a	n/a
	16010907	31.72	-109.99	9	0.05	8	9.8	11	n/a	n/a	n/a
	16010913	31.83	-110.90	9	0.05	6	6.0	6	n/a	n/a	n/a
Little Washita (LW)	16023302	34.86	-98.08	33	0.45	8	10.4	12	8	8.9	12
	16020905	34.92	-98.23	9	0.05	4	4.0	4	n/a	n/a	n/a
	16020906	34.92	-98.14	9	0.45	4	4.0	4	4	4.0	4
	16020907	34.92	-98.04	9	0.45	4	4.0	4	4	4.0	4
Fort Cobb (FC)	16033302	35.38	-98.64	33	0.45	8	10.4	11	8	9.4	11
	16030911	35.38	-98.57	9	0.45	4	4.0	4	4	4.0	4
	16030916	35.29	-98.48	9	0.45	4	4.0	4	4	4.0	4
Little River (LR)	16043302	31.67	-83.60	33	0.30	8	17.2	19	8	15.7	18
	16040901	31.72	-83.73	9	0.30	8	8.0	8	6	6.2	8
St Josephs (SJ)	16063302	41.39	-85.01	33	0.05	8	8.3	9	n/a	n/a	n/a
	16060907	41.45	-84.97	9	0.05	7	7.0	7	n/a	n/a	n/a
South Fork (SF)	16073302	42.42	-93.41	33	0.50	8	16.6	19	8	11.8	16
	16070909	42.42	-93.53	9	0.50	4	4.0	4	4	4.0	4
	16070910	42.42	-93.44	9	0.50	4	4.0	4	4	4.0	4
	16070911	42.42	-93.35	9	0.50	4	4.0	4	4	4.0	4
Monte Buey (MB)	19023301	-32.91	-62.51	33	0.05	8	9.8	12	n/a	n/a	n/a
	19020902	-33.01	-62.49	9	0.05	5	5.0	5	n/a	n/a	n/a
Tonzi Ranch (TZ)	25013301	38.45	-120.95	33	0.40	8	12.8	20	8	14.0	10
	25010911	38.43	-120.95	9	0.40	8	14.4	26	8	18.0	11
Kenaston (KN)	27013301	51.47	-106.48	33	0.50	8	25.7	30	8	22.7	30
	27010910	51.39	-106.51	9	0.05	8	8.0	8	n/a	n/a	n/a
	27010911	51.39	-106.42	9	0.50	8	12.5	14	8	11.4	14
Valencia (VA)	41010906	39.57	-1.26	9	0.05	7	7.0	7	n/a	n/a	n/a
Niger (NI)	45013301	13.57	2.66	33	0.05	6	6.0	6	n/a	n/a	n/a
	45010902	13.57	2.66	9	0.05	4	4.0	4	n/a	n/a	n/a
Benin (BN)	45023301	9.83	1.73	33	0.05	7	7.0	7	n/a	n/a	n/a
	45020902	9.77	1.68	9	0.05	5	5.0	5	n/a	n/a	n/a
TxSON (TX)	48013301	30.35	-98.73	33	0.50	8	28.1	29	8	22.8	24
	48010902	30.43	-98.81	9	0.50	8	9.6	10	8	8.7	10
	48010911	30.28	-98.73	9	0.50	8	14.4	15	8	13.4	14
HOBE (HB)	67013301	55.97	9.10	33	0.05	8	11.2	15	n/a	n/a	n/a
	67010901	55.97	9.10	9	0.05	5	5.0	5	n/a	n/a	n/a

Across the reference pixels listed in Table 3, the average number of individual surface soil moisture sensors that contribute to a given 33 km reference pixel ranges between 6.0 and 28.1, with a mean value of 13.4. The corresponding number of sensor profiles for root zone soil moisture ranges between 8.9 and 22.8, with a mean value of 15.1. At the 9 km scale, 13 of the 31 reference pixels are based on just 4 individual sensor profiles, while most of the rest of the 9 km reference pixels consist of about 10 sensor profiles each. The mean number of surface soil moisture sensors per 9 km reference pixel is 6.7, and the corresponding number of root zone profiles is 7.1. The sampling density (sensors per unit area) is therefore higher for the 9 km reference pixels than for the 33 km reference pixels. Recall that Table 3 corrects a minor error in the average number of sensors reported in Table 3 of Reichle et al. (2021b); the averages shown here also apply to the Version 5 assessment of Reichle et al. (2021b).

For most reference pixels, individual sensor profiles occasionally drop out temporarily. If the sensor that drops out is installed in a particularly wet or a particularly dry location (relative to reference pixel average conditions), not having this sensor contribute to the reference pixel average will result in an artificial discontinuity in the time series of the reference pixel average soil moisture. In the assessment of Version 4 and earlier L4_SM products, this effect was mitigated only for reference pixels with 8 or fewer individual sensor profiles; for these reference pixels, quality-controlled in situ measurements from all contributing sensor profiles needed to be available for the computation of the reference pixel average.

As in the Version 5 assessment, the processing of the in situ measurements for the present Version 6 assessment includes an additional safeguard against discontinuities caused by temporary sensor dropout. In the revised processing used here, the time series from each individual sensor is first converted from volumetric soil moisture units into standard-normal deviates, based on the time series mean and variance of the measurements at the individual sensor. Next, a normalized reference pixel average time series is computed by averaging the standard-normal deviate time series from each individual sensor. Finally, the resulting normalized reference pixel average time series is converted back into volumetric units based on the reference pixel average of the soil moisture climatologies from the individual sensors. By averaging the measurements from the individual sensors in the normalized space, the reference pixel average time series in volumetric units is less sensitive to the dropping out of sensors that are installed in a particularly wet or dry location (relative to reference pixel average conditions).

Core site metrics are provided separately for the 9 km and 33 km reference pixels. Metrics are computed directly against the (reference pixel average) in situ measurements. Because the latter contain measurement error, we present the metrics as the mean *difference* (MD), RMS *difference* (RMSD), and unbiased RMS *difference* (ubRMSD), along with the correlation and anomaly correlation. Because of the in situ measurement error, the primary metrics of interest – that is, the RMSE and ubRMSE – are less than the RMSD and ubRMSD, respectively. Similarly, the (anomaly) correlation vs. the true soil moisture exceeds the (anomaly) correlation that is directly determined against the imperfect in situ measurements.

Summary metrics are obtained by averaging across the metrics from all individual reference pixels at the given scale. For the 9 km metrics, we first average each metric across the 9 km reference pixels within each site, separately for each site and weighted by the number of measurements that contribute to the metric at a given 9 km reference pixel. Second, we average the resulting individual site-average metrics across all sites. This approach gives equal weight to each site and differs from the straight average over all 9 km reference pixels that was used in earlier assessments (Reichle et al. 2015, 2016, 2017a), which somewhat arbitrarily gave more weight to sites that had more 9 km reference pixels. (We computed summary metrics using both methods and found the results to be close. That is, the conclusions remain the same regardless of how exactly the average metric is computed.)

Statistical uncertainty in the ubRMSD, R, and anomaly R metrics is estimated using 95% confidence intervals, which are computed at each site based on the number of samples in the time series (with a correction for temporal autocorrelation). We refer to changes in metrics as statistically significant whenever the confidence intervals do not overlap. It is important to keep in mind that the confidence intervals are

themselves uncertain and only provide practical guidance as to whether the skill differences may be meaningful. Statistical uncertainty estimates for the MD are not provided because the upscaling error is considerably larger for the bias than for the second-order metrics (Chen et al. 2019).

Finally, in situ measurements are used for validation only when the model (or assimilation) estimates indicate non-frozen and snow-free conditions (Reichle et al. 2015, their section 6.2.1). Because the soil temperature and snow states differ somewhat between the L4_SM product and the model-only (Open Loop) simulation examined here, in situ measurements were used only if both datasets indicate favorable validation conditions. This cross-masking ensures that the metrics are directly comparable across both datasets.

6.2.2 Results

In this section, we investigate the summary metrics for soil moisture at the core validation sites. These metrics are illustrated in Figures 9 and 10. Probably the most important result is that the average ubRMSE for surface and root zone soil moisture for the Version 6 L4_SM product at both the 9 km and the 33 km scales meets the accuracy requirement (section 4) of $\text{ubRMSE} \leq 0.04 \text{ m}^3 \text{ m}^{-3}$.

For a more in-depth analysis, we first compare the skill of the Version 6 (Vv6032) L4_SM product to that of the Version 5 (Vv5030) product. There is no discernible difference between the two versions in the average ubRMSD values for both the surface and the root zone soil moisture across the 9 km and the 33 km reference pixels (Figure 9a). For both versions, the ubRMSD at the 9 km (33 km) scale is 0.040 (0.037) $\text{m}^3 \text{ m}^{-3}$ for surface soil moisture and 0.027 (0.024) $\text{m}^3 \text{ m}^{-3}$ for root zone soil moisture. The Version 6 product has slightly better correlation and anomaly correlation skill for surface soil moisture than the Version 5 product, although neither change is statistically significant at the 5% level, as indicated by the overlapping 95% confidence intervals (Figure 10). There is no discernible difference between the versions for the root zone soil moisture (anomaly) correlation. On the other hand, the Version 6 product has a slightly larger average MD for surface soil moisture and a somewhat larger average absolute MD for root zone soil moisture (Figure 9b,c).

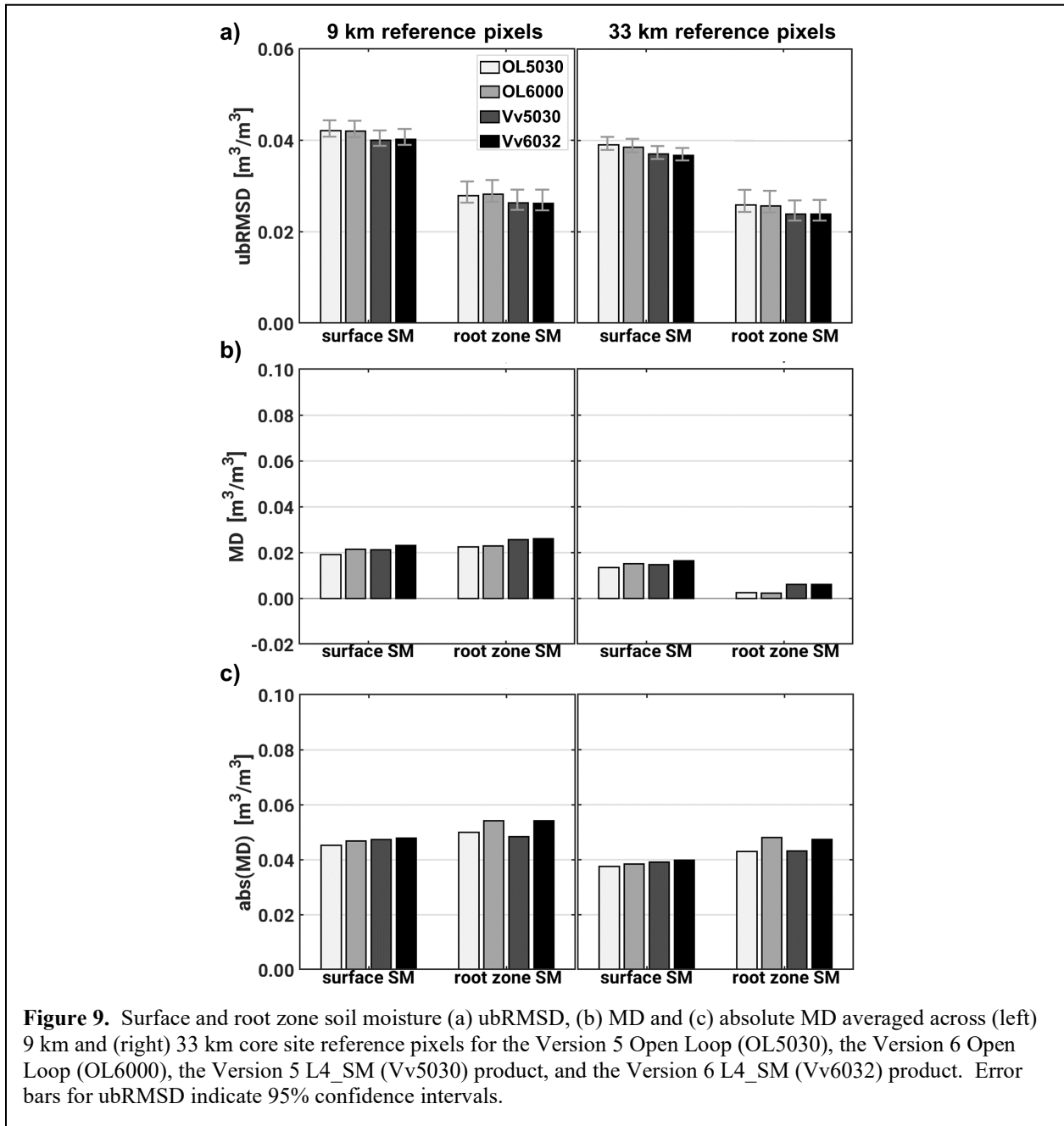
It is not surprising that the skill of the Version 5 and 6 products is so similar. Eleven of the 19 core validation sites are in North America, where both L4_SM versions use the same daily precipitation corrections (based on the CPCU product) and have only minor differences, including the band for high-latitude tapering, the reference precipitation climatology (Figure 3c), and the years of data used to compute the Tb scaling parameters (section 5.3). A closer inspection of the soil moisture performance metrics for each site (Tables A1-A4) confirms that the largest performance differences between the L4_SM versions are at the core validation sites in Africa (Niger, Benin) and Tibet (Ngari), where the CPCU precipitation product is either not used (Africa) or based on a sparse gauge network (Tibet; Reichle et al. 2021b, their Figure 1c).

Next, we compare the skill of the L4_SM (Vv6032) product to that of the model-only Open Loop (OL6000) estimates. For the ubRMSD metrics at the 9 km and the 33 km scales (Figure 9a), the surface and root zone soil moisture skill of the Version 5 product slightly exceeds that of OL6000, demonstrating the positive impact of assimilating SMAP Tb observations. For example, at the 9 km scale the surface soil moisture ubRMSD is 0.040 $\text{m}^3 \text{ m}^{-3}$ for Vv6032 surface soil moisture and 0.042 $\text{m}^3 \text{ m}^{-3}$ for OL6000. However, the ubRMSD improvement of the L4_SM product over the model-only simulation is not statistically significant at the 5% level.

When factoring in the measurement error of the reference pixel-average in situ observations, which Chen et al. (2019) estimate to be at least $\sim 0.01\text{-}0.02 \text{ m}^3 \text{ m}^{-3}$ (in terms of ubRMSE), the Version 6 L4_SM product clearly meets the above-mentioned accuracy requirement.

The average MD (Figure 9b) and average absolute MD (Figure 9c) values for surface and root zone soil moisture tend to be slightly worse for the Version 6 product than for the model-only (OL6000) estimates, but these differences are much smaller than the upscaling uncertainty (Chen et al. 2019).

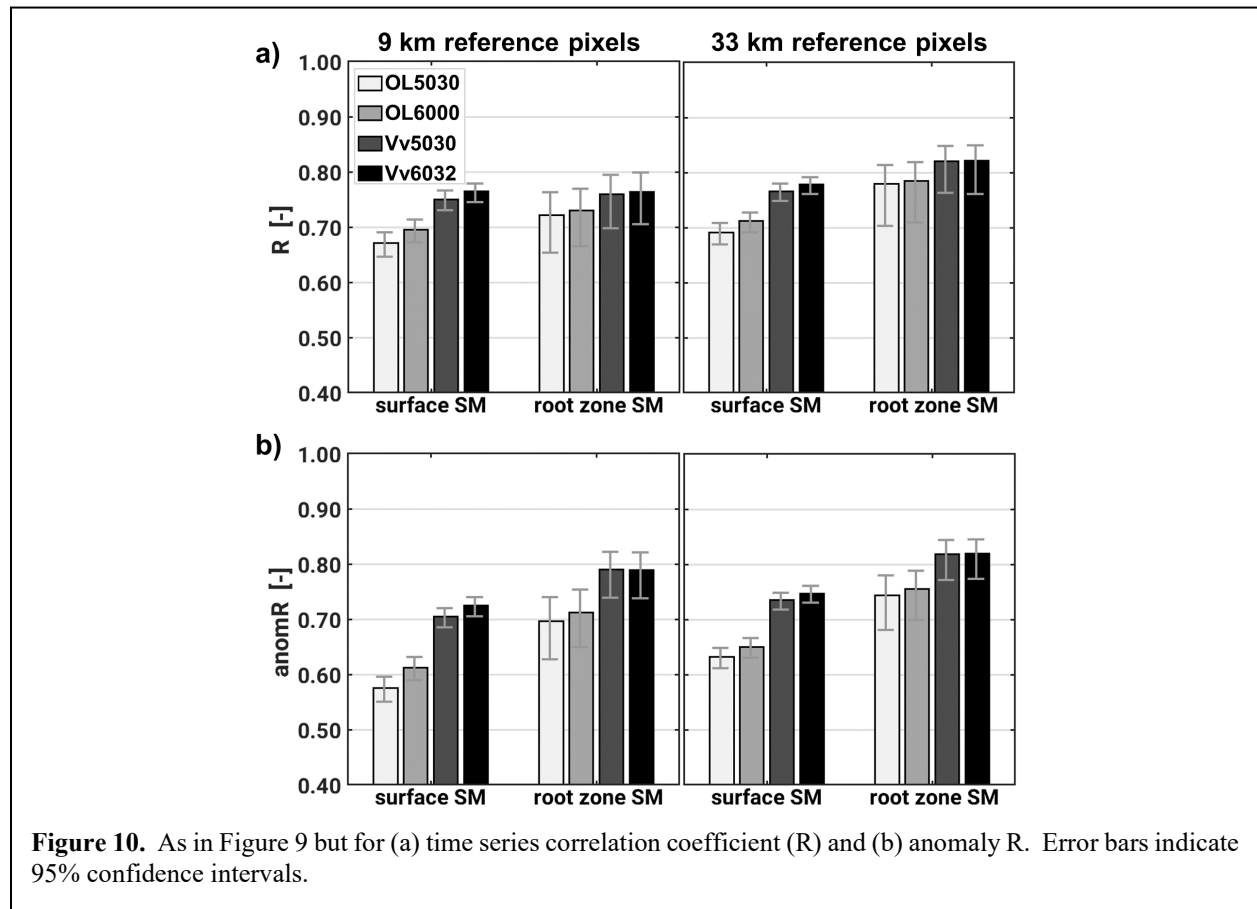
Across-the-board improvements are seen in the L4_SM soil moisture over the model-only Open Loop estimates in terms of R (Figure 10a) and anomaly R (Figure 10b) skill. The improvements range from 0.03 to 0.11 and are statistically significant for surface soil moisture at both the 9 km and 33 km scales.



Next, we compare the skill values at 9 km to those at 33 km. The L4_SM and Open Loop skill values at 33 km are better for all metrics than the corresponding values at 9 km (Figures 9 and 10), which is consistent with the fact that the model forcing data and the assimilated SMAP Tb observations are all at resolutions of about 30 km or greater. The information used to downscale the assimilated information primarily stems from the land model parameters, which are at the finer, 9 km resolution; this information is expected to have a modest impact at best. It is therefore not a surprise that the estimates at 33 km are more skillful than those at 9 km.

Finally, we compare the skill of the surface estimates to that of the root zone estimates. Across both scales, for nearly all metrics and for both the L4_SM and Open Loop estimates, the skill of the root zone soil moisture estimates is better than that of the surface estimates. This result makes sense because there is much more variability in surface soil moisture. It is important to keep in mind, however, that the root zone metrics are computed from only a subset of the sites used for the computation of the surface metrics.

For completeness, Tables A5-A8 list the ubRMSD, MD, R, and anomaly R metrics vs. core site in situ measurements for surface soil temperature at 6am and 6pm local time and for the 9 km and 33 km scales. The metrics are shown for the both the Version 5 and Version 6 estimates from the Open Loops and the L4_SM products. There are no meaningful differences in the average metrics between the Open Loop and L4_SM estimates or between the two versions. See Reichle et al. (2018b) for additional discussion of surface soil temperature skill. For reference, Table A9 lists the Version 6 L4_SM metrics categorized by land cover, as shown for Version 5 in Table XII of Colliander et al. (2021).



6.3 Sparse Networks

This section provides an assessment of the L4_SM soil moisture estimates using in situ measurements from additional regional and continental-scale networks. Unlike the SMAP core sites, the networks used in this subsection usually have just one sensor (or profile of sensors) located within a given 9 km EASEv2 grid cell; hereinafter, we refer to these networks as “sparse” networks (Colliander et al. 2021). The point-scale measurements from sparse networks are, of course, generally not representative of the grid cell average conditions estimated by the L4_SM algorithm. On the other hand, sparse networks offer in situ measurements in a larger variety of environments and provide data quasi-operationally with very short latency. See Reichle et al. (2015) for further discussion of the advantages and limitations of using sparse networks in the L4_SM validation process.

6.3.1 Method

The in situ measurements used here are identical to those used in the Version 5 assessment report (Reichle et al. 2021b). This subsection is a lightly edited version of the corresponding section 6.2.2 of Reichle et al. (2021b).

This assessment report focuses on metrics obtained from a direct comparison of the L4_SM product to in situ measurements, that is, metrics derived without using triple collocation approaches that attempt to correct for errors in the in situ measurements (Chen et al. 2016; Gruber et al. 2016). The values of the time series correlation metrics provided here are thus lower than those that would be obtained with the aid of triple collocation, and they are therefore conservative estimates of the true skill. Note also that the *relative* performance of the products under investigation does not depend on the use of triple collocation approaches (Dong et al. 2020).

The skill of the L4_SM estimates was computed using all available in situ measurements (after quality control) at 3-hourly time steps, and this skill was compared to that of the model-only Open Loop estimates. For sparse networks, we used the same requirements for the minimum number of data values as for core validation sites (section 6.2). Note that quality control generally excludes in situ measurements when the ground is frozen (see Reichle et al. 2015, Appendix C). Instantaneous L4_SM data from the “aup” Collection and corresponding Open Loop data were taken directly from the standard 9 km EASEv2 grid cell that includes the sensor location (that is, the data product estimates are not interpolated bilinearly or otherwise to the precise location of the in situ sensor locations). Metrics were computed for surface and root zone soil moisture against in situ measurements from the USDA Soil Climate Analysis Network (SCAN), the NOAA US Climate Reference Network (USCRN), the Oklahoma (OK) Mesonet, the OZNet-Murrumbidgee network, and the SMOSMania network (Table 4). The average metrics were computed based on a clustering algorithm that assigns the weights given to each location based on the density of sites in the surrounding region (De Lannoy and Reichle 2016). As for the core site metrics, statistical uncertainty estimates in the form of 95% confidence intervals are provided for the second-order metrics (ubRMSD, R, and anomaly R) but not for the MD metrics because the upscaling error for the latter is considerably larger (Chen et al. 2019).

Measurements used for L4_SM validation cover most of the contiguous United States (SCAN, USCRN, OK Mesonet), parts of the Murrumbidgee basin in Australia (OZNet), and an area in southwestern France (SMOSMania). The in situ measurements from the sparse network sites were subjected to extensive automated and manual quality control procedures by the L4_SM team following Liu et al. (2011), which removed spikes, temporal inhomogeneities, oscillations, and other artifacts that are commonly seen in these automated measurements. In our experience, the manual inspection and quality control is an indispensable step in the process. Table 4 also lists the number of sites with sufficient data after quality control.

Table 4. Overview of sparse networks, with indication of the sensor depths, number of sites, and data periods used here. Values in parentheses indicate the number of sites for which the anomaly R metric was computed. The anomaly R metric was only available for sites with sufficient data to compute a seasonally varying climatology. Count of USCRN (OK Mesonet) sites includes 4 (1) site(s) with undetermined IGBP land cover classification.

Network	Region	Sensor Depths (m)	Number of Sites				Period (MM/DD/YYYY)	Reference
			Surface		Root Zone			
SCAN	USA	0.05, 0.10, 0.20, 0.50	135	(134)	109	(107)	04/01/2015 - 03/31/2021	Schaefer et al. 2007
USCRN	USA	0.05, 0.10, 0.20, 0.50	111	(111)	78	(76)	04/01/2015 - 03/31/2021	Bell et al. 2013; Diamond et al. 2013
OK Mesonet	Okla. USA	0.05, 0.25, 0.60	118	(116)	77	(76)	04/01/2015 - 05/01/2018	McPherson et al. 2007
OZNet	Australia	0.04, 0.45	43	(43)	19	(19)	04/01/2015 - 09/01/2020	Smith et al. 2012
SMOSMania	France	0.05, 0.20	21	(21)	21	(21)	04/01/2015 - 12/31/2019	Calvet et al. 2007
All Networks			428	(425)	304	(299)		

A total of 428 sites provided surface soil moisture measurements, and 304 provided root zone soil moisture measurements. Most of the sites are in the continental United States, including more than 100 each in the USCRN and SCAN networks, and another 118 sites in Oklahoma alone from the OK Mesonet. The OZNet network contributes 43 sites with surface soil moisture measurements, of which 19 sites also provide root zone measurements. Finally, 21 sites with surface and root zone soil moisture measurements were used from the SMOSMania network. Three (five) sites do not have sufficient numbers of measurements for the computation of the surface (root zone) soil moisture climatology that is needed to determine the anomaly R skill.

Table 4 also lists the sensor depths that were used to compute the in situ root zone soil moisture. As with the core validation sites, vertical averages for SCAN, USCRN, and OK Mesonet are weighted by the spacing of the sensor depths within the 0-100 cm layer corresponding to the L4_SM estimates, and the average is only computed if all sensors within a given profile provide measurements after quality control. For SCAN and USCRN sites, some measurements at 100 cm depth are available, but these deeper layer measurements are not of the quality and quantity required for L4_SM validation and are therefore not used here. For OZNet and SMOSMania, in situ root zone soil moisture is given by the measurements at the 45 cm and 20 cm depth, respectively; that is, no vertical average is computed.

6.3.2 Results

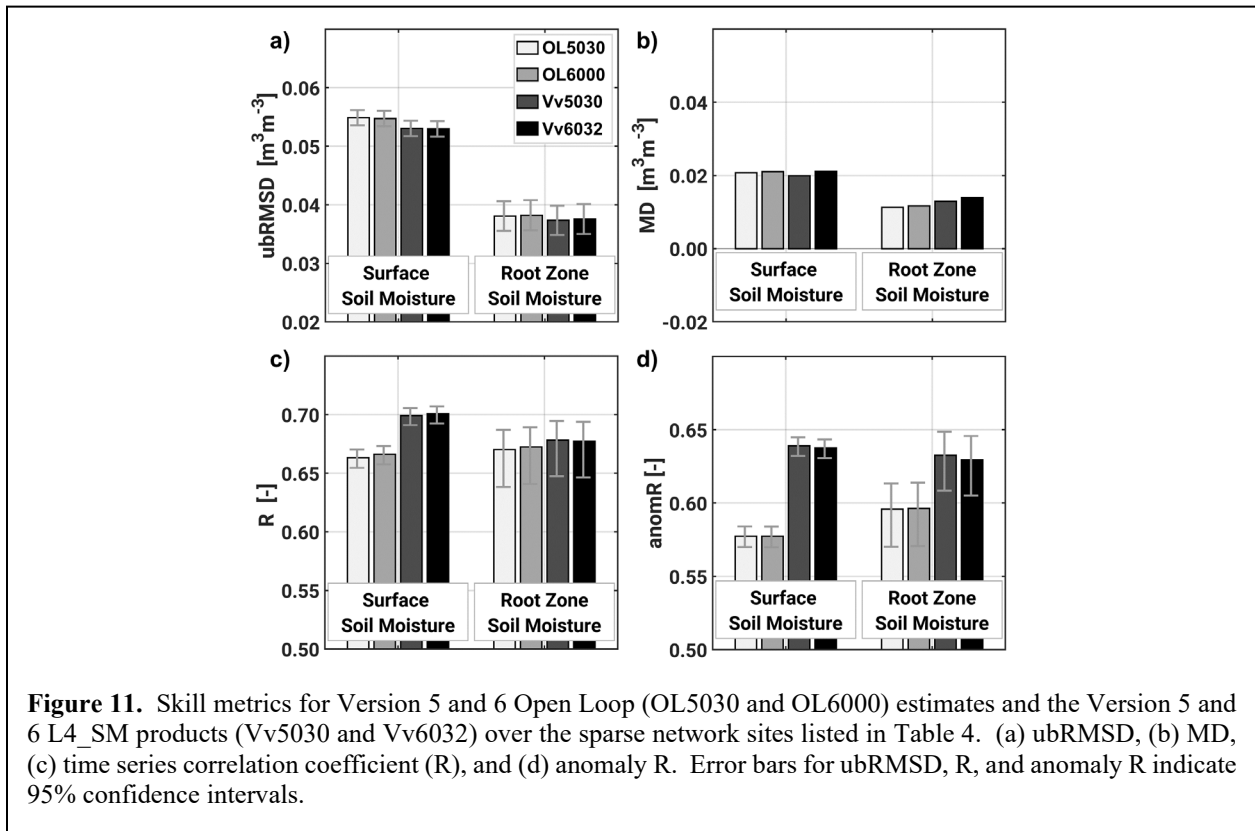
Figure 11 shows the Open Loop and L4_SM metrics for Versions 5 and 6 averaged across all sparse network sites. The two L4_SM versions (Vv5030, Vv6032) have nearly identical skill metrics. As with the core site validation, this is not surprising because most of the sparse network sites are in North America, where the Version 5 and 6 modeling systems both use CPCU-based daily precipitation corrections and have only minor differences as discussed above.

Compared to the Open Loop estimates, both L4_SM product versions have generally lower ubRMSD and higher R and anomaly R values, with improvements that are statistically significant at the 5% level for the surface soil moisture correlation metrics (Figure 11). This again demonstrates the additional information contributed by the assimilation of the SMAP Tb observations in the L4_SM system.

As with the core site validation results, the ubRMSD and MD values vs. the sparse network measurements are smaller (better) for root zone soil moisture than for surface soil moisture (Figure 11), which again reflects the fact that root zone soil moisture generally varies less in time than surface soil moisture.

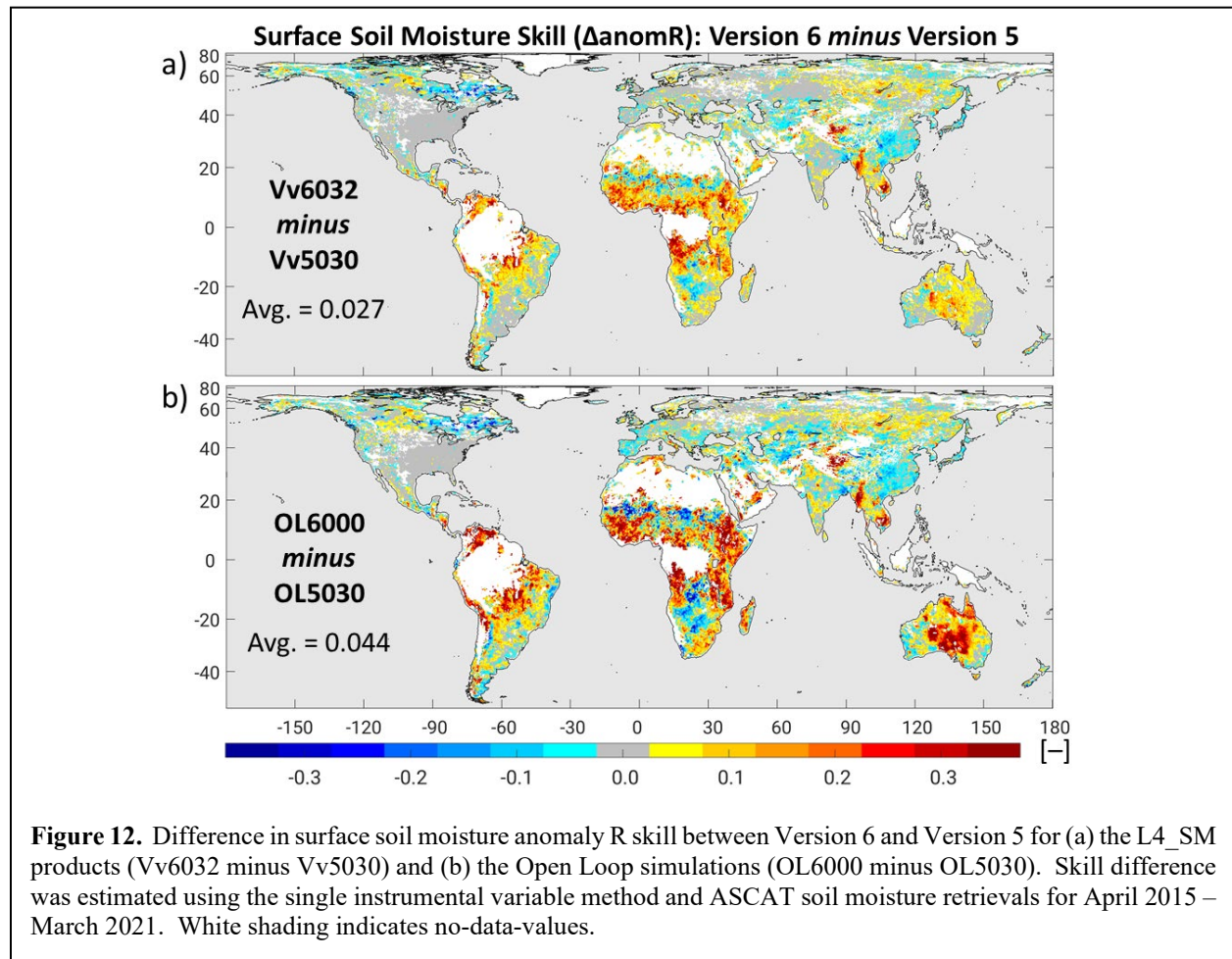
Like the core sites, the sparse network sites are in regions with high-quality precipitation measurements, owing to the generally dense gauge network in CONUS, Western Europe, and southeastern Australia (Reichle et al. 2021a, their Figure 1c). Larger improvements from the assimilation of SMAP observations are generally seen where the precipitation forcing is based on fewer gauges (section 6.4).

Overall, the evaluation of skill for the sparse network sites yields results that are very similar to those obtained for the core validation sites. The beneficial impact of assimilating SMAP Tb observations is greatest for surface soil moisture, with smaller improvements in root zone soil moisture estimates. Finally, it is important to keep in mind that the skill metrics presented here underestimate the true skill because these metrics are based on a direct comparison against in situ measurements (which are subject to error). Therefore, the sparse network ubRMSD values suggest that the L4_SM estimates would meet the formal accuracy requirement across a very wide variety of surface conditions, beyond those that are covered by the relatively few core validation sites that have been available to date for formal verification of the accuracy requirement. One caveat, however, is that the sparse network results do not provide an entirely independent validation because SCAN and USCRN measurements were used to calibrate an earlier version (NRv7.2) of the model (Reichle et al. 2018b). Nevertheless, the sparse network results provide additional confidence in the conclusions drawn from the core validation site comparisons.



6.4 Satellite Soil Moisture Retrievals

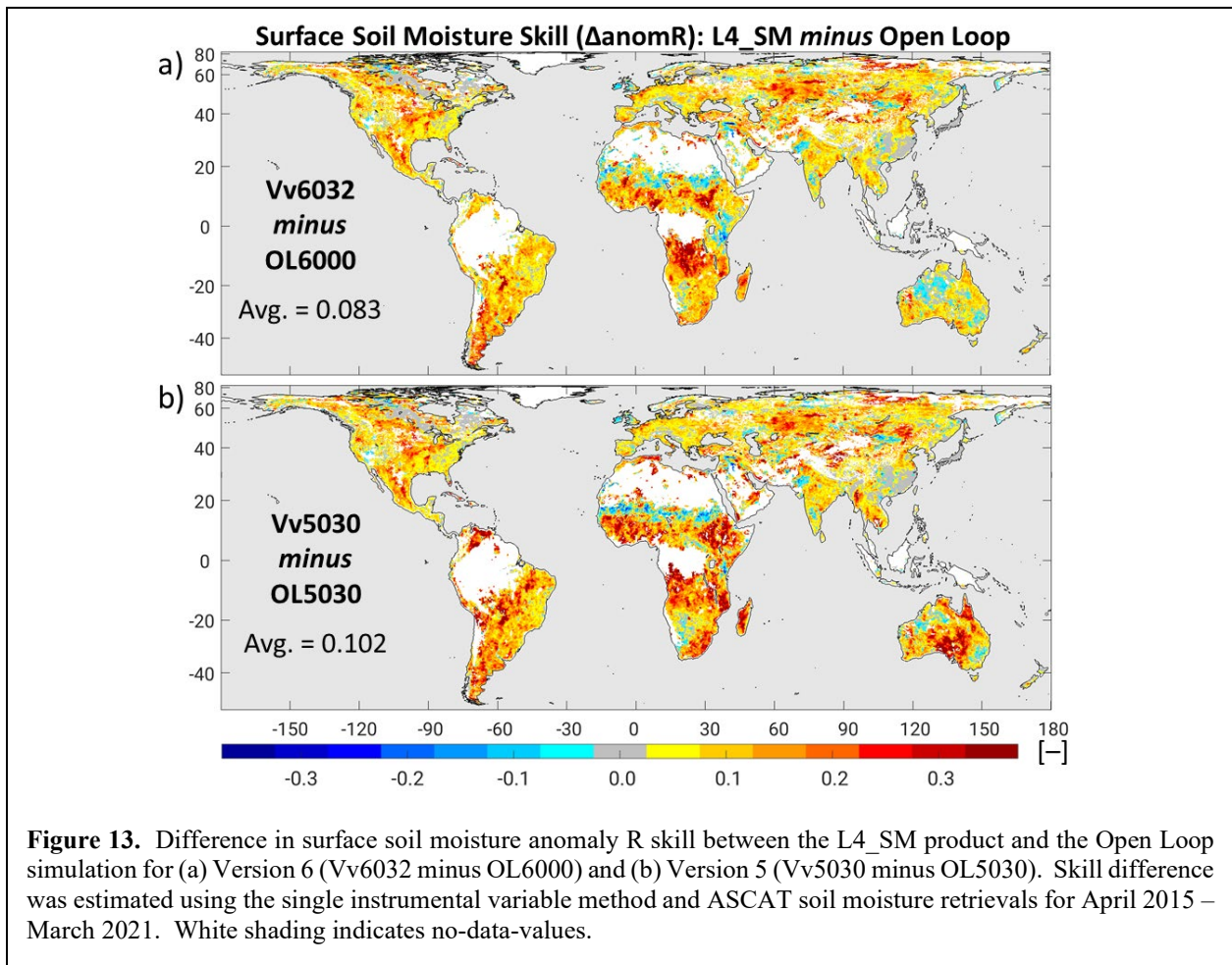
Reichle et al. (2021a) quantified the contribution of the SMAP Tb analysis to the anomaly time series correlation skill of the L4_SM surface soil moisture based on the instrumental variable (IV) method and independent soil moisture retrievals from the Advanced Scatterometer (ASCAT; Wagner et al. 2013), an active microwave (radar) instrument. In a nutshell, the IV method obtains the difference in skill (vs. the unknown true soil moisture) between the L4_SM and model-only estimates through the respective sample correlation skill values vs. the independent ASCAT satellite observations. This ASCAT-based IV approach was validated at the SMAP core validation sites using the grid cell-scale in situ measurements (Reichle et al. 2021a, their Figure 4). Their findings apply to the Version 4 L4_SM product.



Here, we apply the IV approach to determine the skill differences between the L4_SM products and the Open Loop simulations of Versions 5 and 6 using ASCAT soil moisture retrievals for April 2015 to March 2021. Figure 12a shows the surface soil moisture anomaly R difference between the Version 6 and Version 5 L4_SM products. In the global average, the anomaly R skill in Version 6 exceeds that of Version 5 by 0.03. The improvements are concentrated in the Southern Hemisphere, with improvements up to 0.3 seen in the regions surrounding the tropical rainforests of South America and Africa. The skill improvements are also considerable in central Australia as well as in Myanmar and Vietnam. The skill

improvements in these regions are not surprising. In Africa, the Version 5 product uses only uncorrected (albeit climatologically rescaled) precipitation from the GEOS Forward Processing (FP) weather analysis (Lucchesi 2018; Reichle et al. 2018b, 2019). The use of IMERG-based precipitation corrections there clearly results in a net increase in the soil moisture skill. The strong improvements in central Australia and Myanmar are also expected, given the problems with the CPCU precipitation product in these regions (Reichle et al. 2017c, 2021a). A modest degradation in the surface soil moisture anomaly R skill is seen in portions of southern Africa and the northern Sahel, China, and northeastern Canada (Figure 12a), suggesting that in these regions the gauge-based CPCU precipitation is more skillful than the IMERG-Final precipitation at sub-monthly time scales.

The anomaly R skill differences for the Version 6 and Version 5 Open Loop simulations are shown in Figure 12b; these Open Loop skill differences are an amplified version of the skill differences seen in the L4_SM product (Figure 12a), with a global average anomaly R difference of 0.04 and skill differences greater than 0.3 in many regions. This is particularly true for central Australia. Here, the considerably worse skill in OL5030 is caused by the very poor quality of the CPCU precipitation data there. The assimilation of SMAP Tb observations in Vv5030 makes up for most of the poor skill caused by the CPCU errors.



Stark contrasts between the Version 5 and 6 systems can also be seen in the improvement of the L4_SM skill over that of the corresponding Open Loop simulation for the two versions (Figure 13). In Version 5, the assimilation of SMAP Tb observations greatly improves the Vv5030 skill in central Australia (Figure 13b); again, the Vv5030 skill here is depressed because of the errors in the CPCU precipitation used in the Version 5 modeling system. In Version 6, the skill improvement from the SMAP Tb assimilation is much smaller in central Australia (Figure 13a), which shows that the IMERG-based precipitation corrections in Version 6 have considerably improved the skill of the Version 6 modeling system there. In the global average, the assimilation of the SMAP Tb observations improves the surface soil moisture anomaly R skill by 0.08 in Version 6, down from an improvement by 0.10 in Version 5, which again reflects the improvements in the Version 6 modeling system (Figure 12b).

6.5 Data Assimilation Diagnostics

This section provides an evaluation of the L4_SM data assimilation diagnostics, including the statistics of the observation-minus-forecast (O-F) Tb residuals, the observation-minus-analysis (O-A) residuals, and the analysis increments. Because the L4_SM algorithm assimilates Tb observations, the O-F and O-A diagnostics are in terms of brightness temperature (that is, in “observation space”). The analysis increments are, strictly speaking, in the space of the Catchment model prognostic variables that make up the “state vector”, including the “root zone excess”, “surface excess”, and “top-layer ground heat content” (Reichle et al. 2014b). For the discussion below, the soil moisture increments have been converted into equivalent volumetric soil moisture content in units of $\text{m}^3 \text{m}^{-3}$ and into water flux terms in units of mm d^{-1} .

A key element of the analysis update is the downscaling and inversion of the observational information from the 36 km grid of the assimilated Tb observations into the modeled geophysical variables on the 9 km grid, based on the simulated error characteristics, which vary dynamically and spatially. An example and illustration of a single analysis update can be found in Reichle et al. (2017b, their section 3b).

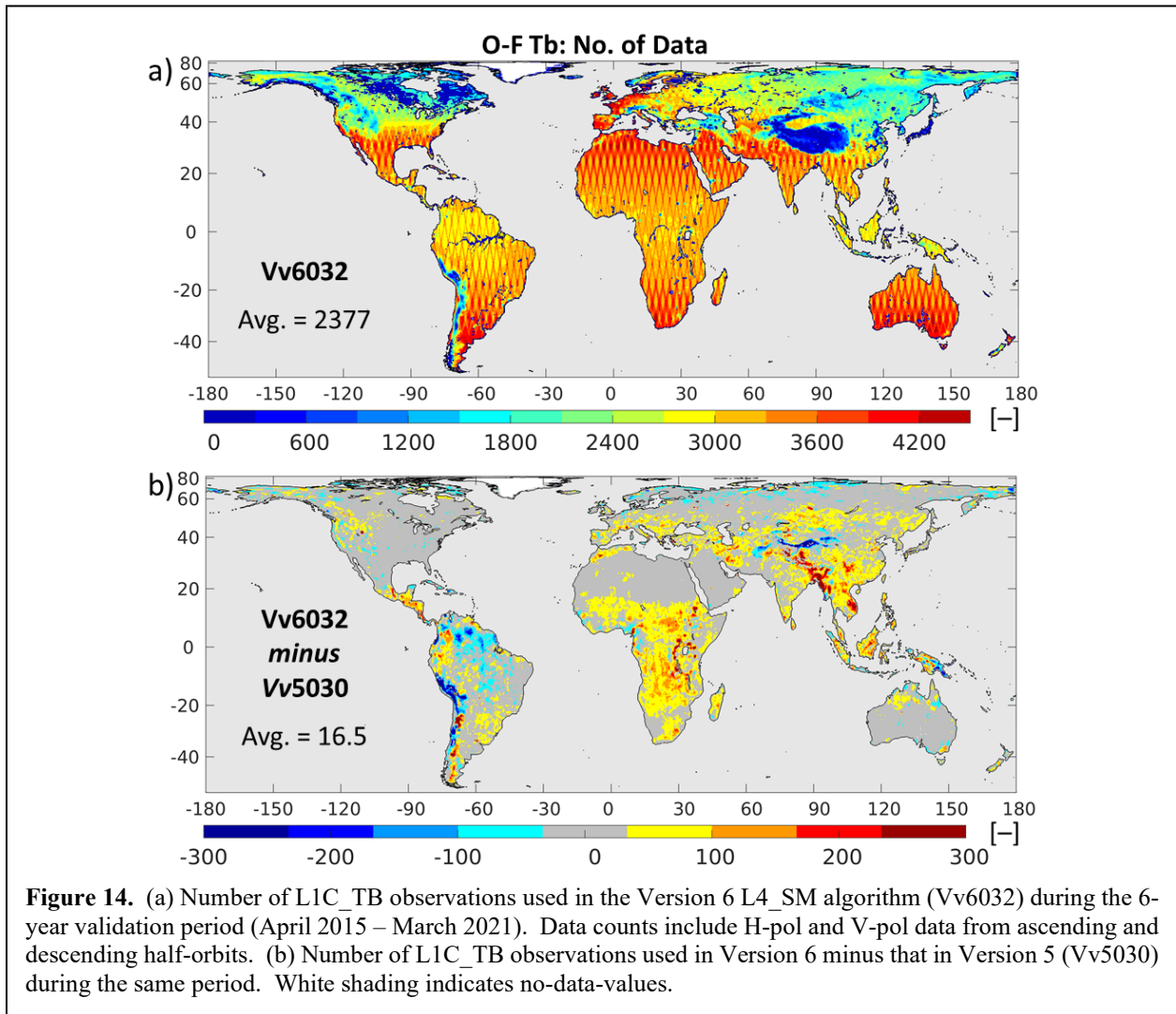
6.5.1 Observation-Minus-Forecast Residuals

Figure 14a shows the total number of L1C_TB observations that were assimilated at each grid cell in Version 5 during the assessment period (April 2015 – March 2021). This count includes H- and V-pol observations from ascending and descending orbits. The average data count (per 36 km grid cell) across the globe is approximately 2,377 for the 6-year (2,192-day) period. Few or no SMAP Tb observations are assimilated in high-elevation and mountainous areas (including the Rocky Mountains, the Andes, the Himalayas, and Tibet), in the vicinity of lakes (such as in northern Canada), and next to major rivers (including the Amazon and the Congo). In the high latitudes, the much shorter warm (unfrozen) season also results in lower counts of assimilated Tb observations, although this is somewhat mitigated by SMAP’s polar orbit, which results in more frequent revisit times there. The remaining gaps in coverage might reflect a lack of sufficient numbers of SMAP observations to provide the required climatological information for the computation of the (seasonally varying) Tb scaling parameters during the times of the year when conditions are suitable for a soil moisture analysis. Note, however, that the L4_SM product provides soil moisture estimates everywhere, even if in some regions the L4_SM estimates are not based on the assimilation of SMAP observations and rely only on the information in the model and forcing data.

In the global average, the count of assimilated observations for Version 6 increased slightly, by 16.5 per 36 km grid cell (~0.7%), from that of Version 5 (Figure 14b). There is a modest increase across much of Africa (except for the Sahara Desert) and southeast Asia. Larger increases of up to several hundred additional assimilated observations are seen in Myanmar, Vietnam, and pockets of the Southern Andes. In contrast, in the central Andes and parts of southern Venezuela, the assimilated observations count decreased by up to several hundred. The primary reason for these differences is the change in the precipitation forcing

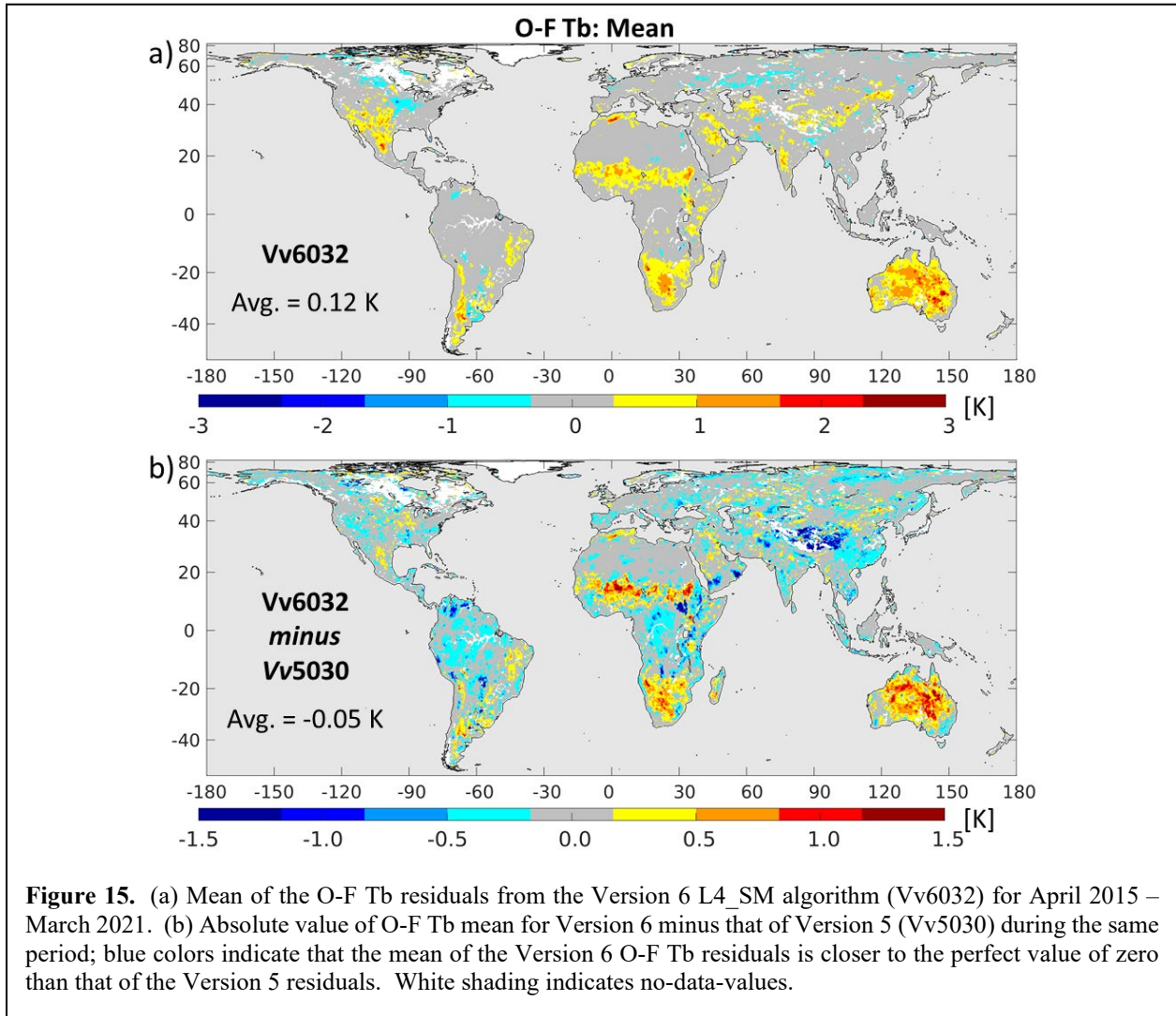
and its impact on the model-based quality control steps of the L4_SM algorithm. Specifically, Tb observations are not assimilated in the L4_SM algorithm if the precipitation rate exceeds 50 mm d^{-1} in the hour preceding the Tb analysis. This precipitation threshold is a crude detector of excessive, temporary ponding of rainwater at the surface during very heavy rain events. For the most part, the regions where the mean precipitation rate decreased from Version 5 to Version 6 of L4_SM (Figure 3c) match those where the number of assimilated Tb observations increased (Figure 14b), and the regions where the mean precipitation rate increased match those where the assimilated Tb count decreased. (Note that the switch from CPCU-based to IMERG-based daily precipitation corrections changes the entire probability distribution function of the L4_SM hourly precipitation forcing, not just the long-term mean precipitation rate.)

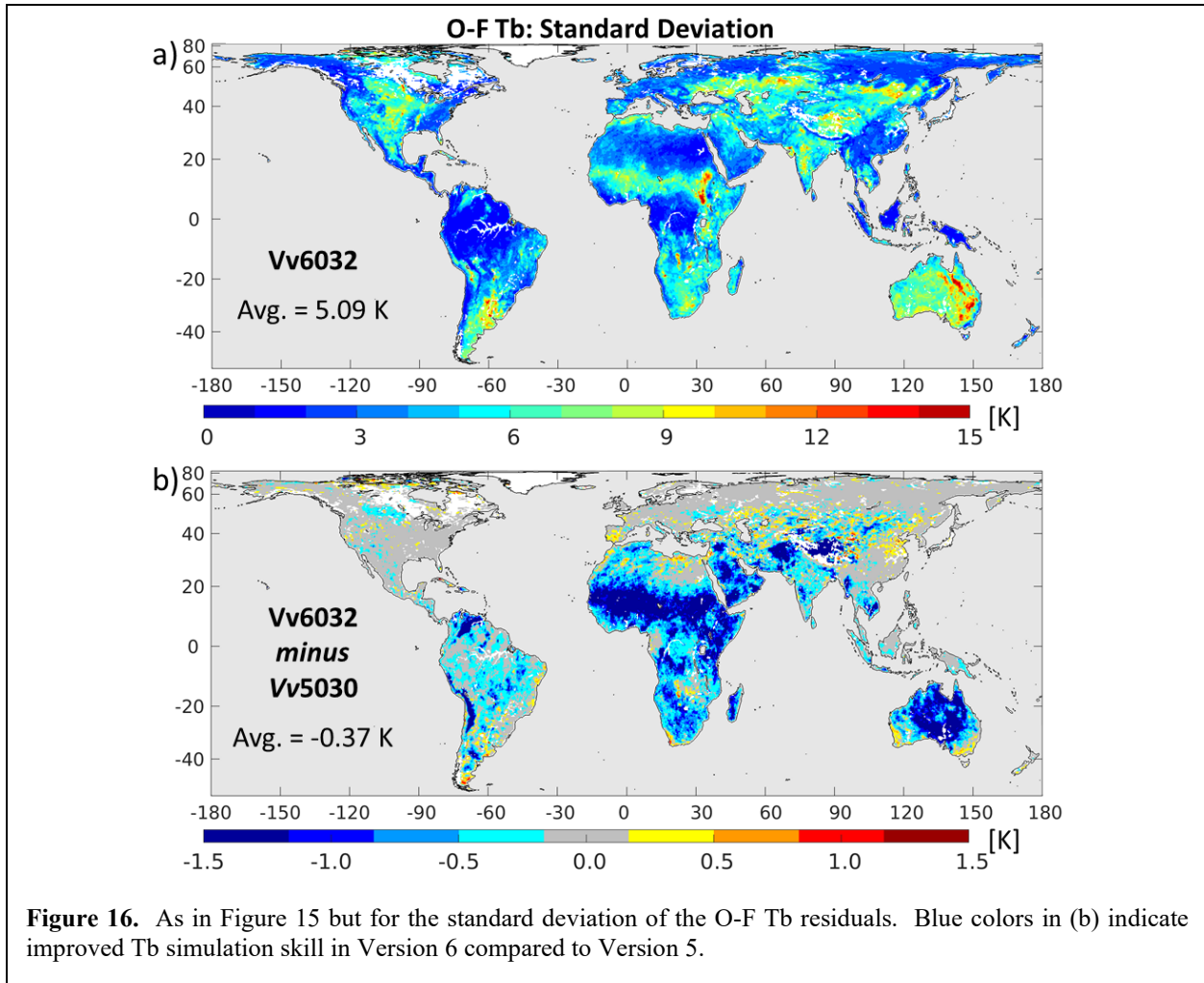
Some of the differences in the assimilated observations count between the L4_SM versions (Figure 14b) are likely related to indirect impacts of the precipitation changes on the model-based Tb quality control. Precipitation differences also cause differences in simulated snow mass (Figure 8) and soil temperature (via both snow melt and the latent heat flux; Figure 6), which are used to screen for snow-covered or frozen soil conditions.



The major (science) version of the assimilated L1C_TB observations has not changed between Versions 5 and 6 of L4_SM (section 5.2). The few changes between the two L4_SM versions in the minor processing version (or CRID) of the assimilated L1C_TB granules play at most a minor role in explaining the differences in the count of the assimilated SMAP Tb observations (Figure 14b).

Next, Figure 15a shows the global distribution of the time series mean of the O-F Tb residuals for Version 6. The time mean values of the O-F Tb residuals are typically small and mostly range from -3 to 3 K, with an overall bias of just 0.12 K and a mean absolute bias of just 0.24 K. Compared to Version 5, the global average of the absolute mean O-F Tb residuals decreased slightly (by 0.05 K), albeit with regional differences of up to ± 1.5 K (Figure 15b). The mean O-F Tb residuals in Version 6 are closer to the perfect value of zero in much of tropical South America, central Africa, and China. They are closer to zero in Version 5 in the Sahel, southern Africa, and most of Australia. The small degradation in the Version 6 algorithm calibration in the latter regions may be related to the continued use in Version 6 of microwave radiative transfer model parameters that were calibrated for the Version 5 modeling system, which cannot be fully compensated by the Version 6 Tb scaling parameters.



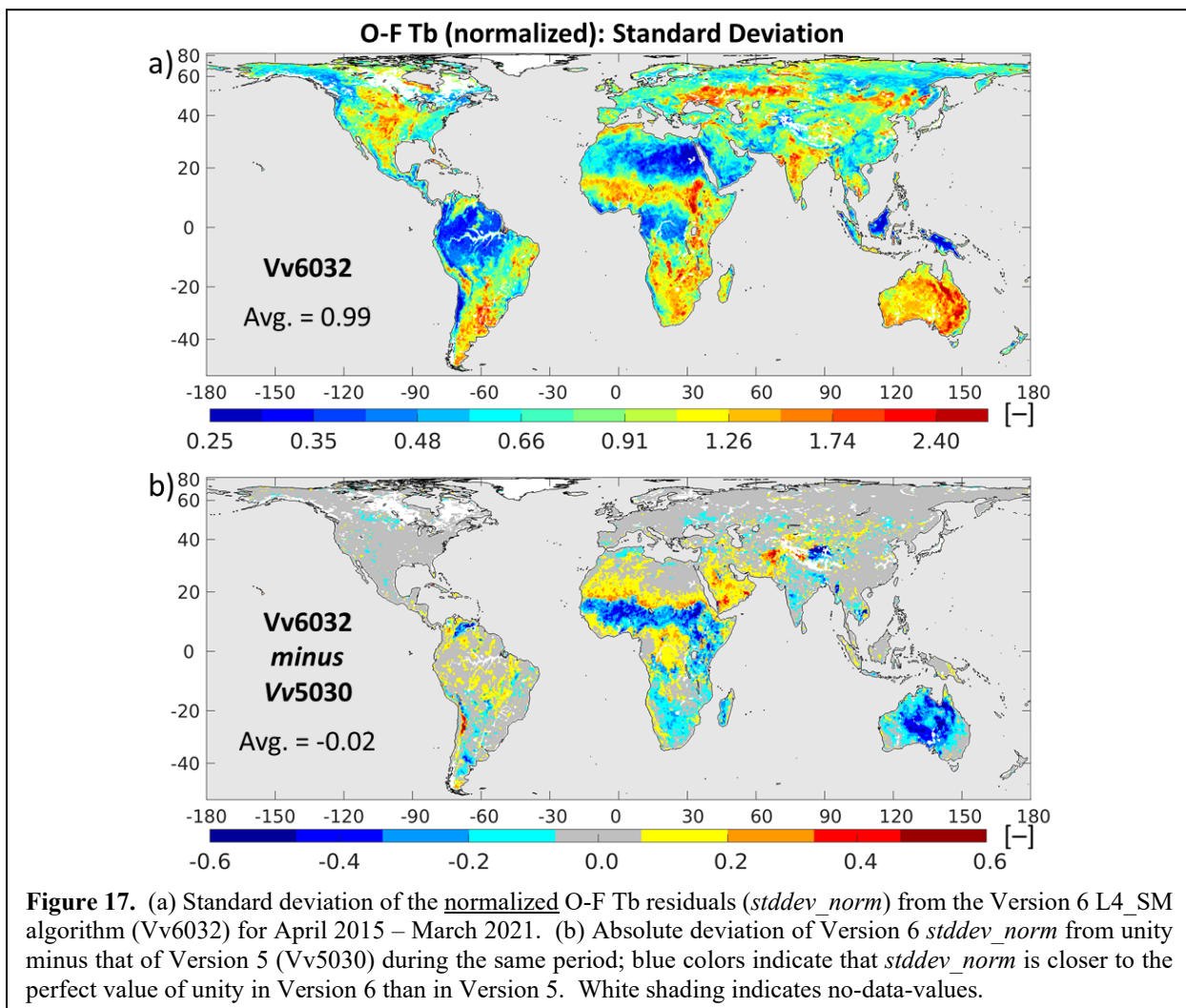


The time series standard deviation of the O-F Tb residuals ranges from a few Kelvins to around 15 K in a few small regions (Figure 16a). Higher values are found in central North America, southern South America, southern Africa, the Sahel, central Asia, India, and Australia. These regions have sparse or modest vegetation cover and typically exhibit strong variability in soil moisture conditions. The O-F Tb residuals are generally smallest in more densely vegetated regions, including the eastern United States, the Amazon basin, and tropical Africa. Small values are also found in the high latitudes, including Alaska and Siberia, and in the Sahara Desert. The global (spatial) average of the O-F Tb standard deviation is just 5.1 K in Version 6, compared to 5.5 K in Version 5. The Version 6 modeling system is clearly better able to predict the observed Tb just prior to each analysis, particularly across much of Africa, the Arabian Peninsula, and Australia but also in parts of South America and central Asia (Figure 16b). These considerable improvements in the Tb simulation skill of Version 6 are consistent with the improvements in the surface soil moisture anomaly correlation skill, which were derived independently (Figure 12). Both results reflect the improved, primarily IMERG-based precipitation forcing of Version 6 compared to the CPCU-based precipitation of Version 5. The spatially averaged time series standard deviation of the Tb O-A residuals is 3.3 K in Version 6, which is reduced by 0.2 K from that of the Version 5 system (not shown).

Finally, Figure 17a shows the standard deviation of the normalized O-F Tb residuals (*stddev_norm*), which measures the consistency between the simulated errors and the actual errors. Specifically, the O-F Tb residuals are normalized with the standard deviation of their expected total error, which is the sum (in a

covariance sense) of the error in the observations (including instrument errors and errors of representativeness) and the error in the Tb model forecasts (Reichle et al. 2015, their Appendix B). The parameters that determine the expected error standard deviations are key inputs to the ensemble-based L4_SM assimilation algorithm. If they are chosen such that the expected errors are fully consistent with the actual errors, the metric shown in Figure 17a should be unity everywhere. If the *stddev_norm* metric is less than one, the actual errors are overestimated by the assimilation system, and if the metric is greater than one, the actual errors are underestimated.

The global average of the *stddev_norm* metric in Version 6 is 0.99, which suggests that, on average, the simulated error standard deviation nearly matches that of the actual errors (Figure 17a). This is an improvement from the corresponding global average value metric of 1.07 in Version 5 (Reichle et al. 2021b, their Figure 14), where the actual errors were somewhat underestimated on average. As in Version 5, however, the Version 6 metric varies greatly across the globe (Figure 17a). Typical values are either too low or too high. In the Amazon basin, the eastern US, tropical Africa, Indonesia, and portions of the high northern latitudes, *stddev_norm* values are around 0.5 or less, and thus the actual errors there are considerably overestimated by the modeling system. Conversely, *stddev_norm* values range from 1.25 to 2.5 in much of central North America, eastern Brazil, Argentina, the Sahel, southern Africa, India, central Asia, and Australia, meaning that the actual errors in these regions are considerably underestimated.



Finally, Figure 17b compares the absolute difference of *stddev_norm* from unity between Version 6 and Version 5. In the Sahel, southern Africa, and particularly in central Australia, the consistency of the simulated and actual errors is considerably improved in Version 6 compared to Version 5. The improvements in central Australia in Version 6 again reflect the improved, IMERG-based precipitation forcing there. In central Africa, the southern Sahara Desert, and the Arabian Peninsula, the overestimation of the actual errors got slightly worse in Version 6 compared to Version 5, but these regions are of lesser interest for soil moisture estimation, owing to their persistently very dry or persistently very wet conditions. In the global average, the absolute difference of the *stddev_norm* metric from the perfect value of unity is reduced by 0.02 in Version 6 compared to Version 5. More work, however, is needed to further improve the calibration of the input parameters that determine the model and observation errors in the L4_SM system.

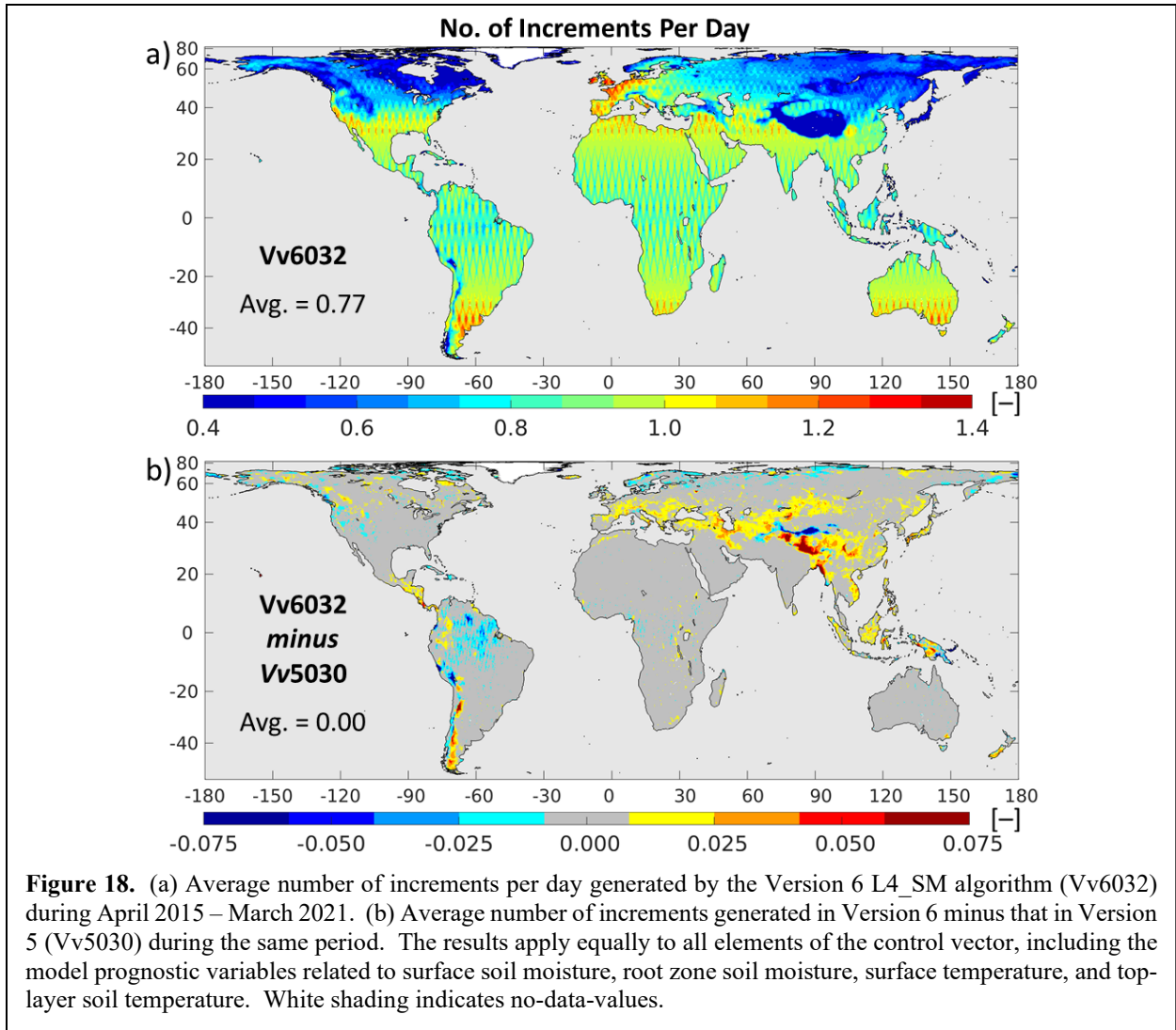
6.5.2 Increments

The number of times an analysis increment is applied at a given 9 km EASEv2 grid cell during the validation period depends on the count of assimilated observations in the vicinity (that is, within the 1.25-degree “localization” radius of influence; Reichle et al. 2017b). For simplicity, we compute the number of increments, separately for each 9 km grid cell, by counting the number of times the absolute analysis-minus-forecast difference in the 3-hourly analysis update output exceeded $10^{-5} \text{ m}^3 \text{ m}^{-3}$ for surface soil moisture or 0.001 K for surface temperature².

As in Version 5, the average number of increments in Version 6 is 0.77 per day over the 6-year validation period, which means that there are approximately four increments applied every five days on average, either from an ascending or a descending overpass. The overall pattern of the increments count (Figure 18a) follows that of the count of the assimilated Tb observations (Figure 14a). Similarly, the difference in the number of increments between Version 6 and Version 5 (Figure 18b) looks like that of the assimilated observations (Figure 14b) except in much of Africa, where the number of assimilated Tb observations increased by up to 5% but the number of increments remained essentially the same. The reason for this discrepancy remains unclear and requires further study.

The time mean values of the analysis increments for surface and root zone soil moisture are shown in Figure 19a and c, respectively. In the global average, the net increments are only -0.020 mm d^{-1} for surface soil moisture and 0.043 mm d^{-1} for root zone soil moisture (or -7.3 and 16 mm per year , respectively). Regionally, however, the mean increments can be up to $\sim 0.5 \text{ mm d}^{-1}$ and constitute a non-negligible fraction of the water balance. Generally, the pattern of the mean soil moisture increments reflects the long-term mean bias in the O-F Tb residuals (Figure 15a). They are largest in the central US, eastern South America, Africa, India, portions of central Asia, and southeastern Australia. Interestingly, the mean surface soil moisture increments are generally negative (drying) while the mean root zone soil moisture increments are generally positive (wetting). The magnitude of the mean increments in Version 6 is generally similar to that of Version 5 for surface soil moisture (Figure 19b), except for a few regions in South America, Africa and Australia. The differences in magnitude are a bit larger for the mean increments in root zone soil moisture (Figure 19d; note the different color scale). For both surface and root zone soil moisture, the global average of the magnitude of the mean increments in the two versions is nearly identical.

² In previous L4_SM versions, this approach provided a useful approximation of the number and statistics of the increments. Unfortunately, in Version 6 the approach produces noisy results when the published analysis and forecast fields are used, owing to the lossy compression of the published aup files (section 5.3). To compute the statistics of the Version 6 increments here, we thus used binary data that were written before the lossy compression. The binary data can be made available upon request. Future versions will apply only lossless compression to the aup output.



Finally, Figure 20 shows the time series standard deviation of the increments in surface and root zone soil moisture. This metric measures the typical magnitude of instantaneous increments. Typical increments in surface soil moisture are on the order of $0.02\text{--}0.03\text{ m}^3\text{ m}^{-3}$ in the central US, Argentina, the Sahel, southern Africa, India, portions of central Asia, and most of Australia (Figure 20a). In the same regions, root zone soil moisture increments are typically on the order of $0.002\text{--}0.006\text{ m}^3\text{ m}^{-3}$ (Figure 20c). Over densely vegetated regions, in particular the tropical forests, surface and root zone soil moisture increments are generally negligible, reflecting the fact that in those areas the measured SMAP Tb observations are mostly sensitive to the dense vegetation and are only marginally sensitive to soil moisture. Compared to Version 5, the typical magnitude of the instantaneous increments is reduced across much of Africa for both surface and root zone soil moisture (Figure 20b and d), which again reflects the improved, IMERG-based precipitation forcing in Version 6. For the same reason, the instantaneous surface soil moisture increments in central Australia are also smaller in Version 6 than in Version 5 (Figure 20b). However, in central Australia the magnitude of the instantaneous root zone soil moisture increments increased in Version 6 (Figure 20d). Here, the revised precipitation climatology and the improved, IMERG-based precipitation forcing result in slightly wetter average soil moisture in Version 6 (Figure 5), which strengthens the coupling of the surface and root zone layers and thereby facilitates the propagation of the SMAP-observed

surface soil moisture information (contained in the assimilated Tb observations) into the deeper soil layers. It is quite likely that the root zone soil moisture skill in central Australia improved in Version 6 along with that of the Version 6 surface soil moisture (Figure 12a).

6.5.3 Uncertainty Estimates

The L4_SM data product also includes error estimates for key output variables, including surface and root zone soil moisture as well as surface soil temperature. These uncertainty estimates vary dynamically and geographically because they are computed as the standard deviation of a given output variable across the ensemble of land surface states at a given time and location. (The ensemble is an integral part of the ensemble Kalman filter employed in the L4_SM algorithm, and the ensemble average provides the estimate of the variable under consideration (Reichle 2008).) By construction, the uncertainty estimates represent only the random component of the uncertainty. Bias and other structural errors such as errors in the dynamic range are not included.

The estimated uncertainties for soil moisture and soil temperature of Version 6 are nearly identical to those of Version 5 (for the latter, see Reichle et al. 2021b, their section 6.5.3 and Figure 18). That is, the improved skill of the Version 6 estimates, including in much of Africa and central Australia, is not reflected in reduced uncertainty estimates. Owing to the lack of high-quality in situ measurements in these regions, it is unclear if the consistency between the soil moisture uncertainty estimates and the actual soil moisture errors is better in Version 6 than in Version 5. Given the improved consistency between the simulated and actual Tb errors in Version 6 (Figure 17b), the Version 6 soil moisture uncertainty estimates are likely no worse in relation to the actual errors than the Version 5 soil moisture uncertainty estimates.

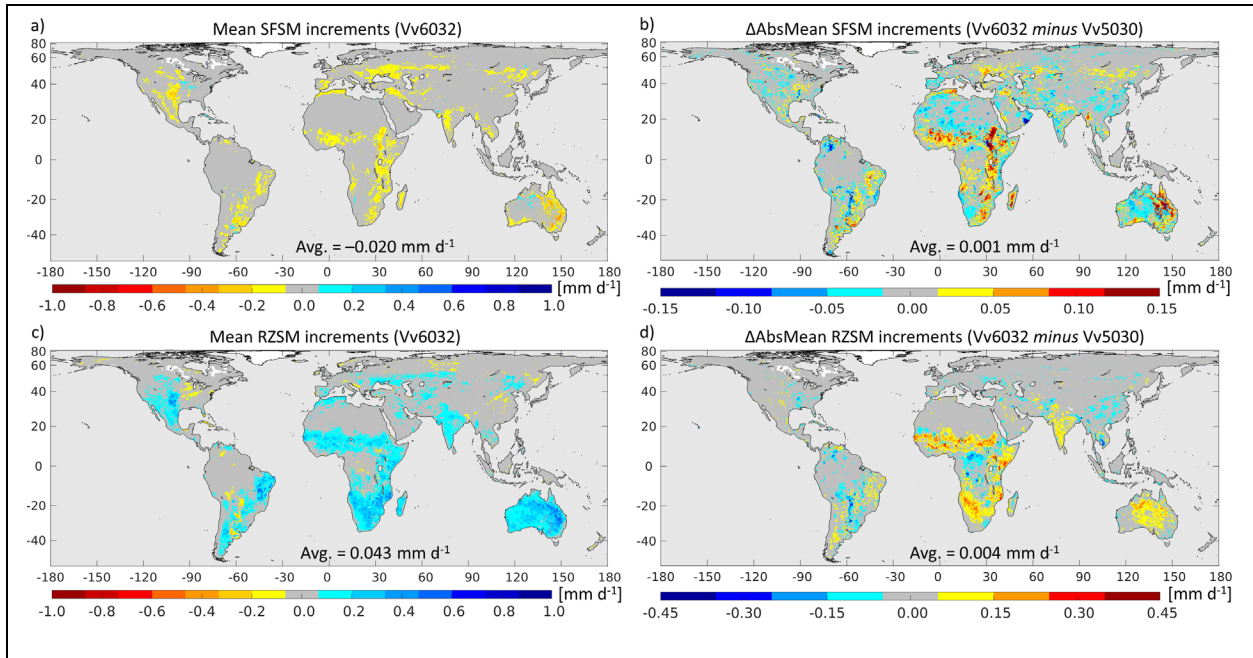


Figure 19. Time series mean of the increments for (a) surface and (c) root zone soil moisture from the Version 6 L4_SM algorithm (Vv6032) for Apr 2015 – March 2021 in equivalent flux units (mm d^{-1}). Absolute value of increments for Version 6 minus that of Version 5 (Vv5030) during the same period for (b) surface and (d) root zone soil moisture; blue colors in (b) and (d) indicate that the mean of the Version 6 increments is closer to the perfect value of zero than that of the Version 5 increments. Note the different color scales in (b) and (d). White shading indicates no-data-values.

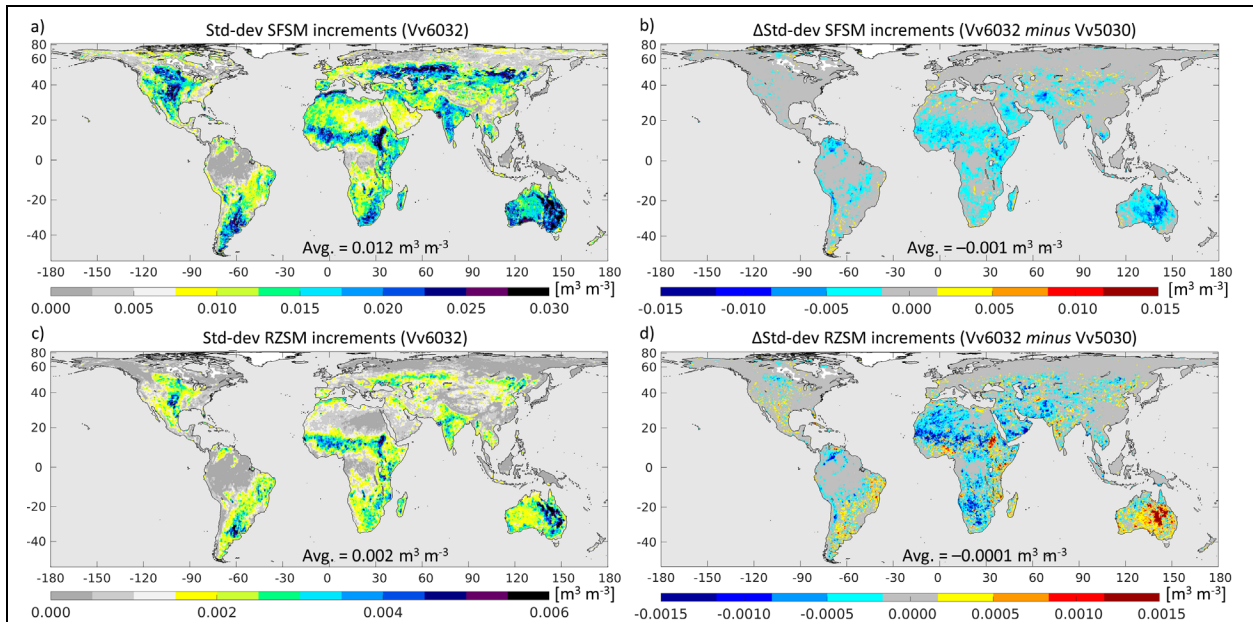


Figure 20. As in Figure 19 but for time series standard deviation of the increments in volumetric soil moisture units ($\text{m}^3 \text{m}^{-3}$). Blue colors in (b) and (d) indicate that the standard deviation of the Version 6 increments is closer to the perfect value of zero than that of the Version 5 increments. See text for explanation of increased standard deviation in Version 6 in Australia.

7 LIMITATIONS AND PLAN FOR FUTURE IMPROVEMENTS

Several limitations and avenues for future development are revealed by the assessment of the Version 6 L4_SM product presented above and by Version 4 and 5 validation results (Reichle et al. 2018b, 2019, 2021a,b) that still apply to Version 6.

7.1 L4_SM Algorithm Calibration and Temporal Homogeneity

Compared to earlier versions, the calibration of the Version 6 L4_SM algorithm utilized longer records of model-only Tb data and SMAP Tb observations. There are, however, still regions with a residual bias in the O-F Tb residuals (Figure 15a), which in turn leads to non-zero long-term mean soil moisture analysis increments (Figure 19a and c). Further improvements in the L4_SM algorithm calibration will be facilitated by an even longer record of SMAP observations and matching model-only Tb estimates. By themselves, however, longer records for the computation of the Tb scaling parameters are not sufficient.

First, version changes in the GEOS FP system (Lucchesi 2018) during the SMAP period adversely impact the homogeneity of the surface meteorological forcing data that are needed to calibrate the L4_SM algorithm and to generate the L4_SM data product. A forthcoming GEOS reanalysis product for the 21st century (R21C) is expected to be available in 2023. This new reanalysis dataset will provide a more homogeneous record of surface meteorological forcing data during the SMAP period and will also be more consistent with the future operational FP version that will provide the surface meteorological forcing data for L4_SM forward processing. We plan to use the R21C data (once they are available) in future L4_SM versions for both calibration and L4_SM processing.

Second, the microwave radiative transfer model parameters used in the Version 6 L4_SM algorithm are identical to those used in the Version 5 algorithm, which were calibrated using SMOS data and the Version 5 modeling system. Recalibration of the microwave radiative transfer model parameters requires a substantial computational effort, which prevented the derivation of an updated set of parameters for the Version 6 system and instead forced us to rely on the Tb scaling parameters alone to minimize bias in the simulated Tb versus the assimilated Tb. Moreover, preliminary research suggests that the L4_SM algorithm could be improved by using microwave soil roughness parameters and a vegetation optical depth (VOD) climatology based on SMAP Tb observations, both of which are by-products of the dual-channel algorithm of the SMAP Level 2 passive soil moisture retrievals (O'Neill et al. 2021). Using Level 2 VOD information should improve upon the current L4_SM approach of determining VOD from optical data, which are a poor surrogate for vegetation optical depth. The next version of the L4_SM algorithm should thus rely on some combination of recalibrated microwave radiative transfer model parameters and parameters taken from the dual-channel retrieval algorithm.

7.2 Impact of Ensemble Perturbations

In their assessment of the Version 5 L4_SM product, Reichle et al. (2021b, their section 6.1) found that nonlinearities in the generation of the multiplicative perturbations applied to the precipitation and shortwave forcing cause a small bias relative to the unperturbed forcing, which contributed to a small bias in the Version 5 L4_SM soil moisture relative to the corresponding Nature Run v8.3. Following the suggestion of Reichle et al. (2021b), the limits for multiplicative perturbations were relaxed in the Version 6 algorithm, but this change reduced the bias in the perturbed shortwave forcing only marginally (section 6.1, Figure 7). Moreover, we were unable to derive an approximate correction term as suggested by Reichle et al. (2021b). It also remains unclear if anything can be done to reduce the well-known wet soil moisture bias in arid regions that stems from the fact that at the dry end, soil moisture perturbations can only be positive

(wetting). Reducing the standard deviation of the perturbations would reduce this bias, but it would also make the L4_SM algorithm insensitive to errors in the model forecast soil moisture (for lack of sufficient ensemble spread in the EnKF analysis). More work is needed to understand and remedy the residual bias seen in the ensemble-based L4_SM assimilation algorithm.

7.3 Precipitation Data

As suggested by Reichle et al. (2021b), the daily precipitation corrections in the Version 6 L4_SM algorithm are primarily based on IMERG data, with the CPCU product used only in North America and for spin-up (section 5.3). It is important to keep in mind, however, that the IMERG-Final data used for L4_SM reprocessing through 29 June 2021 (Vv6032) are informed by monthly totals from precipitation gauges. Beginning on 30 Jun 2021, the daily precipitation corrections in the Version 6 L4_SM algorithm (Vv6030) are based on IMERG-Late data, which are not informed by monthly gauge totals and are therefore presumably of somewhat lesser quality. Preliminary results obtained during the development of the R21C reanalysis suggest that daily precipitation corrections with IMERG-Late indeed reduce the skill of simulated soil moisture compared to using IMERG-Final but still provide a net improvement compared to using CPCU. Additional research is in progress to determine the impact of switching from IMERG-Final to IMERG-Late inputs on the L4_SM soil moisture skill.

More research is also necessary to determine the exact cause of and eliminate the snowfall and snow mass artefact along 60°N latitude (Figure 8).

Finally, the GPM project plans to change the IMERG processing algorithm from version 06B to a new major version in 2022. Additional research will be needed to assess the impact of the upcoming IMERG version change on the quality of the L4_SM product.

7.4 Peatland and Permafrost Modeling

Research into improving the Catchment model parameterization for peat soils (Bechtold et al. 2019) and research into Tb data assimilation in peatlands (Bechtold et al. 2020) provide encouraging results. Additional research suggests that relatively simple model revisions can improve the Catchment model skill in permafrost regions (Tao et al. 2017, 2019). Implementing these model advances in the L4_SM algorithm should improve the skill of the L4_SM product in the high latitudes, where the coupling with the carbon cycle is of particular interest in the context of the SMAP science objectives (Entekhabi et al. 2010).

8 SUMMARY AND CONCLUSIONS

This report provides an assessment of Version 6 of the SMAP L4_SM product. The validation covers the period from 1 April 2015, 0z to 1 April 2021, 0z. **The most important change in the Version 6 algorithm is the improved precipitation forcing.** Specifically, the revised algorithm uses an updated, seasonally varying reference climatology and daily precipitation corrections that are primarily based on IMERG observations (section 5.3). Two different IMERG products are used: (i) IMERG-Final, which is derived from satellite observations and corrected to monthly gauge totals and (ii) IMERG-Late, which is a satellite-only product with a ~14-hour latency suitable for L4_SM operations. The revised precipitation reference climatology is from the IMERG-Final product in the 60°N-60°S latitude band; poleward of 60°N and 60°S latitude, the climatology is from IMERG-Final where available and from the GPCPv2.3 product elsewhere. The daily precipitation corrections in the Version 6 algorithm are based on IMERG data except in North America, where the CPCU gauge-only product is used as in Version 5. The corrections use IMERG-Final data for Version 6 L4_SM reprocessing through 29 June 2021 and IMERG-Late data thereafter, owing to the ~3.5-month latency of the IMERG-Final product. Additional updates in the Version 6 algorithm include (i) the recalibration of the Tb scaling parameters over a longer, 6-year period, (ii) a minor adjustment of a parameter in the multiplicative perturbations scheme for precipitation and shortwave forcing, and (iii) the lossy compression of the output to reduce the total data volume, which was inadvertently missing in Version 5 (section 5.3).

The Version 6 L4_SM product was validated using in situ soil moisture measurements from SMAP core validation sites and sparse networks. Additionally, independent soil moisture retrievals from ASCAT were used to determine anomaly correlation skill differences between the Version 5 and 6 soil moisture estimates. The product was further evaluated through an assessment of the data assimilation diagnostics generated by the L4_SM algorithm, such as the O-F Tb residuals and the soil moisture increments.

The global pattern of arid and humid regions is well captured by the Version 6 L4_SM soil moisture estimates (Figure 4). There is no change in the global average soil moisture between Version 5 and Version 6. An analysis of the time-averaged precipitation and soil moisture illustrates the key differences in the climatology of the Version 6 L4_SM product relative to Version 5 (Figures 3 and 5). Owing to substantial changes in the regional and continental precipitation climatology, the Version 6 soil moisture climatology is wetter in much of South America and Australia and drier in much of Africa and parts of East Asia. These changes are also reflected in the surface turbulent fluxes and surface and soil temperatures (Figure 6). Because of these climatological differences, the Version 5 and 6 products should *not* be combined into a single dataset for use in applications outside of CONUS.

When compared to in situ measurements from the SMAP core validation sites, the Version 6 surface soil moisture ubRMSD is $0.040 \text{ m}^3 \text{ m}^{-3}$ at the 9 km scale and $0.037 \text{ m}^3 \text{ m}^{-3}$ at the 33 km scale (Figure 9, Table A1). For root zone soil moisture, the ubRMSD is $0.027 \text{ m}^3 \text{ m}^{-3}$ at the 9 km scale and $0.024 \text{ m}^3 \text{ m}^{-3}$ at the 33 km scale (Figure 9, Table A3). These metrics are unchanged from those of the Version 5 product. When factoring in the measurement error of the in situ measurements (conservatively estimated to be ~0.01-0.02 $\text{m}^3 \text{ m}^{-3}$), the **Version 6 L4_SM surface and root zone soil moisture clearly meets the product accuracy requirement** ($\text{ubRMSE} \leq 0.04 \text{ m}^3 \text{ m}^{-3}$). It is important to keep in mind that whereas the surface soil moisture in situ measurements are typically at ~5 cm depth, the L4_SM estimates are for the 0-5 cm soil layer. As with the error in the in situ measurements themselves, this mismatch in layer depths adversely impacts all given validation metrics. There are minor differences between the Version 5 and 6 correlation and mean difference metrics. For surface soil moisture, the correlation and anomaly correlation are slightly larger in Version 6 than in Version 5, but the differences are not statistically significant at the 5% level (Figure 10, Table A2); no differences are seen in the correlation metrics for root zone soil moisture (Figure 10, Table A4). For both surface and root zone soil moisture, the MD is slightly larger in Version 6 than in Version 5 (Figure 9, Tables A1 and A3). Since most of the core sites are in North America, where the daily

precipitation corrections in both Versions 5 and 6 are based on the CPCU gauge product, it is not surprising that core site performance metrics for the two versions are very close.

The assimilation of SMAP Tb observations is beneficial for the Version 6 L4_SM surface and root zone soil moisture estimates, with improvements over the model-only Open Loop (OL6000) that are consistent across the 9 km and 33 km scales and across the ubRMSD and correlation metrics (Figures 9 and 10). For surface soil moisture, the correlation improvements are statistically significant at the 5% level. The Open Loop ubRMSD metrics are essentially the same in Versions 5 and 6, and so are the ubRMSD improvements from the SMAP Tb assimilation. The Open Loop correlation skills are slightly higher in Version 6 compared to Version 5 while the correlation improvements from SMAP Tb assimilation (that is, the L4_SM minus Open Loop skill differences) are slightly smaller in Version 6 than in Version 5.

The comparison with in situ measurements from a global set of sparse networks corroborates the results obtained for the core validation sites (Figure 11).

The key improvements in Version 6 are manifested in large parts of South America, Africa, and central Australia, as well as in Myanmar and Vietnam, as shown by an Instrumental Variable analysis using independent surface soil moisture retrievals from ASCAT (Figure 12a). In these regions, the IMERG-based daily precipitation corrections in Version 6 represent a clear advantage over the precipitation forcing used in Version 5, which relied on GEOS FP precipitation in Africa and CPCU-corrected precipitation elsewhere. The latter was supported by very sparse or faulty gauge measurements in the regions that show the strongest improvements in Version 6. Moreover, the skill improvements from Version 5 to Version 6 are larger for the corresponding Open Loop data than for the L4_SM products (Figure 12b). As intended, the SMAP Tb assimilation partly makes up for precipitation errors (Figure 13), and these improvements are larger in the lower-skill Version 5 system.

The data assimilation diagnostics further broaden the validation to the global domain. The global average number of Tb observations assimilated in the Version 6 system is nearly identical to that in Version 5 (Figure 14). Owing to the differences in the precipitation climatology and intensity, however, the model-based quality control causes some regional differences in the number of assimilated Tb observations between the two versions, primarily in mountainous regions and regions where the precipitation climatology changed most considerably. The time mean, globally averaged analysis increments in surface and root zone soil moisture are very small (Figure 19). Regionally, however, time mean increments can be as large as 0.5 mm d⁻¹. These biases are caused by modest biases in the O-F Tb residuals in the L4_SM product that can be up to ±3 K in small regions (Figure 15). The assimilation diagnostics further reveal that, on a regional basis, the errors in Tb are typically over- or underestimated considerably by the L4_SM system (Figure 17). However, the Version 6 assimilation diagnostics are generally improved over those of Version 5. Most importantly, the time series standard deviation of the O-F Tb residuals is reduced from 5.5 K in Version 5 to 5.1 K in Version 6 (Figure 16). These improvements in the Tb simulation skill in the Version 6 system are again concentrated in South America, Africa, central Australia, Myanmar, and Vietnam. The improvements in the Version 6 system are also evident in the generally smaller instantaneous analysis increments for surface and root zone soil moisture (Figure 20), since the same or better product skill (e.g., Figure 12) can be achieved with smaller soil moisture adjustments from the Tb analysis. Australia is an exception. Here, the magnitude of the analysis increments increased for root zone soil moisture, presumably because the wetter soil moisture conditions in Version 6 strengthen the coupling between the surface and root zone soil moisture and facilitate enhanced propagation of the surface-layer information contained in the SMAP Tb observations into the deeper soil.

Ensemble-based uncertainty estimates for the analyzed surface soil moisture, root zone soil moisture, surface temperature, and top layer soil temperature are also provided with the product. These uncertainty estimates are designed to reflect the random error in key geophysical product fields. The Version 5 and 6 uncertainty estimates are essentially the same. It is unclear if the consistency between the uncertainty estimates and the actual errors in the product has improved in Version 6 in the regions where the Version 6

skill changed the most, including South America, Africa, and central Australia. Owing to a lack of suitable independent observations in these regions, the ubRMSD skill in these regions cannot be established reliably.

Based on the results presented in this report, the public release of Version 6 of the L4_SM data product is recommended. Additional validation of the Version 6 product should more closely examine the impact of using daily precipitation corrections that are based on the satellite-only IMERG-Late product instead of the satellite-gauge IMERG-Final product (section 7.3). Additionally, the IMERG version upgrade that is planned for 2022 will necessitate an investigation of its impact on the L4_SM product skill (section 7.3).

Possible avenues for future development include the use of the forthcoming GEOS R21C reanalysis that will provide a more temporally homogeneous record of surface meteorological forcing data (section 7.1), the recalibration of the microwave radiative transfer parameters in the latest modeling system and/or the use of soil roughness or vegetation optical depth information from the dual-channel algorithm of the SMAP Level 2 passive soil moisture product (section 7.1), and the use of improved Catchment model physics for peatlands and permafrost (section 7.4). It remains unclear if anything can be done to further lessen the residual bias caused by the ensemble perturbations (section 7.2). Moreover, calibration of the system with longer records should further reduce the residual regional bias in the O-F Tb residuals and the resulting impact of non-zero long-term mean analysis increments on the water balance. Similarly, longer records of in situ measurements will permit more extensive validation. Additionally, the expected public availability of tower flux measurements for the SMAP period will support the evaluation of L4_SM latent and sensible heat flux estimates. These developments will be addressed in future work.

ACKNOWLEDGEMENTS

This report was made possible by the contributions of many individuals from the SMAP Project, the SMAP Science Team, the SMAP Cal/Val Partner Program, and the NASA Global Modeling and Assimilation Office. The NASA SMAP mission and the NASA Modeling, Analysis, and Prediction program supported the research. Computational resources were provided by the NASA High-End Computing Program through the NASA Center for Climate Simulation at the Goddard Space Flight Center. This research was also supported by the U.S. Department of Agriculture (USDA), Agricultural Research Service, and the USDA Long-Term Agroecosystem Research (LTAR) network. USDA is an equal opportunity provider and employer.

APPENDIX

Performance Metrics at Core Validation Site Reference Pixels

Tables A1-A8 in this Appendix provide a complete listing of the performance metrics, including ubRMSD, MD, R, and anomaly R, for all 9 km and 33 km core site reference pixels. Metrics are provided for surface soil moisture, root zone soil moisture, surface soil temperature at 6am local time, and surface soil temperature at 6pm local time for the L4_SM Vv6032 and Vv5030 product versions as well as for the model-only OL6000 and OL5030 estimates. Table A9 provides the L4_SM Vv6032 performance metrics for the 9 km reference pixels categorized by land cover.

Table A1. Surface soil moisture ubRMSD and MD at individual core site reference pixels and averaged over 33 km and 9 km reference pixels, including average and average absolute metrics across all sites (bottom rows labeled “All”). Information for 33 km reference pixels is shown in bold font. Italics indicate Version 6 L4_SM metrics.

Site name	Reference pixel		Surface soil moisture								
	ID	Horiz. scale (km)	ubRMSD (m3 m-3)					MD (m3 m-3)			
			OL6000	Vv6032	OL5030	Vv5030	95% conf. interval	OL6000	Vv6032	OL5030	Vv5030
RM	03013302	33	0.029	0.037	0.028	0.037	0.005	0.049	0.051	0.043	0.046
	03010903	9	0.028	0.036	0.029	0.036	0.003	0.122	0.136	0.127	0.142
	03010908	9	0.040	0.047	0.038	0.047	0.007	-0.013	-0.011	-0.015	-0.013
RC	04013302	33	0.042	0.040	0.042	0.041	0.011	-0.002	0.004	-0.010	-0.003
	04010907	9	0.041	0.040	0.041	0.041	0.008	-0.013	-0.010	-0.027	-0.023
	04010910	9	0.048	0.047	0.048	0.046	0.013	-0.033	-0.033	-0.022	-0.021
YC	07013301	33	0.045	0.033	0.045	0.036	0.007	-0.007	-0.012	-0.014	-0.022
	07010902	9	0.072	0.058	0.075	0.061	0.013	-0.047	-0.044	-0.057	-0.056
	07010916	9	0.051	0.043	0.052	0.045	0.009	-0.002	-0.011	-0.010	-0.019
CR	09013301	33	0.036	0.052	0.037	0.049	0.007	-0.030	-0.030	-0.021	-0.021
	09010906	9	0.030	0.051	0.031	0.048	0.005	0.025	0.024	0.034	0.034
NG	12033301	33	0.020	0.020	0.030	0.030	0.005	-0.032	-0.033	-0.017	-0.015
WG	16013302	33	0.026	0.029	0.026	0.029	0.002	0.025	0.033	0.024	0.031
	16010906	9	0.027	0.028	0.027	0.028	0.002	-0.004	0.008	-0.006	0.005
	16010907	9	0.027	0.031	0.028	0.031	0.002	0.022	0.033	0.021	0.031
	16010913	9	0.033	0.038	0.030	0.037	0.003	0.100	0.104	0.092	0.094
LW	16023302	33	0.037	0.030	0.037	0.030	0.003	-0.041	-0.042	-0.043	-0.043
	16020905	9	0.048	0.042	0.048	0.042	0.004	0.000	0.002	-0.005	-0.001
	16020906	9	0.044	0.037	0.043	0.037	0.004	-0.011	-0.014	-0.015	-0.015
	16020907	9	0.041	0.035	0.040	0.034	0.005	-0.042	-0.045	-0.046	-0.047
FC	16033302	33	0.038	0.036	0.038	0.036	0.003	-0.024	-0.022	-0.034	-0.033
	16030911	9	0.050	0.040	0.050	0.040	0.004	-0.046	-0.040	-0.056	-0.052
	16030916	9	0.037	0.034	0.037	0.033	0.003	-0.026	-0.024	-0.034	-0.032
LR	16043302	33	0.041	0.039	0.041	0.040	0.003	0.003	0.003	0.002	0.002
	16040901	9	0.034	0.032	0.033	0.031	0.003	0.076	0.084	0.074	0.081
SJ	16063302	33	0.044	0.041	0.044	0.040	0.006	0.136	0.132	0.132	0.129
	16060907	9	0.045	0.042	0.047	0.041	0.014	0.067	0.061	0.062	0.056
SF	16073302	33	0.055	0.047	0.055	0.048	0.007	0.027	0.025	0.029	0.027
	16070909	9	0.060	0.053	0.061	0.054	0.007	-0.013	-0.012	-0.012	-0.013
	16070910	9	0.061	0.054	0.062	0.055	0.006	0.031	0.030	0.033	0.031
	16070911	9	0.064	0.056	0.065	0.057	0.007	0.044	0.042	0.047	0.045
MB	19023301	33	0.040	0.037	0.039	0.036	0.007	-0.056	-0.055	-0.068	-0.071
	19020902	9	0.040	0.035	0.042	0.036	0.008	-0.047	-0.055	-0.060	-0.071
TZ	25013301	33	0.045	0.040	0.039	0.034	0.011	0.027	0.025	0.012	0.014
	25010911	9	0.050	0.046	0.042	0.037	0.010	0.025	0.021	0.006	0.007
KN	27013301	33	0.042	0.039	0.042	0.038	0.007	-0.005	-0.004	0.020	0.019
	27010910	9	0.032	0.029	0.032	0.029	0.006	-0.039	-0.029	-0.013	-0.005
	27010911	9	0.040	0.035	0.041	0.036	0.007	-0.065	-0.060	-0.040	-0.037
VA	41010906	9	0.028	0.026	0.029	0.027	0.006	0.066	0.064	0.066	0.066
NI	45013301	33	0.039	0.036	0.041	0.038	0.006	0.063	0.081	0.036	0.058
	45010902	9	0.039	0.036	0.041	0.039	0.005	0.072	0.088	0.045	0.067
BN	45023301	33	0.048	0.047	0.051	0.047	0.008	0.119	0.120	0.126	0.128
	45020902	9	0.048	0.046	0.051	0.047	0.007	0.118	0.120	0.124	0.127
TX	48013301	33	0.034	0.028	0.034	0.028	0.004	0.031	0.030	0.032	0.030
	48010902	9	0.040	0.036	0.039	0.036	0.004	0.068	0.067	0.068	0.067
	48010911	9	0.038	0.032	0.038	0.032	0.004	0.075	0.074	0.077	0.076
HB	67013301	33	0.033	0.031	0.034	0.031	0.008	-0.014	-0.015	-0.012	-0.014
	67010901	9	0.046	0.046	0.045	0.045	0.021	-0.018	-0.016	-0.015	-0.013
All	Average	33	0.039	0.037	0.039	0.037	0.001	0.015	0.016	0.013	0.015
	Average	9	0.042	0.040	0.042	0.040	0.002	0.023	0.025	0.021	0.023
	Avg. Abs.	33	n/a	n/a	n/a	n/a	n/a	0.038	0.040	0.037	0.039
	Avg. Abs.	9	Same as average.					0.049	0.050	0.047	0.049

Table A2. As in Table A1 but for R and anomaly R.

Site name	Reference pixel		Surface soil moisture									
			R (dimensionless)					anomaly R (dimensionless)				
	ID	Horiz. scale (km)	OL6000	Vv6032	OL5030	Vv5030	95% conf. interval	OL6000	Vv6032	OL5030	Vv5030	95% conf. interval
RM	03013302	33	0.80	0.82	0.82	0.82	0.05	0.64	0.73	0.69	0.75	0.05
	03010903	9	0.61	0.63	0.62	0.63	0.07	0.58	0.65	0.61	0.66	0.06
	03010908	9	0.71	0.69	0.74	0.70	0.07	0.49	0.59	0.56	0.60	0.07
RC	04013302	33	0.63	0.70	0.62	0.68	0.16	0.61	0.70	0.61	0.68	0.19
	04010907	9	0.64	0.69	0.63	0.66	0.14	0.60	0.71	0.61	0.71	0.14
	04010910	9	0.70	0.72	0.70	0.74	0.12	0.53	0.68	0.52	0.67	0.15
YC	07013301	33	0.86	0.92	0.87	0.90	0.04	0.80	0.90	0.82	0.90	0.04
	07010902	9	0.85	0.90	0.84	0.88	0.05	0.74	0.84	0.73	0.84	0.06
	07010916	9	0.82	0.88	0.82	0.86	0.05	0.78	0.85	0.77	0.85	0.05
CR	09013301	33	0.70	0.62	0.68	0.64	0.07	0.66	0.66	0.62	0.66	0.07
	09010906	9	0.71	0.68	0.67	0.68	0.07	0.64	0.71	0.58	0.70	0.06
NG	12033301	33	0.67	0.68	0.66	0.66	0.13	0.48	0.51	0.46	0.47	0.15
WG	16013302	33	0.75	0.80	0.74	0.80	0.04	0.71	0.78	0.70	0.78	0.04
	16010906	9	0.67	0.72	0.65	0.72	0.05	0.64	0.70	0.61	0.70	0.05
	16010907	9	0.68	0.72	0.66	0.72	0.05	0.64	0.70	0.61	0.70	0.05
	16010913	9	0.74	0.80	0.75	0.81	0.05	0.73	0.81	0.73	0.81	0.04
LW	16023302	33	0.72	0.85	0.73	0.85	0.03	0.70	0.85	0.70	0.85	0.03
	16020905	9	0.65	0.75	0.66	0.75	0.05	0.60	0.72	0.61	0.72	0.05
	16020906	9	0.67	0.79	0.68	0.79	0.04	0.65	0.80	0.66	0.80	0.04
	16020907	9	0.68	0.80	0.69	0.81	0.06	0.68	0.78	0.68	0.79	0.05
FC	16033302	33	0.70	0.84	0.71	0.84	0.04	0.67	0.84	0.67	0.84	0.03
	16030911	9	0.67	0.81	0.66	0.81	0.04	0.63	0.83	0.64	0.83	0.04
	16030916	9	0.70	0.82	0.70	0.82	0.03	0.69	0.82	0.70	0.82	0.03
LR	16043302	33	0.70	0.74	0.70	0.74	0.05	0.67	0.72	0.67	0.72	0.05
	16040901	9	0.79	0.81	0.79	0.80	0.05	0.77	0.79	0.77	0.79	0.04
SJ	16063302	33	0.64	0.71	0.63	0.71	0.11	0.47	0.67	0.45	0.66	0.10
	16060907	9	0.66	0.72	0.63	0.72	0.16	0.45	0.66	0.41	0.66	0.13
SF	16073302	33	0.63	0.74	0.62	0.73	0.07	0.67	0.80	0.67	0.80	0.05
	16070909	9	0.58	0.69	0.56	0.68	0.08	0.65	0.79	0.64	0.78	0.05
	16070910	9	0.54	0.67	0.53	0.66	0.08	0.59	0.75	0.59	0.75	0.06
	16070911	9	0.51	0.64	0.50	0.63	0.08	0.53	0.70	0.53	0.70	0.06
MB	19023301	33	0.57	0.75	0.57	0.76	0.05	0.60	0.75	0.60	0.78	0.05
	19020902	9	0.58	0.78	0.55	0.79	0.08	0.63	0.79	0.61	0.81	0.08
TZ	25013301	33	0.93	0.94	0.92	0.94	0.04	0.69	0.72	0.67	0.73	0.07
	25010911	9	0.92	0.92	0.90	0.92	0.05	0.67	0.69	0.64	0.70	0.07
KN	27013301	33	0.57	0.71	0.57	0.71	0.09	0.67	0.76	0.64	0.74	0.08
	27010910	9	0.61	0.75	0.62	0.75	0.09	0.67	0.76	0.65	0.75	0.08
	27010911	9	0.64	0.77	0.63	0.76	0.08	0.67	0.75	0.64	0.73	0.08
VA	41010906	9	0.56	0.67	0.55	0.65	0.16	0.65	0.73	0.65	0.73	0.16
NI	45013301	33	0.61	0.73	0.32	0.55	0.16	n/a	n/a	n/a	n/a	n/a
	45010902	9	0.58	0.70	0.25	0.48	0.15	0.56	0.65	0.16	0.44	0.13
BN	45023301	33	0.71	0.74	0.68	0.73	0.08	0.57	0.69	0.32	0.47	0.08
	45020902	9	0.77	0.80	0.74	0.78	0.07	0.54	0.66	0.32	0.47	0.07
TX	48013301	33	0.83	0.91	0.83	0.91	0.03	0.78	0.88	0.78	0.88	0.04
	48010902	9	0.74	0.83	0.74	0.83	0.05	0.67	0.78	0.67	0.79	0.05
	48010911	9	0.78	0.87	0.79	0.87	0.04	0.72	0.83	0.72	0.84	0.04
HB	67013301	33	0.78	0.82	0.78	0.82	0.05	0.67	0.76	0.68	0.77	0.06
	67010901	9	0.80	0.82	0.83	0.83	0.10	0.39	0.59	0.46	0.63	0.18
All	Average	33	0.71	0.78	0.69	0.77	0.02	0.65	0.75	0.63	0.73	0.02
	Average	9	0.69	0.76	0.67	0.75	0.02	0.61	0.73	0.58	0.71	0.02

Table A3. As in Table A1 but for root zone soil moisture.

Site name	Reference pixel		Root zone soil moisture									
			ubRMSD (m3 m-3)					MD (m3 m-3)				
	ID	Horiz. scale (km)	OL6000	V6032	OL5030	V5030	95% conf. interval	OL6000	V6032	OL5030	V5030	
RM	03013302	33	n/a	n/a	n/a	n/a	n/a	n/a	n/a	n/a	n/a	n/a
	03010903	9	n/a	n/a	n/a	n/a	n/a	n/a	n/a	n/a	n/a	n/a
	03010908	9	n/a	n/a	n/a	n/a	n/a	n/a	n/a	n/a	n/a	n/a
RC	04013302	33	n/a	n/a	n/a	n/a	n/a	n/a	n/a	n/a	n/a	n/a
	04010907	9	n/a	n/a	n/a	n/a	n/a	n/a	n/a	n/a	n/a	n/a
	04010910	9	n/a	n/a	n/a	n/a	n/a	n/a	n/a	n/a	n/a	n/a
YC	07013301	33	0.012	0.011	0.010	0.007	0.006	-0.110	-0.098	-0.111	-0.100	
	07010902	9	n/a	n/a	n/a	n/a	n/a	n/a	n/a	n/a	n/a	
	07010916	9	n/a	n/a	n/a	n/a	n/a	n/a	n/a	n/a	n/a	
CR	09013301	33	n/a	n/a	n/a	n/a	n/a	n/a	n/a	n/a	n/a	
	09010906	9	n/a	n/a	n/a	n/a	n/a	n/a	n/a	n/a	n/a	
NG	12033301	33	n/a	n/a	n/a	n/a	n/a	n/a	n/a	n/a	n/a	
WG	16013302	33	n/a	n/a	n/a	n/a	n/a	n/a	n/a	n/a	n/a	
	16010906	9	n/a	n/a	n/a	n/a	n/a	n/a	n/a	n/a	n/a	
	16010907	9	n/a	n/a	n/a	n/a	n/a	n/a	n/a	n/a	n/a	
	16010913	9	n/a	n/a	n/a	n/a	n/a	n/a	n/a	n/a	n/a	
LW	16023302	33	0.030	0.027	0.030	0.027	0.004	-0.033	-0.033	-0.035	-0.034	
	16020905	9	n/a	n/a	n/a	n/a	n/a	n/a	n/a	n/a	n/a	
	16020906	9	0.030	0.027	0.030	0.026	0.005	-0.008	-0.008	-0.010	-0.010	
	16020907	9	0.035	0.032	0.034	0.031	0.008	-0.029	-0.031	-0.032	-0.033	
FC	16033302	33	0.028	0.022	0.029	0.023	0.003	0.036	0.049	0.027	0.039	
	16030911	9	0.033	0.028	0.034	0.028	0.005	-0.003	0.011	-0.012	0.001	
	16030916	9	0.025	0.023	0.025	0.023	0.003	-0.004	0.005	-0.012	-0.001	
LR	16043302	33	0.029	0.029	0.030	0.029	0.003	0.066	0.067	0.066	0.066	
	16040901	9	0.027	0.028	0.027	0.027	0.003	0.095	0.100	0.093	0.097	
SJ	16063302	33	n/a	n/a	n/a	n/a	n/a	n/a	n/a	n/a	n/a	
	16060907	9	n/a	n/a	n/a	n/a	n/a	n/a	n/a	n/a	n/a	
SF	16073302	33	0.034	0.034	0.034	0.035	0.006	0.009	0.009	0.010	0.010	
	16070909	9	0.037	0.037	0.038	0.038	0.006	-0.046	-0.044	-0.045	-0.045	
	16070910	9	0.038	0.037	0.038	0.038	0.005	0.031	0.031	0.032	0.032	
	16070911	9	0.036	0.036	0.037	0.036	0.005	0.022	0.021	0.024	0.023	
MB	19023301	33	n/a	n/a	n/a	n/a	n/a	n/a	n/a	n/a	n/a	
	19020902	9	n/a	n/a	n/a	n/a	n/a	n/a	n/a	n/a	n/a	
TZ	25013301	33	0.023	0.025	0.026	0.028	0.014	0.044	0.041	0.032	0.032	
	25010911	9	0.027	0.028	0.027	0.029	0.013	0.048	0.045	0.032	0.033	
KN	27013301	33	0.026	0.022	0.025	0.021	0.011	-0.041	-0.035	-0.017	-0.015	
	27010910	9	n/a	n/a	n/a	n/a	n/a	n/a	n/a	n/a	n/a	
	27010911	9	0.028	0.023	0.027	0.022	0.008	-0.064	-0.055	-0.039	-0.034	
VA	41010906	9	n/a	n/a	n/a	n/a	n/a	n/a	n/a	n/a	n/a	
NI	45013301	33	n/a	n/a	n/a	n/a	n/a	n/a	n/a	n/a	n/a	
	45010902	9	n/a	n/a	n/a	n/a	n/a	n/a	n/a	n/a	n/a	
BN	45023301	33	n/a	n/a	n/a	n/a	n/a	n/a	n/a	n/a	n/a	
	45020902	9	n/a	n/a	n/a	n/a	n/a	n/a	n/a	n/a	n/a	
TX	48013301	33	0.023	0.020	0.023	0.020	0.005	0.046	0.048	0.047	0.049	
	48010902	9	0.026	0.022	0.026	0.022	0.005	0.112	0.113	0.111	0.112	
	48010911	9	0.021	0.018	0.020	0.017	0.004	0.106	0.107	0.107	0.109	
HB	67013301	33	n/a	n/a	n/a	n/a	n/a	n/a	n/a	n/a	n/a	
	67010901	9	n/a	n/a	n/a	n/a	n/a	n/a	n/a	n/a	n/a	
All	Average	33	0.026	0.024	0.026	0.024	0.002	0.002	0.006	0.002	0.006	
	Average	9	0.029	0.027	0.029	0.027	0.002	0.024	0.027	0.024	0.027	
	Avg. Abs.	33	n/a	n/a	n/a	n/a	n/a	0.048	0.047	0.043	0.043	
	Avg. Abs.	9	Same as average.					0.053	0.053	0.049	0.047	

Table A4. As in Table A1 but for root zone soil moisture R and anomaly R.

Site name	Reference pixel		Root zone soil moisture										
	ID	Horiz. scale (km)	R (dimensionless)					anomaly R (dimensionless)					
			OL6000	Vv6032	OL5030	Vv5030	95% conf. interval	OL6000	Vv6032	OL5030	Vv5030	95% conf. interval	
RM	03013302	33	n/a	n/a	n/a	n/a	n/a	n/a	n/a	n/a	n/a	n/a	n/a
	03010903	9	n/a	n/a	n/a	n/a	n/a	n/a	n/a	n/a	n/a	n/a	n/a
	03010908	9	n/a	n/a	n/a	n/a	n/a	n/a	n/a	n/a	n/a	n/a	n/a
RC	04013302	33	n/a	n/a	n/a	n/a	n/a	n/a	n/a	n/a	n/a	n/a	n/a
	04010907	9	n/a	n/a	n/a	n/a	n/a	n/a	n/a	n/a	n/a	n/a	n/a
	04010910	9	n/a	n/a	n/a	n/a	n/a	n/a	n/a	n/a	n/a	n/a	n/a
YC	07013301	33	0.87	0.93	0.90	0.96	0.21	n/a	n/a	n/a	n/a	n/a	n/a
	07010902	9	n/a	n/a	n/a	n/a	n/a	n/a	n/a	n/a	n/a	n/a	n/a
	07010916	9	n/a	n/a	n/a	n/a	n/a	n/a	n/a	n/a	n/a	n/a	n/a
CR	09013301	33	n/a	n/a	n/a	n/a	n/a	n/a	n/a	n/a	n/a	n/a	n/a
	09010906	9	n/a	n/a	n/a	n/a	n/a	n/a	n/a	n/a	n/a	n/a	n/a
NG	12033301	33	n/a	n/a	n/a	n/a	n/a	n/a	n/a	n/a	n/a	n/a	n/a
WG	16013302	33	n/a	n/a	n/a	n/a	n/a	n/a	n/a	n/a	n/a	n/a	n/a
	16010906	9	n/a	n/a	n/a	n/a	n/a	n/a	n/a	n/a	n/a	n/a	n/a
	16010907	9	n/a	n/a	n/a	n/a	n/a	n/a	n/a	n/a	n/a	n/a	n/a
	16010913	9	n/a	n/a	n/a	n/a	n/a	n/a	n/a	n/a	n/a	n/a	n/a
LW	16023302	33	0.72	0.80	0.73	0.80	0.10	0.68	0.82	0.68	0.82	0.09	
	16020905	9	n/a	n/a	n/a	n/a	n/a	n/a	n/a	n/a	n/a	n/a	
	16020906	9	0.62	0.73	0.64	0.74	0.13	0.59	0.74	0.60	0.75	0.13	
	16020907	9	0.68	0.75	0.70	0.78	0.16	n/a	n/a	n/a	n/a	n/a	
FC	16033302	33	0.72	0.83	0.71	0.82	0.09	0.67	0.82	0.66	0.81	0.09	
	16030911	9	0.73	0.83	0.70	0.82	0.10	0.65	0.82	0.64	0.81	0.09	
	16030916	9	0.72	0.79	0.70	0.78	0.09	0.64	0.76	0.62	0.76	0.09	
LR	16043302	33	0.66	0.66	0.65	0.66	0.11	0.60	0.63	0.60	0.63	0.10	
	16040901	9	0.61	0.60	0.61	0.60	0.15	0.66	0.66	0.66	0.65	0.13	
SJ	16063302	33	n/a	n/a	n/a	n/a	n/a	n/a	n/a	n/a	n/a	n/a	
	16060907	9	n/a	n/a	n/a	n/a	n/a	n/a	n/a	n/a	n/a	n/a	
SF	16073302	33	0.62	0.63	0.62	0.61	0.18	0.74	0.86	0.75	0.87	0.10	
	16070909	9	0.58	0.60	0.56	0.57	0.18	0.73	0.86	0.72	0.86	0.10	
	16070910	9	0.44	0.46	0.42	0.44	0.20	0.60	0.81	0.61	0.83	0.11	
	16070911	9	0.44	0.46	0.43	0.44	0.20	0.55	0.74	0.57	0.78	0.12	
MB	19023301	33	n/a	n/a	n/a	n/a	n/a	n/a	n/a	n/a	n/a	n/a	
	19020902	9	n/a	n/a	n/a	n/a	n/a	n/a	n/a	n/a	n/a	n/a	
TZ	25013301	33	0.94	0.93	0.93	0.92	0.11	0.82	0.78	0.79	0.79	0.18	
	25010911	9	0.94	0.92	0.92	0.90	0.13	0.83	0.79	0.79	0.80	0.16	
KN	27013301	33	0.84	0.85	0.79	0.85	0.23	0.89	0.91	0.84	0.89	0.15	
	27010910	9	n/a	n/a	n/a	n/a	n/a	n/a	n/a	n/a	n/a	n/a	
	27010911	9	0.89	0.89	0.82	0.88	0.14	0.90	0.91	0.82	0.89	0.11	
VA	41010906	9	n/a	n/a	n/a	n/a	n/a	n/a	n/a	n/a	n/a	n/a	
NI	45013301	33	n/a	n/a	n/a	n/a	n/a	n/a	n/a	n/a	n/a	n/a	
	45010902	9	n/a	n/a	n/a	n/a	n/a	n/a	n/a	n/a	n/a	n/a	
BN	45023301	33	n/a	n/a	n/a	n/a	n/a	n/a	n/a	n/a	n/a	n/a	
	45020902	9	n/a	n/a	n/a	n/a	n/a	n/a	n/a	n/a	n/a	n/a	
TX	48013301	33	0.91	0.94	0.91	0.94	0.07	0.89	0.93	0.89	0.93	0.06	
	48010902	9	0.79	0.85	0.79	0.85	0.12	0.72	0.80	0.72	0.81	0.12	
	48010911	9	0.89	0.92	0.90	0.93	0.07	0.88	0.92	0.88	0.93	0.06	
HB	67013301	33	n/a	n/a	n/a	n/a	n/a	n/a	n/a	n/a	n/a	n/a	
	67010901	9	n/a	n/a	n/a	n/a	n/a	n/a	n/a	n/a	n/a	n/a	
All	Average	33	0.79	0.82	0.78	0.82	0.05	0.75	0.82	0.74	0.82	0.04	
	Average	9	0.73	0.76	0.72	0.76	0.05	0.72	0.79	0.70	0.80	0.04	

Table A5. As in Table A1 but for surface soil temperature at 6am local time.

Site name	Reference pixel		Surface Soil Temperature (6am)								
	ID	Horiz. scale (km)	ubRMSD (K)					MD (K)			
			O16000	Vv6032	O15030	Vv5030	95% conf. interval	O16000	Vv6032	O15030	Vv5030
RM	03013302	33	1.8	1.8	1.8	1.8	0.5	-3.6	-3.6	-3.5	-3.5
	03010903	9	1.9	1.9	1.9	1.9	0.5	-4.1	-4.1	-4.1	-4.2
	03010908	9	1.5	1.5	1.5	1.5	0.4	-3.1	-3.2	-3.1	-3.1
RC	04013302	33	2.3	2.3	2.3	2.3	0.7	0.9	0.9	1.0	1.0
	04010907	9	1.5	1.5	1.5	1.5	0.6	0.9	0.9	1.0	1.0
	04010910	9	2.1	2.1	2.1	2.1	0.9	-0.5	-0.5	-0.6	-0.6
YC	07013301	33	2.4	2.4	2.4	2.4	0.5	-3.8	-3.8	-3.7	-3.8
	07010902	9	1.9	1.8	1.9	1.8	0.4	-2.5	-2.6	-2.4	-2.5
	07010916	9	2.3	2.3	2.3	2.3	0.5	-3.1	-3.2	-3.1	-3.2
CR	09013301	33	1.2	1.2	1.2	1.2	0.3	-0.8	-0.8	-0.8	-0.9
	09010906	9	1.2	1.2	1.2	1.2	0.3	-0.9	-0.9	-0.9	-0.9
NG	12033301	33	2.1	2.0	2.2	2.2	0.7	-4.9	-4.9	-5.3	-5.3
WG	16013302	33	1.5	1.5	1.5	1.5	0.3	-2.1	-2.2	-2.1	-2.2
	16010906	9	1.9	1.9	1.9	1.9	0.4	-1.5	-1.7	-1.5	-1.7
	16010907	9	1.5	1.5	1.5	1.5	0.3	-3.1	-3.2	-3.0	-3.2
	16010913	9	2.0	1.9	2.0	1.9	0.5	-2.2	-2.2	-2.1	-2.1
LW	16023302	33	1.8	1.8	1.8	1.8	0.5	-1.7	-1.8	-1.7	-1.8
	16020905	9	2.0	2.0	2.1	2.0	0.6	-1.8	-1.8	-1.7	-1.8
	16020906	9	1.9	1.9	1.9	1.9	0.5	-1.7	-1.7	-1.7	-1.7
	16020907	9	1.7	1.7	1.7	1.7	0.7	-1.6	-1.6	-1.6	-1.6
FC	16033302	33	1.7	1.7	1.7	1.7	0.5	-1.8	-1.8	-1.7	-1.8
	16030911	9	1.5	1.5	1.5	1.5	0.6	-1.6	-1.6	-1.5	-1.5
	16030916	9	1.4	1.4	1.4	1.4	1.4	-1.3	-1.4	-1.2	-1.3
LR	16043302	33	1.8	1.8	1.8	1.8	0.4	-2.3	-2.3	-2.3	-2.3
	16040901	9	1.5	1.5	1.5	1.5	0.4	-2.2	-2.2	-2.1	-2.2
SJ	16063302	33	1.7	1.7	1.7	1.7	0.6	-1.3	-1.3	-1.3	-1.3
	16060907	9	1.6	1.6	1.6	1.6	0.8	-1.5	-1.5	-1.5	-1.5
SF	16073302	33	1.6	1.6	1.6	1.6	0.5	-1.7	-1.7	-1.7	-1.7
	16070909	9	1.5	1.5	1.5	1.5	0.5	-1.4	-1.4	-1.4	-1.4
	16070910	9	1.5	1.5	1.5	1.5	0.5	-1.8	-1.8	-1.8	-1.8
	16070911	9	1.5	1.5	1.5	1.5	0.4	-1.9	-1.9	-1.9	-1.9
MB	19023301	33	1.5	1.6	1.5	1.6	0.3	-1.6	-1.7	-1.5	-1.5
	19020902	9	n/a	n/a	n/a	n/a	n/a	n/a	n/a	n/a	n/a
TZ	25013301	33	n/a	n/a	n/a	n/a	n/a	n/a	n/a	n/a	n/a
	25010911	9	n/a	n/a	n/a	n/a	n/a	n/a	n/a	n/a	n/a
KN	27013301	33	1.5	1.5	1.4	1.4	0.5	-0.6	-0.6	-0.7	-0.8
	27010910	9	1.2	1.2	1.2	1.2	0.4	-0.9	-1.0	-1.1	-1.1
	27010911	9	1.5	1.5	1.4	1.4	0.5	-0.9	-1.0	-1.1	-1.1
VA	41010906	9	n/a	n/a	n/a	n/a	n/a	n/a	n/a	n/a	n/a
NI	45013301	33	n/a	n/a	n/a	n/a	n/a	n/a	n/a	n/a	n/a
	45010902	9	n/a	n/a	n/a	n/a	n/a	n/a	n/a	n/a	n/a
BN	45023301	33	n/a	n/a	n/a	n/a	n/a	n/a	n/a	n/a	n/a
	45020902	9	n/a	n/a	n/a	n/a	n/a	n/a	n/a	n/a	n/a
TX	48013301	33	1.3	1.3	1.3	1.3	0.2	-2.0	-2.0	-2.0	-2.0
	48010902	9	1.4	1.4	1.4	1.4	0.3	-2.5	-2.5	-2.5	-2.5
	48010911	9	1.6	1.5	1.5	1.5	0.3	-2.1	-2.1	-2.1	-2.1
HB	67013301	33	1.1	1.1	1.1	1.1	0.3	-0.6	-0.6	-0.6	-0.6
	67010901	9	1.0	1.0	1.0	1.0	0.5	-0.5	-0.5	-0.5	-0.5
All	Average	33	1.7	1.7	1.7	1.7	0.1	-1.8	-1.9	-1.8	-1.9
	Average	9	1.6	1.6	1.6	1.6	0.1	-1.7	-1.7	-1.7	-1.7
	Average Abs	33	n/a	n/a	n/a	n/a	n/a	2.0	2.0	2.0	2.0
	Average Abs	9	n/a	n/a	n/a	n/a	n/a	1.7	1.8	1.7	1.8

Table A6. As in Table A1 but for 6am surface soil temperature R and anomaly R.

Site name	Reference pixel		Surface Soil Temperature (6am)									
			R (dimensionless)					anomaly R (dimensionless)				
	ID	Horiz. scale (km)	OL6000	VV6032	OL5030	VV5030	95% conf. interval	OL6000	VV6032	OL5030	VV5030	95% conf. interval
RM	03013302	33	0.98	0.98	0.98	0.98	0.01	0.89	0.90	0.90	0.90	0.02
	03010903	9	0.98	0.98	0.98	0.98	0.01	0.87	0.88	0.88	0.88	0.02
	03010908	9	0.98	0.98	0.98	0.98	0.01	0.89	0.90	0.90	0.90	0.02
RC	04013302	33	0.96	0.96	0.96	0.96	0.03	n/a	n/a	n/a	n/a	n/a
	04010907	9	0.98	0.98	0.98	0.98	0.01	n/a	n/a	n/a	n/a	n/a
	04010910	9	0.96	0.96	0.96	0.96	0.03	n/a	n/a	n/a	n/a	n/a
YC	07013301	33	0.95	0.95	0.95	0.95	0.02	0.74	0.75	0.74	0.75	0.04
	07010902	9	0.97	0.97	0.97	0.97	0.01	0.85	0.86	0.85	0.86	0.02
	07010916	9	0.97	0.98	0.97	0.98	0.01	0.85	0.86	0.85	0.86	0.02
CR	09013301	33	0.98	0.98	0.98	0.98	0.01	0.94	0.94	0.94	0.94	0.01
	09010906	9	0.98	0.98	0.98	0.98	0.01	0.94	0.94	0.94	0.94	0.01
NG	12033301	33	0.90	0.91	0.90	0.89	0.11	n/a	n/a	n/a	n/a	n/a
WG	16013302	33	0.98	0.98	0.98	0.98	0.01	0.89	0.90	0.89	0.90	0.02
	16010906	9	0.97	0.97	0.97	0.97	0.02	0.84	0.85	0.84	0.85	0.02
	16010907	9	0.98	0.98	0.98	0.98	0.01	0.89	0.90	0.89	0.90	0.02
	16010913	9	0.98	0.98	0.98	0.98	0.01	n/a	n/a	n/a	n/a	n/a
LW	16023302	33	0.98	0.98	0.98	0.98	0.01	0.91	0.92	0.92	0.92	0.01
	16020905	9	0.98	0.98	0.98	0.98	0.01	0.91	0.91	0.91	0.91	0.01
	16020906	9	0.98	0.98	0.98	0.98	0.01	0.91	0.91	0.91	0.91	0.01
	16020907	9	0.98	0.99	0.98	0.99	0.01	n/a	n/a	n/a	n/a	n/a
FC	16033302	33	0.99	0.99	0.99	0.99	0.01	0.91	0.92	0.91	0.92	0.01
	16030911	9	0.99	0.99	0.99	0.99	0.01	n/a	n/a	n/a	n/a	n/a
	16030916	9	0.98	0.98	0.98	0.98	0.05	n/a	n/a	n/a	n/a	n/a
LR	16043302	33	0.97	0.97	0.97	0.97	0.01	0.90	0.90	0.90	0.90	0.02
	16040901	9	0.98	0.98	0.98	0.98	0.01	0.94	0.94	0.94	0.94	0.02
SJ	16063302	33	0.97	0.97	0.97	0.97	0.02	0.91	0.91	0.91	0.91	0.03
	16060907	9	0.97	0.97	0.97	0.97	0.02	n/a	n/a	n/a	n/a	n/a
SF	16073302	33	0.98	0.98	0.98	0.98	0.01	0.92	0.92	0.92	0.92	0.01
	16070909	9	0.98	0.98	0.98	0.98	0.01	0.93	0.93	0.93	0.93	0.02
	16070910	9	0.98	0.98	0.98	0.98	0.01	0.92	0.92	0.92	0.92	0.02
	16070911	9	0.98	0.98	0.98	0.98	0.01	0.92	0.92	0.92	0.92	0.02
MB	19023301	33	0.96	0.96	0.96	0.96	0.02	0.89	0.88	0.90	0.88	0.02
	19020902	9	n/a	n/a	n/a	n/a	n/a	n/a	n/a	n/a	n/a	n/a
TZ	25013301	33	n/a	n/a	n/a	n/a	n/a	n/a	n/a	n/a	n/a	n/a
	25010911	9	n/a	n/a	n/a	n/a	n/a	n/a	n/a	n/a	n/a	n/a
KN	27013301	33	0.97	0.97	0.97	0.97	0.02	0.89	0.89	0.89	0.89	0.03
	27010910	9	0.98	0.98	0.98	0.98	0.01	0.93	0.93	0.93	0.93	0.02
	27010911	9	0.97	0.97	0.97	0.97	0.02	0.89	0.89	0.90	0.90	0.02
VA	41010906	9	n/a	n/a	n/a	n/a	n/a	n/a	n/a	n/a	n/a	n/a
NI	45013301	33	n/a	n/a	n/a	n/a	n/a	n/a	n/a	n/a	n/a	n/a
	45010902	9	n/a	n/a	n/a	n/a	n/a	n/a	n/a	n/a	n/a	n/a
BN	45023301	33	n/a	n/a	n/a	n/a	n/a	n/a	n/a	n/a	n/a	n/a
	45020902	9	n/a	n/a	n/a	n/a	n/a	n/a	n/a	n/a	n/a	n/a
TX	48013301	33	0.98	0.99	0.98	0.99	0.01	0.93	0.93	0.93	0.93	0.01
	48010902	9	0.98	0.98	0.98	0.98	0.01	0.90	0.91	0.90	0.91	0.01
	48010911	9	0.98	0.98	0.98	0.98	0.01	0.90	0.90	0.90	0.90	0.01
HB	67013301	33	0.98	0.98	0.98	0.98	0.01	n/a	n/a	n/a	n/a	n/a
	67010901	9	0.98	0.98	0.98	0.98	0.02	n/a	n/a	n/a	n/a	n/a
All	Average	33	0.97	0.97	0.97	0.97	0.01	0.89	0.90	0.90	0.90	0.01
	Average	9	0.98	0.98	0.98	0.98	0.00	0.90	0.91	0.90	0.91	0.01

Table A7. As in Table A1 but for surface soil temperature at 6pm local time.

Site name	Reference pixel		Surface Soil Temperature (6pm)								
			ubRMSD (K)					MD (K)			
	ID	Horiz. scale (km)	OL6000	Vv6032	OL5030	Vv5030	95% conf. interval	OL6000	Vv6032	OL5030	Vv5030
RM	03013302	33	1.7	1.7	1.7	1.7	0.5	-1.5	-1.6	-1.4	-1.5
	03010903	9	2.1	2.1	2.1	2.1	0.6	-2.6	-2.7	-2.6	-2.7
	03010908	9	1.5	1.6	1.5	1.6	0.5	-1.0	-1.1	-1.0	-1.1
RC	04013302	33	2.2	2.2	2.2	2.2	0.6	1.5	1.4	1.6	1.5
	04010907	9	1.5	1.5	1.5	1.5	0.6	1.0	0.9	1.1	1.1
	04010910	9	2.0	2.0	2.0	2.0	0.8	0.3	0.3	0.1	0.1
YC	07013301	33	2.1	2.1	2.1	2.1	0.4	-0.6	-0.7	-0.6	-0.6
	07010902	9	1.5	1.5	1.5	1.5	0.3	0.3	0.2	0.4	0.3
	07010916	9	1.6	1.6	1.6	1.6	0.3	-0.1	-0.1	0.0	-0.1
CR	09013301	33	1.7	1.7	1.7	1.7	0.4	-0.5	-0.7	-0.6	-0.7
	09010906	9	1.7	1.7	1.7	1.7	0.3	-0.6	-0.7	-0.7	-0.8
NG	12033301	33	4.1	4.1	4.1	4.0	1.0	-8.9	-8.9	-9.5	-9.5
WG	16013302	33	2.0	1.9	2.0	1.9	0.4	-0.7	-0.9	-0.7	-0.8
	16010906	9	2.4	2.4	2.4	2.3	0.5	-0.4	-0.7	-0.4	-0.6
	16010907	9	1.9	1.9	1.9	1.9	0.4	-1.3	-1.6	-1.3	-1.5
	16010913	9	2.7	2.6	2.7	2.6	0.6	-1.5	-1.6	-1.4	-1.4
LW	16023302	33	1.9	1.9	1.9	1.9	0.6	-0.3	-0.3	-0.2	-0.3
	16020905	9	2.1	2.1	2.1	2.1	0.7	-0.2	-0.2	-0.1	-0.2
	16020906	9	2.0	2.0	2.0	2.0	0.6	-0.2	-0.2	-0.1	-0.2
	16020907	9	1.8	1.7	1.8	1.7	0.8	-0.5	-0.5	-0.4	-0.4
FC	16033302	33	1.8	1.8	1.8	1.8	0.6	-0.1	-0.2	0.1	-0.1
	16030911	9	1.6	1.6	1.7	1.6	0.7	-0.1	-0.2	0.0	-0.1
	16030916	9	1.4	1.4	1.4	1.4	1.4	-0.2	-0.2	-0.1	-0.1
LR	16043302	33	1.8	1.7	1.8	1.7	0.4	-1.5	-1.5	-1.5	-1.5
	16040901	9	1.6	1.6	1.6	1.6	0.5	-1.4	-1.4	-1.4	-1.4
SJ	16063302	33	1.8	1.8	1.8	1.8	0.7	-0.4	-0.4	-0.4	-0.4
	16060907	9	1.6	1.6	1.6	1.6	1.0	-0.7	-0.7	-0.7	-0.6
SF	16073302	33	1.7	1.7	1.7	1.7	0.6	-0.5	-0.5	-0.5	-0.5
	16070909	9	1.6	1.6	1.6	1.6	0.5	-0.6	-0.6	-0.6	-0.6
	16070910	9	1.8	1.8	1.8	1.8	0.6	-1.0	-1.0	-1.0	-1.0
	16070911	9	1.7	1.7	1.7	1.7	0.5	-1.1	-1.1	-1.1	-1.1
MB	19023301	33	2.2	2.3	2.1	2.3	0.5	0.6	0.5	0.8	0.8
	19020902	9	1.6	1.7	1.6	1.7	0.5	-0.7	-0.6	-0.5	-0.4
TZ	25013301	33	n/a	n/a	n/a	n/a	n/a	n/a	n/a	n/a	n/a
	25010911	9	n/a	n/a	n/a	n/a	n/a	n/a	n/a	n/a	n/a
KN	27013301	33	2.1	2.1	2.1	2.1	0.7	1.2	1.1	0.9	0.9
	27010910	9	1.8	1.8	1.8	1.8	0.5	0.4	0.2	0.1	0.0
	27010911	9	2.1	2.1	2.1	2.0	0.6	0.5	0.3	0.2	0.1
VA	41010906	9	n/a	n/a	n/a	n/a	n/a	n/a	n/a	n/a	n/a
NI	45013301	33	n/a	n/a	n/a	n/a	n/a	n/a	n/a	n/a	n/a
	45010902	9	n/a	n/a	n/a	n/a	n/a	n/a	n/a	n/a	n/a
BN	45023301	33	n/a	n/a	n/a	n/a	n/a	n/a	n/a	n/a	n/a
	45020902	9	n/a	n/a	n/a	n/a	n/a	n/a	n/a	n/a	n/a
TX	48013301	33	1.7	1.6	1.7	1.6	0.3	-1.7	-1.7	-1.7	-1.7
	48010902	9	1.8	1.8	1.8	1.8	0.4	-1.8	-1.8	-1.8	-1.8
	48010911	9	2.0	1.9	2.0	1.9	0.4	-2.0	-2.0	-2.0	-2.0
HB	67013301	33	1.1	1.1	1.1	1.1	0.4	-1.5	-1.5	-1.5	-1.5
	67010901	9	1.4	1.4	1.4	1.4	0.7	-1.7	-1.7	-1.7	-1.7
All	Average	33	2.0	2.0	2.0	2.0	0.1	-1.0	-1.1	-1.0	-1.1
	Average	9	1.7	1.7	1.7	1.7	0.2	-0.7	-0.8	-0.7	-0.7
	Average Abs	33	n/a	n/a	n/a	n/a	n/a	1.4	1.5	1.5	1.5
	Average Abs	9	n/a	n/a	n/a	n/a	n/a	0.9	0.9	0.8	0.9

Table A8. As in Table A1 but for 6pm surface soil temperature R and anomaly R.

Site name	Reference pixel		Surface Soil Temperature (6pm)									
			R (dimensionless)					anomaly R (dimensionless)				
	ID	Horiz. scale (km)	OL6000	VV6032	OL5030	VV5030	95% conf. interval	OL6000	VV6032	OL5030	VV5030	95% conf. interval
RM	03013302	33	0.99	0.99	0.99	0.99	0.01	0.91	0.92	0.91	0.92	0.02
	03010903	9	0.99	0.99	0.99	0.99	0.01	0.90	0.92	0.90	0.91	0.02
	03010908	9	0.98	0.98	0.98	0.98	0.01	0.87	0.88	0.87	0.88	0.02
RC	04013302	33	0.96	0.96	0.96	0.96	0.03	n/a	n/a	n/a	n/a	n/a
	04010907	9	0.98	0.98	0.98	0.98	0.01	n/a	n/a	n/a	n/a	n/a
	04010910	9	0.97	0.97	0.97	0.97	0.02	n/a	n/a	n/a	n/a	n/a
YC	07013301	33	0.96	0.96	0.96	0.96	0.02	0.78	0.79	0.77	0.78	0.03
	07010902	9	0.98	0.98	0.98	0.98	0.01	0.90	0.90	0.90	0.90	0.02
	07010916	9	0.98	0.98	0.98	0.98	0.01	0.89	0.91	0.89	0.90	0.02
CR	09013301	33	0.97	0.97	0.97	0.97	0.01	0.92	0.93	0.92	0.92	0.02
	09010906	9	0.98	0.97	0.97	0.97	0.01	0.92	0.93	0.92	0.93	0.02
NG	12033301	33	0.82	0.83	0.82	0.83	0.14	n/a	n/a	n/a	n/a	n/a
WG	16013302	33	0.98	0.98	0.98	0.98	0.01	0.88	0.90	0.88	0.90	0.02
	16010906	9	0.97	0.97	0.97	0.97	0.01	0.85	0.87	0.85	0.87	0.02
	16010907	9	0.98	0.98	0.98	0.98	0.01	0.87	0.89	0.87	0.89	0.02
	16010913	9	0.98	0.98	0.98	0.98	0.01	n/a	n/a	n/a	n/a	n/a
LW	16023302	33	0.98	0.98	0.98	0.98	0.01	0.90	0.91	0.90	0.91	0.02
	16020905	9	0.98	0.98	0.98	0.98	0.01	0.88	0.89	0.88	0.89	0.02
	16020906	9	0.98	0.98	0.98	0.98	0.01	0.89	0.89	0.89	0.89	0.02
	16020907	9	0.98	0.98	0.98	0.98	0.02	n/a	n/a	n/a	n/a	n/a
FC	16033302	33	0.98	0.98	0.98	0.98	0.01	0.90	0.91	0.90	0.91	0.02
	16030911	9	0.98	0.98	0.98	0.98	0.01	n/a	n/a	n/a	n/a	n/a
	16030916	9	0.98	0.98	0.98	0.98	0.05	n/a	n/a	n/a	n/a	n/a
LR	16043302	33	0.97	0.97	0.97	0.97	0.02	0.88	0.88	0.88	0.88	0.02
	16040901	9	0.97	0.97	0.97	0.97	0.02	0.90	0.91	0.90	0.91	0.03
SJ	16063302	33	0.98	0.98	0.98	0.98	0.02	0.91	0.91	0.91	0.91	0.03
	16060907	9	0.98	0.98	0.97	0.98	0.03	n/a	n/a	n/a	n/a	n/a
SF	16073302	33	0.98	0.98	0.98	0.98	0.01	0.92	0.92	0.92	0.92	0.02
	16070909	9	0.98	0.98	0.98	0.98	0.01	0.93	0.93	0.93	0.92	0.02
	16070910	9	0.98	0.98	0.98	0.98	0.01	0.91	0.91	0.91	0.91	0.02
	16070911	9	0.98	0.98	0.98	0.98	0.01	0.91	0.91	0.91	0.91	0.02
MB	19023301	33	0.93	0.93	0.94	0.92	0.03	0.72	0.70	0.73	0.70	0.05
	19020902	9	0.97	0.96	0.97	0.96	0.03	n/a	n/a	n/a	n/a	n/a
TZ	25013301	33	n/a	n/a	n/a	n/a	n/a	n/a	n/a	n/a	n/a	n/a
	25010911	9	n/a	n/a	n/a	n/a	n/a	n/a	n/a	n/a	n/a	n/a
KN	27013301	33	0.95	0.95	0.95	0.95	0.03	0.88	0.88	0.88	0.88	0.03
	27010910	9	0.97	0.97	0.97	0.97	0.02	0.91	0.91	0.91	0.91	0.02
	27010911	9	0.95	0.95	0.95	0.96	0.03	0.88	0.88	0.88	0.88	0.03
VA	41010906	9	n/a	n/a	n/a	n/a	n/a	n/a	n/a	n/a	n/a	n/a
NI	45013301	33	n/a	n/a	n/a	n/a	n/a	n/a	n/a	n/a	n/a	n/a
	45010902	9	n/a	n/a	n/a	n/a	n/a	n/a	n/a	n/a	n/a	n/a
BN	45023301	33	n/a	n/a	n/a	n/a	n/a	n/a	n/a	n/a	n/a	n/a
	45020902	9	n/a	n/a	n/a	n/a	n/a	n/a	n/a	n/a	n/a	n/a
TX	48013301	33	0.98	0.98	0.98	0.98	0.01	0.91	0.92	0.91	0.93	0.01
	48010902	9	0.98	0.98	0.98	0.98	0.01	0.88	0.89	0.88	0.89	0.02
	48010911	9	0.97	0.98	0.97	0.98	0.01	0.87	0.89	0.87	0.89	0.02
HB	67013301	33	0.98	0.98	0.98	0.98	0.01	n/a	n/a	n/a	n/a	n/a
	67010901	9	0.98	0.98	0.98	0.98	0.03	n/a	n/a	n/a	n/a	n/a
All	Average	33	0.96	0.96	0.96	0.96	0.01	0.87	0.88	0.88	0.88	0.01
	Average	9	0.98	0.98	0.98	0.98	0.01	0.89	0.90	0.89	0.90	0.01

Table A9. Metrics for Version 6 (Vv6032) L4_SM surface (SF) and root zone (RZ) soil moisture at the 9 km scale categorized based on land cover.

L4 (9-km, 3-hourly)		ubRMSD		MD		RMSD		R		Anomaly R		No. of 9-km ref. pixels		Avg. no. of 3-hr data per ref. pix.	
		(m3/m3)		(m3/m3)		(m3/m3)		(-)		(-)					
Land Cover	Site Name	SF	RZ	SF	RZ	SF	RZ	SF	RZ	SF	RZ	SF	RZ	SF	RZ
Grasslands	Reynolds Creek	0.044	n/a	-0.021	n/a	0.049	n/a	0.70	n/a	0.70	n/a	2	n/a	3,219	n/a
	TxSON	0.034	0.020	0.071	0.110	0.078	0.112	0.85	0.89	0.81	0.86	2	2	17,282	15,332
	Fort Cobb	0.037	0.025	-0.032	0.008	0.049	0.042	0.82	0.81	0.83	0.79	2	2	12,165	8,662
	Little Washita	0.038	0.029	-0.019	-0.019	0.046	0.036	0.78	0.74	0.77	0.74	3	2	9,168	3,849
	Niger	0.036	n/a	0.088	n/a	0.095	n/a	0.70	n/a	0.65	n/a	1	n/a	1,053	n/a
	Yanco	0.050	n/a	-0.027	n/a	0.058	n/a	0.89	n/a	0.84	n/a	2	n/a	10,207	n/a
	Average		0.040	0.025	0.010	0.033	0.063	0.063	0.79	0.81	0.77	0.80			
Croplands	South Fork	0.054	0.036	0.020	0.002	0.062	0.049	0.67	0.50	0.74	0.80	3	3	9,309	4,913
	Kenaston	0.032	0.023	-0.044	-0.055	0.055	0.059	0.76	0.89	0.76	0.91	2	1	5,200	2,921
	Carman	0.051	n/a	0.024	n/a	0.056	n/a	0.68	n/a	0.71	n/a	1	n/a	8,274	n/a
	Monte Buey	0.035	n/a	-0.055	n/a	0.065	n/a	0.78	n/a	0.79	n/a	1	n/a	3,737	n/a
	REMEDIHUS	0.041	n/a	0.063	n/a	0.094	n/a	0.66	n/a	0.62	n/a	2	n/a	9,686	n/a
	HOBE	0.046	n/a	-0.016	n/a	0.049	n/a	0.82	n/a	0.59	n/a	1	n/a	1,067	n/a
	St Josephs	0.042	n/a	0.061	n/a	0.073	n/a	0.72	n/a	0.66	n/a	1	n/a	2,409	n/a
Average		0.043	0.030	0.007	-0.026	0.065	0.054	0.73	0.70	0.70	0.86				
Crops/natural	Little River	0.032	0.028	0.084	0.100	0.090	0.104	0.81	0.60	0.79	0.66	1	1	4,284	3,465
Open shrubs	Walnut Gulch	0.033	n/a	0.048	n/a	0.062	n/a	0.75	n/a	0.73	n/a	3	n/a	12,341	n/a
Woody savannas	Tonzi Ranch	0.046	0.028	0.021	0.045	0.051	0.047	0.92	0.92	0.69	0.79	1	1	10,326	3,662
Savannas	Valencia	0.026	n/a	0.064	n/a	0.069	n/a	0.67	n/a	0.73	n/a	1	n/a	1,766	n/a
	Benin	0.046	n/a	0.120	n/a	0.128	n/a	0.80	n/a	0.66	n/a	1	n/a	6,637	n/a

REFERENCES

- Bechtold, M., G. J. M. De Lannoy, R. D. Koster, R. H. Reichle, S. P. Mahanama, et al. (2019), PEAT-CLSM: A Specific Treatment of Peatland Hydrology in the NASA Catchment Land Surface Model, *Journal of Advances in Modeling Earth Systems*, *11*, 2130-2162, doi:10.1029/2018MS001574.
- Bechtold, M., G. J. M. De Lannoy, R. H. Reichle, D. Roose, N. Balliston, I. Burdun, K. Devito, J. Kurbatova, M. Strack, and E. A. Zarov (2020), Improved Groundwater Table and L-band Brightness Temperature Estimates for Northern Hemisphere Peatlands Using New Model Physics and SMOS Observations in a Global Data Assimilation Framework, *Remote Sensing of Environment*, *246*, 111805, doi:10.1016/j.rse.2020.111805.
- Bell, J. E., Palecki, M. A., Baker, C. B., Collins, W. G., Lawrimore, J. H., Leeper, R. D., Hall, M. E., Kochendorfer, J., Meyers, T. P., Wilson, T., & Diamond, H. J. (2013), U.S. Climate Reference Network soil moisture and temperature observations, *Journal of Hydrometeorology*, *14*, 977–988, doi:10.1175/jhm-d-12-0146.1.
- Bircher, S., N. Skou, K. H. Jensen, J. P. Walker, and L. Rasmussen (2012), A soil moisture and temperature network for SMOS validation in Western Denmark, *Hydrology and Earth System Sciences*, *16*, 1445–1463, doi:10.5194/hess-16-1445-2012.
- Bosch, D. D., J. M. Sheridan, and L. K. Marshall (2007), Precipitation, soil moisture, and climate database, Little River Experimental Watershed, Georgia, United States, *Water Resources Research*, *43*, doi:10.1029/2006wr005834.
- Brodzik, M. J., B. Billingsley, T. Haran, B. Raup, and M. H. Savoie (2012), EASE-Grid 2.0: Incremental but significant improvements for Earth-gridded data sets, *ISPRS Int. J. Geoinf.*, *1*, 32–45, doi:10.3390/ijgi1010032.
- Caldwell, T. G., T. Bongiovanni, M. H. Cosh, C. Halley, and M. H. Young (2018), Field and Laboratory Evaluation of the CS655 Soil Water Content Sensor, *Vadose Zone Journal*, *17*, 170214, doi:10.2136/vzj2017.12.0214.
- Calvet, J.-C., N. Fritz, F. Froissard, D. Suquia, A. Petitpa, and B. Piguet (2007), In situ soil moisture observations for the CAL/VAL of SMOS: the SMOSMANIA network, 2007 IEEE International Geoscience and Remote Sensing Symposium, doi:10.1109/igarss.2007.4423019.
- CEOS (2015), Committee on Earth Observation Satellites (CEOS) Working Group on Calibration and Validation (WGCV): <http://calvalportal.ceos.org>, CEOS WGCV Land Products Sub-Group: <http://lpvs.gsfc.nasa.gov>. Accessed 7 October 2015.
- Chan, S., E. G. Njoku, and A. Colliander (2020), *SMAP LIC Radiometer Half-Orbit 36 km EASE-Grid Brightness Temperatures, Version 5*. NASA National Snow and Ice Data Center Distributed Active Archive Center, doi:10.5067/JJ5FL7FRLKJI.
- Chen, F., W. T. Crow, A. Colliander, M. Cosh, T. J. Jackson, R. Bindlish, R. H. Reichle, S. K. Chan, D. D. Bosch, P. J. Starks, D. C. Goodrich, M. Seyfried (2016), Application of Triple Collocation in Ground-based Validation of Soil Moisture Active/Passive (SMAP) Level 2 Data Products, *IEEE Journal of Selected Topics in Applied Earth Observations and Remote Sensing*, submitted.
- Chen, F. et al. (2019), Uncertainty of Reference Pixel Soil Moisture Averages Sampled at SMAP Core Validation Sites, *Journal of Hydrometeorology*, *20*, 1553–1569, doi:10.1175/jhm-d-19-0049.1.
- Clewley, D., J. B. Whitcomb, R. Akbar, A. R. Silva, A. Berg, J. R. Adams, T. Caldwell, D. Entekhabi, and M. Moghaddam (2017), A Method for Upscaling In Situ Soil Moisture Measurements to Satellite Footprint Scale Using Random Forests, *IEEE Journal of Selected Topics in Applied Earth Observations and Remote Sensing*, *10*(6), 2663–2673, doi:10.1109/jstars.2017.2690220.
- Colliander, A., S. Chan, N. Das, S. Kim, S. Dunbar, T. Jackson, C. Derksen, K. McDonald, J. Kimball, E. Njoku, R. Reichle, and B. Weiss (2014), SMAP L2-L4 Data Products Calibration and Validation Plan, Soil Moisture Active Passive (SMAP) Mission Science Document. JPL D-79463, Jet Propulsion Laboratory, Pasadena, CA.

- Colliander, A., et al. (2017a), SMAP/In Situ Core Validation Site Land Surface Parameters Match-Up Data, Version 1. NASA National Snow and Ice Data Center DAAC, doi:10.5067/DXAVIXLY18KM.
- Colliander, A. et al. (2017b), Validation of SMAP surface soil moisture products with core validation sites, *Remote Sensing of Environment*, 191, 215–231, doi:10.1016/j.rse.2017.01.021.
- Colliander, A., R. H. Reichle, W. T. Crow, M. H. Cosh, et al. (2021), Validation of Soil Moisture Data Products from the NASA SMAP Mission, *IEEE Journal of Selected Topics in Applied Earth Observations and Remote Sensing*, in press, doi: 10.1109/JSTARS.2021.3124743.
- Coopersmith, E. J., M. H. Cosh, W. A. Petersen, J. Prueger, and J. J. Niemeier (2015), Soil Moisture Model Calibration and Validation: An ARS Watershed on the South Fork Iowa River, *Journal of Hydrometeorology*, 16, 1087–1101, doi:10.1175/jhm-d-14-0145.1.
- Cosh, M. H., T. J. Jackson, P. Starks, and G. Heathman (2006), Temporal stability of surface soil moisture in the Little Washita River watershed and its applications in satellite soil moisture product validation, *Journal of Hydrology*, 323, 168–177, doi:10.1016/j.jhydrol.2005.08.020.
- Cosh, M. H., P. J. Starks, J. A. Guzman, and D. N. Moriasi (2014), Upper Washita River Experimental Watersheds: Multiyear Stability of Soil Water Content Profiles, *Journal of Environmental Quality*, 43, 1328–1333, doi:10.2134/jeq2013.08.0318.
- De Lannoy, G. J. M., R. H. Reichle, and V. R. N. Pauwels (2013), Global Calibration of the GEOS-5 L-band Microwave Radiative Transfer Model over Nonfrozen Land Using SMOS Observations, *Journal of Hydrometeorology*, 14, 765–785, doi:10.1175/JHM-D-12-092.1.
- De Lannoy, G. J. M., R. H. Reichle, and J. A. Vrugt (2014a), Uncertainty Quantification of GEOS-5 L-Band Radiative Transfer Model Parameters using Bayesian Inference and SMOS Observations, *Remote Sensing of Environment*, 148, 146–157, doi:10.1016/j.rse.2014.03.030.
- De Lannoy, G. J. M., R. D. Koster, R. H. Reichle, S. P. P. Mahanama, and Q. Liu (2014b), An Updated Treatment of Soil Texture and Associated Hydraulic Properties in a Global Land Modeling System, *Journal of Advances in Modeling Earth Systems*, 6, 957–979, doi:10.1002/2014MS000330.
- De Lannoy, G. J. M., and R. H. Reichle (2016), Global Assimilation of Multiangle and Multipolarization SMOS Brightness Temperature Observations into the GEOS-5 Catchment Land Surface Model for Soil Moisture Estimation, *Journal of Hydrometeorology*, 17, 669–691, doi:10.1175/JHM-D-15-0037.1.
- Diamond, H. J. et al. (2013), U.S. Climate Reference Network after One Decade of Operations: Status and Assessment, *Bulletin of the American Meteorological Society*, 94, 485–498, doi:10.1175/bams-d-12-00170.1.
- Dong, J., W. T. Crow, K. J. Tobin, M. H. Cosh, D. D. Bosch, P. J. Starks, M. Seyfried, and C. Holifield-Collins (2020), Comparison of microwave remote sensing and land surface modeling for surface soil moisture climatology estimation, *Remote Sensing of Environment*, 242, 111756, doi:10.1016/j.rse.2020.111756.
- Entekhabi, D., R. H. Reichle, R. D. Koster, and W. T. Crow (2010), Performance Metrics for Soil Moisture Retrievals and Application Requirements, *Journal of Hydrometeorology*, 11, 832–840, doi:10.1175/2010JHM1223.1.
- Entekhabi, D., et al. (2014), SMAP Handbook, *JPL Publication*, JPL 400-1567, NASA Jet Propulsion Laboratory, Pasadena, California, USA, 182 pp.
- Galle, S. et al. (2018), AMMA-CATCH, a Critical Zone Observatory in West Africa Monitoring a Region in Transition, *Vadose Zone Journal*, 17(1), 0, doi:10.2136/vzj2018.03.0062.
- Gelaro, R., et al. (2017), The Modern-Era Retrospective Analysis for Research and Applications, Version-2 (MERRA-2), *Journal of Climate*, 30, 5419–5454, doi:10.1175/JCLI-D-16-0758.1.
- González-Zamora, Á., N. Sánchez, J. Martínez-Fernández, Á. Gumuzzio, M. Piles, and E. Olmedo (2015), Long-term SMOS soil moisture products: A comprehensive evaluation across scales and methods in the Duero Basin (Spain), *Physics and Chemistry of the Earth, Parts A/B/C*, 83–84, 123–136, doi:10.1016/j.pce.2015.05.009.

- Gruber, A., C.-H. Su, S. Zwieback, W. Crow, W. Dorigo, and W. Wagner (2016), Recent advances in (soil moisture) triple collocation analysis, *International Journal of Applied Earth Observation and Geoinformation*, 45B, 200-211, doi: 10.1016/j.jag.2015.09.002.
- Gruber, A., et al. (2020), Validation practices for satellite soil moisture retrievals: What are (the) errors?, *Remote Sensing of Environment*, 244, 111806, doi:10.1016/j.rse.2020.111806.
- Heathman, G. C., M. H. Cosh, V. Merwade, and E. Han (2012), Multi-scale temporal stability analysis of surface and subsurface soil moisture within the Upper Cedar Creek Watershed, Indiana, *CATENA*, 95, 91–103, doi:10.1016/j.catena.2012.03.008.
- Helfand, H. M., and Schubert, S. D. (1995), Climatology of the Simulated Great Plains Low-Level Jet and Its Contribution to the Continental Moisture Budget of the United States, *Journal of Climate*, 8, 784-806, doi:10.1175/1520-0442(1995)008<0784:cotsgp>2.0.co;2.
- Jackson, T. J., A. Colliander, J. Kimball, R. Reichle, C. Derksen, W. Crow, D. Entekhabi, P. O’Neill, and E. Njoku (2014), SMAP Science Data Calibration and Validation Plan (Revision A), Soil Moisture Active Passive (SMAP) Mission Science Document. JPL D-52544, Jet Propulsion Laboratory, Pasadena, CA.
- Jensen, K. H., and J. C. Refsgaard (2018), HOBE: The Danish Hydrological Observatory, *Vadose Zone Journal*, 17, 180059, doi:10.2136/vzj2018.03.0059.
- Juglea, S., Y. Kerr, A. Mialon, J.-P. Wigneron, E. Lopez-Baeza, A. Cano, A. Albitar, C. Millan-Scheiding, M. Carmen Antolin, and S. Delwart (2010), Modelling soil moisture at SMOS scale by use of a SVAT model over the Valencia Anchor Station, *Hydrology and Earth System Sciences*, 14(5), 831–846, doi:10.5194/hess-14-831-2010.
- Keefer, T. O., M. S. Moran, and G. B. Paige (2008), Long-term meteorological and soil hydrology database, Walnut Gulch Experimental Watershed, Arizona, United States, *Water Resources Research*, 44, doi:10.1029/2006wr005702.
- Khodayar, S., A. Coll, and E. Lopez-Baeza (2019), An improved perspective in the spatial representation of soil moisture: potential added value of SMOS disaggregated 1-km resolution “all weather” product, *Hydrology and Earth System Sciences*, 23(1), 255–275, doi:10.5194/hess-23-255-2019.
- Koster, R. D., M. J. Suarez, A. Ducharne, M. Stieglitz, and P. Kumar (2000), A catchment-based approach to modeling land surface processes in a general circulation model: 1. Model structure, *J. Geophys. Res.*, 105, 24809–24822, doi:10.1029/2000JD900327.
- Koster, R. D., R. H. Reichle, S. P. P. Mahanama, J. Perket, Q. Liu, and G. Partyka (2020), Land-Focused Changes in the Updated GEOS FP System (Version 5.25), NASA Global Modeling and Assimilation Office Research Brief, 11pp. Available at: https://gmao.gsfc.nasa.gov/researchbriefs/land_changes_GEOS-FP/land_changes_GEOS-FP.pdf.
- Liu, Q., R. H. Reichle, R. Bindlish, M. H. Cosh, W. T. Crow, R. de Jeu, G. J. M. De Lannoy, G. J. Huffman, and T. J. Jackson (2011), The contributions of precipitation and soil moisture observations to the skill of soil moisture estimates in a land data assimilation system, *Journal of Hydrometeorology*, 12, 750-765, doi:10.1175/JHM-D-10-05000.1.
- Louis, J.-F. (1979), A parametric model of vertical eddy fluxes in the atmosphere, *Boundary-Layer Meteorology*, 17, 187-202, doi:10.1007/bf00117978.
- Lucchesi, R. (2018), File specification for GEOS-5 FP, *NASA GMAO Office Note No. 4 (version 1.2)*, 56 pp., NASA Goddard Space Flight Center, Greenbelt, MD, USA. Available at: <https://gmao.gsfc.nasa.gov/pubs>
- McNairn, H. et al. (2015), The Soil Moisture Active Passive Validation Experiment 2012 (SMAPVEX12): Prelaunch Calibration and Validation of the SMAP Soil Moisture Algorithms, *IEEE Transactions on Geoscience and Remote Sensing*, 53, 2784–2801, doi:10.1109/tgrs.2014.2364913.
- McPherson, R. A. et al. (2007), Statewide Monitoring of the Mesoscale Environment: A Technical Update on the Oklahoma Mesonet, *Journal of Atmospheric and Oceanic Technology*, 24, 301–321, doi:10.1175/jtech1976.1.
- Moghaddam, M. et al. (2016), *Soil Moisture Profiles and Temperature Data from SoilSCAPE Sites, USA*, ORNL Distributed Active Archive Center, doi:10.3334/ornl daac/1339.

- Montzka, C., et al. (2020), Soil Moisture Product Validation Good Practices Protocol Version 1.0., In: *Good Practices for Satellite Derived Land Product Validation, Land Product Validation Subgroup (WGCV/CEOS)*, edited by C. Montzka, M. Cosh, J. Nickeson, F. Camacho, 123 pp, doi:10.5067/doc/ceoswgcv/lpv/sm.001.
- O'Neill, P., et al. (2021), Calibration and Validation for the L2/3_SM_P Version 8 and L2/3_SM_P_E Version 5 Data Products, SMAP Project, JPL D-56297, Jet Propulsion Laboratory, Pasadena, CA.
- Panciera, R., et al. (2014), The Soil Moisture Active Passive Experiments (SMAPEX): Toward Soil Moisture Retrieval From the SMAP Mission, *IEEE Transactions on Geoscience and Remote Sensing*, 52, 490–507, doi:10.1109/tgrs.2013.2241774.
- Peng, J., et al. (2020), SMAP Radiometer Brightness Temperature Calibration for the L1B_TB (Version 5), L1C_TB (Version 5), and L1C_TB_E (Version 3) Data Products, SMAP Project, JPL-D 56295, Jet Propulsion Laboratory, Pasadena, CA. Available at: https://nsidc.org/data/smap/data_versions.
- Reichle, R. H. (2008), Data Assimilation Methods in the Earth Sciences, *Advances in Water Resources*, 31, 1411-1418, doi:10.1016/j.advwatres.2008.01.001.
- Reichle, R. H., and Q. Liu (2014), Observation-Corrected Precipitation Estimates in GEOS-5, *NASA Technical Report Series on Global Modeling and Data Assimilation, NASA/TM-2014-104606, Vol. 35*, National Aeronautics and Space Administration, Goddard Space Flight Center, Greenbelt, Maryland, USA, 18pp. Available at: <https://gmao.gsfc.nasa.gov/pubs>.
- Reichle, R. H., and Q. Liu (2021), Observation-Corrected Precipitation for the SMAP Level 4 Soil Moisture (Version 6) Product and the GEOS R21C Reanalysis, *NASA Technical Report Series on Global Modeling and Data Assimilation, NASA/TM-2021-104606, Vol. 59*, National Aeronautics and Space Administration, Goddard Space Flight Center, Greenbelt, Maryland, USA, 28pp.
- Reichle, R. H., G. J. M. De Lannoy, B. A. Forman, C. S. Draper, and Q. Liu (2014a), Connecting Satellite Observations with Water Cycle Variables through Land Data Assimilation: Examples Using the NASA GEOS-5 LDAS, *Surveys in Geophysics*, 35, 577-606, doi:10.1007/s10712-013-9220-8.
- Reichle, R. H., R. Koster, G. De Lannoy, W. Crow, and J. Kimball (2014b), SMAP Level 4 Surface and Root Zone Soil Moisture Data Product: L4_SM Algorithm Theoretical Basis Document (Revision A), Soil Moisture Active Passive (SMAP) Mission Science Document. JPL D-66483, Jet Propulsion Laboratory, Pasadena, CA.
- Reichle, R. H., G. J. M. De Lannoy, Q. Liu, A. Colliander, A. Conaty, T. Jackson, J. Kimball, and R. D. Koster (2015), Soil Moisture Active Passive (SMAP) Project Assessment Report for the Beta-Release L4_SM Data Product, *NASA Technical Report Series on Global Modeling and Data Assimilation, NASA/TM-2015-104606, Vol. 40*, National Aeronautics and Space Administration, Goddard Space Flight Center, Greenbelt, Maryland, USA, 63pp. Available at: <https://gmao.gsfc.nasa.gov/pubs>.
- Reichle, R. H., G. J. M. De Lannoy, Q. Liu, J. V. Ardizzone, F. Chen, A. Colliander, A. Conaty, W. Crow, T. Jackson, J. Kimball, R. D. Koster, and E. B. Smith (2016), Soil Moisture Active Passive Mission L4_SM Data Product Assessment (Version 2 Validated Release), *NASA GMAO Office Note No. 12 (Version 1.0)*, 55pp., NASA Goddard Space Flight Center, Greenbelt, MD, USA. Available at: <https://gmao.gsfc.nasa.gov/pubs>
- Reichle, R. H., et al. (2017a), Assessment of the SMAP Level-4 Surface and Root-Zone Soil Moisture Product Using In Situ Measurements, *Journal of Hydrometeorology*, 18, 2621-2645, doi:10.1175/JHM-D-17-0063.1.
- Reichle, R. H., et al. (2017b), Global Assessment of the SMAP Level-4 Surface and Root-Zone Soil Moisture Product Using Assimilation Diagnostics, *Journal of Hydrometeorology*, 18, 3217-3237, doi:10.1175/JHM-D-17-0130.1.
- Reichle, R. H., Q. Liu, R. D. Koster, C. S. Draper, S. P. P. Mahanama, and G. S. Partyka (2017c), Land surface precipitation in MERRA-2, *Journal of Climate*, 30, 1643-1664, doi:10.1175/JCLI-D-16-0570.1.
- Reichle, R. H., R. A. Lucchesi, J. V. Ardizzone, G.-K. Kim, E. B. Smith, and B. H. Weiss (2018a), Soil Moisture Active Passive (SMAP) Mission Level 4 Surface and Root Zone Soil Moisture (L4_SM)

- Product Specification Document, *NASA GMAO Office Note No. 10 (Version 1.5)*, 83 pp., NASA Goddard Space Flight Center, Greenbelt, MD, USA. Available at: <https://gmao.gsfc.nasa.gov/pubs>.
- Reichle, R. H., Q. Liu, R. D. Koster, J. V. Ardizzone, A. Colliander, W. T. Crow, G. J. M. De Lannoy, and J. S. Kimball (2018b), Soil Moisture Active Passive (SMAP) Project Assessment Report for Version 4 of the L4_SM Data Product, *NASA Technical Report Series on Global Modeling and Data Assimilation, NASA/TM-2018-104606, Vol. 52*, National Aeronautics and Space Administration, Goddard Space Flight Center, Greenbelt, Maryland, USA, 72pp. Available at: <https://gmao.gsfc.nasa.gov/pubs>.
- Reichle, R. H., et al. (2019), Version 4 of the SMAP Level-4 Soil Moisture Algorithm and Data Product, *Journal of Advances in Modeling Earth Systems*, *11*, 3106-3130, doi:10.1029/2019MS001729.
- Reichle, R., G. De Lannoy, R. D. Koster, W. T. Crow, J. S. Kimball, and Q. Liu (2020a), *SMAP L4 Global 3-hourly 9 km EASE-Grid Surface and Root Zone Soil Moisture Analysis Update, Version 5*. NASA National Snow and Ice Data Center Distributed Active Archive Center, doi:10.5067/0D8JT6S27BS9.
- Reichle, R., G. De Lannoy, R. D. Koster, W. T. Crow, J. S. Kimball, and Q. Liu (2020b), *SMAP L4 Global 3-hourly 9 km EASE-Grid Surface and Root Zone Soil Moisture Geophysical Data, Version 5*. NASA National Snow and Ice Data Center Distributed Active Archive Center, doi:10.5067/9LNYIYOBNBR5.
- Reichle, R., G. De Lannoy, R. D. Koster, W. T. Crow, J. S. Kimball, and Q. Liu (2020c), *SMAP L4 Global 3-hourly 9 km EASE-Grid Surface and Root Zone Soil Moisture Land Model Constants, Version 5*. NASA National Snow and Ice Data Center Distributed Active Archive Center, doi:10.5067/5C36BVQZW28K.
- Reichle, R. H., Q. Liu, J. V. Ardizzone, W. T. Crow, G. J. M. De Lannoy, J. Dong, J. S. Kimball, and R. D. Koster (2021a), The Contributions of Gauge-Based Precipitation and SMAP Brightness Temperature Observations to the Skill of the SMAP Level-4 Soil Moisture Product, *Journal of Hydrometeorology*, *22*, 405-424, doi:10.1175/JHM-D-20-0217.1.
- Reichle, R. H., Q. Liu, R. D. Koster, J. V. Ardizzone, A. Colliander, W. T. Crow, G. J. M. De Lannoy, and J. S. Kimball (2021b), Soil Moisture Active Passive (SMAP) Project Assessment Report for Version 5 of the L4_SM Data Product, *NASA Technical Report Series on Global Modeling and Data Assimilation, NASA/TM-2021-104606, Vol. 58*, National Aeronautics and Space Administration, Goddard Space Flight Center, Greenbelt, Maryland, USA, 56pp. Available at: <https://gmao.gsfc.nasa.gov/pubs>.
- Reichle, R., G. De Lannoy, R. D. Koster, W. T. Crow, J. S. Kimball, and Q. Liu (2021c), *SMAP L4 9 km EASE-Grid Surface and Root Zone Soil Moisture Analysis Update, Version 6*. NASA National Snow and Ice Data Center Distributed Active Archive Center, doi:10.5067/08S1A6811J0U.
- Reichle, R., G. De Lannoy, R. D. Koster, W. T. Crow, J. S. Kimball, and Q. Liu (2021d), *SMAP L4 9 km EASE-Grid Surface and Root Zone Soil Moisture Geophysical Data, Version 6*. NASA National Snow and Ice Data Center Distributed Active Archive Center, doi: 10.5067/08S1A6811J0U.
- Reichle, R., G. De Lannoy, R. D. Koster, W. T. Crow, J. S. Kimball, and Q. Liu (2021e), *SMAP L4 9 km EASE-Grid Surface and Root Zone Soil Moisture Land Model Constants, Version 6*. NASA National Snow and Ice Data Center Distributed Active Archive Center, doi:10.5067/MWAFPGI1KMMH.
- Rowlandson, T., S. Impera, J. Belanger, A. A. Berg, B. Toth, and R. Magagi (2015), Use of in situ soil moisture network for estimating regional-scale soil moisture during high soil moisture conditions, *Canadian Water Resources Journal / Revue canadienne des ressources hydriques*, *40*, 343–351, doi:10.1080/07011784.2015.1061948.
- Sanchez, N., J. Martinez-Fernandez, A. Scaini, and C. Perez-Gutierrez (2012), Validation of the SMOS L2 Soil Moisture Data in the REMEDHUS Network (Spain), *IEEE Transactions on Geoscience and Remote Sensing*, *50*, 1602–1611, doi:10.1109/tgrs.2012.2186971.
- Schaefer, G. L., M. H. Cosh, and T. J. Jackson (2007), The USDA Natural Resources Conservation Service Soil Climate Analysis Network (SCAN), *Journal of Atmospheric and Oceanic Technology*, *24*, 2073–2077, doi:10.1175/2007jtecha930.1.

- Seyfried, M. S., M. D. Murdock, C. L. Hanson, G. N. Flerchinger, and S. Van Vactor (2001), Long-Term Soil Water Content Database, Reynolds Creek Experimental Watershed, Idaho, United States, *Water Resources Research*, 37(11), 2847–2851, doi:10.1029/2001wr000419.
- Simard, M., N. Pinto, J. B. Fisher, and A. Baccini (2011), Mapping forest canopy height globally with spaceborne lidar, *J. Geophys. Res.*, 116, G04021, doi:10.1029/2011JG001708.
- Smith, A. B., J. P. Walker, A. W. Western, R. I. Young, K. M. Ellett, R. C. Pipunic, R. B. Grayson, L. Siriwardena, F. H. S. Chiew, and H. Richter (2012), The Murrumbidgee soil moisture monitoring network data set, *Water Resources Research*, 48, doi:10.1029/2012wr011976.
- Tan, J., G. J. Huffman, D. T. Bolvin, and E. J. Nelkin (2019), IMERG V06: Changes to the Morphing Algorithm. *Journal of Atmospheric and Oceanic Technology*, 36, 2471–2482, doi:10.1175/jtech-d-19-0114.1.
- Tao, J., R. H. Reichle, R. D. Koster, B. A. Forman, and Y. Xue (2017), Evaluation and enhancement of permafrost modeling with the NASA Catchment Land Surface Model, *Journal of Advances in Modeling Earth Systems*, 9, 2771-2795, doi:10.1002/2017MS001019.
- Tao, J., R. D. Koster, R. H. Reichle, B. A. Forman, Y. Xue, R. H. Chen, and M. Moghaddam (2019), Permafrost Variability over the Northern Hemisphere Based on the MERRA-2 Reanalysis, *The Cryosphere*, 13, 2087-2110, doi:10.5194/tc-13-2087-2019.
- Tetlock, E., B. Toth, A. Berg, T. Rowlandson, and J. T. Ambadan (2019), An 11-year (2007–2017) soil moisture and precipitation dataset from the Kenaston Network in the Brightwater Creek basin, Saskatchewan, Canada, *Earth System Science Data*, 11, 787–796, doi:10.5194/essd-11-787-2019.
- Thibeault, M., J. M. Caceres, D. Dadamia, A. G. Soldano, M. U. Quirno, J. M. Guerrieri, et al. (2015), Spatial and temporal analysis of the Monte Buey SAOCOM and SMAP core site. In 2015 IEEE International Geoscience and Remote Sensing Symposium (IGARSS), IEEE, doi:10.1109/igarss.2015.7325929.
- Wagner, W., S. Hahn, R. Kidd, T. Melzer, Z. Bartalis, S. Hasenauer, et al. (2013), The ASCAT Soil Moisture Product: A Review of its Specifications, Validation Results, and Emerging Applications, *Meteorologische Zeitschrift*, 22, 5-33, doi:10.1127/0941-2948/2013/0399.
- Wen, X., H. Lu, C. Li, T. Koike, and I. Kaihotsu. (2014), Inter-comparison of soil moisture products from SMOS, AMSR-E, ECWMF and GLDAS over the Mongolia Plateau. In T. J. Jackson, J. M. Chen, P. Gong, and S. Liang (Eds.), *Land Surface Remote Sensing II*, SPIE, doi: 10.1117/12.2068952.

Previous Volumes in This Series

- Volume 1** *Documentation of the Goddard Earth Observing System (GEOS) general circulation model - Version 1*
September 1994
L.L. Takacs, A. Molod, and T. Wang
- Volume 2** *Direct solution of the implicit formulation of fourth order horizontal diffusion for gridpoint models on the sphere*
October 1994
Y. Li, S. Moorthi, and J.R. Bates
- Volume 3** *An efficient thermal infrared radiation parameterization for use in general circulation models*
December 1994
M.-D. Chou and M.J. Suarez
- Volume 4** *Documentation of the Goddard Earth Observing System (GEOS) Data Assimilation System - Version 1*
January 1995
James Pfaendtner, Stephen Bloom, David Lamich, Michael Seablom, Meta Sienkiewicz, James Stobie, and Arlindo da Silva
- Volume 5** *Documentation of the Aries-GEOS dynamical core: Version 2*
April 1995
Max J. Suarez and Lawrence L. Takacs
- Volume 6** *A Multiyear Assimilation with the GEOS-1 System: Overview and Results*
April 1995
Siegfried Schubert, Chung-Kyu Park, Chung-Yu Wu, Wayne Higgins, Yelena Kondratyeva, Andrea Molod, Lawrence Takacs, Michael Seablom, and Richard Rood
- Volume 7** *Proceedings of the Workshop on the GEOS-1 Five-Year Assimilation*
September 1995
Siegfried D. Schubert and Richard B. Rood
- Volume 8** *Documentation of the Tangent Linear Model and Its Adjoint of the Adiabatic Version of the NASA GEOS-1 C-Grid GCM: Version 5.2*
March 1996
Weiyu Yang and I. Michael Navon
- Volume 9** *Energy and Water Balance Calculations in the Mosaic LSM*
March 1996
Randal D. Koster and Max J. Suarez

- Volume 10** *Dynamical Aspects of Climate Simulations Using the GEOS General Circulation Model*
 April 1996
 Lawrence L. Takacs and Max J. Suarez
- Volume 11** *Documentation of the Tangent Linear and Adjoint Models of the Relaxed Arakawa-Schubert Moisture Parameterization Package of the NASA GEOS-1 GCM (Version 5.2)*
 May 1997
 Weiyu Yang, I. Michael Navon, and Ricardo Todling
- Volume 12** *Comparison of Satellite Global Rainfall Algorithms*
 August 1997
 Alfred T.C. Chang and Long S. Chiu
- Volume 13** *Interannual Variability and Potential Predictability in Reanalysis Products*
 December 1997
 Wie Ming and Siegfried D. Schubert
- Volume 14** *A Comparison of GEOS Assimilated Data with FIFE Observations*
 August 1998
 Michael G. Bosilovich and Siegfried D. Schubert
- Volume 15** *A Solar Radiation Parameterization for Atmospheric Studies*
 June 1999
 Ming-Dah Chou and Max J. Suarez
- Volume 16** *Filtering Techniques on a Stretched Grid General Circulation Model*
 November 1999
 Lawrence Takacs, William Sawyer, Max J. Suarez, and Michael S. Fox-Rabinowitz
- Volume 17** *Atlas of Seasonal Means Simulated by the NSIPP-1 Atmospheric GCM*
 July 2000
 Julio T. Bacmeister, Philip J. Pegion, Siegfried D. Schubert, and Max J. Suarez
- Volume 18** *An Assessment of the Predictability of Northern Winter Seasonal Means with the NSIPP1 AGCM*
 December 2000
 Philip J. Pegion, Siegfried D. Schubert, and Max J. Suarez
- Volume 19** *A Thermal Infrared Radiation Parameterization for Atmospheric Studies*
 July 2001
 Ming-Dah Chou, Max J. Suarez, Xin-Zhong Liang, and Michael M.-H. Yan

- Volume 20** *The Climate of the FVCCM-3 Model*
 August 2001 Yehui Chang, Siegfried D. Schubert, Shian-Jiann Lin, Sharon Nebuda, and Bo-Wen Shen
- Volume 21** *Design and Implementation of a Parallel Multivariate Ensemble Kalman Filter for the Poseidon Ocean General Circulation Model*
 September 2001 Christian L. Keppenne and Michele M. Rienecker
- Volume 22** *A Coupled Ocean-Atmosphere Radiative Model for Global Ocean Biogeochemical Models*
 August 2002 Watson W. Gregg
- Volume 23** *Prospects for Improved Forecasts of Weather and Short-term Climate Variability on Subseasonal (2-Week to 2-Month) Time Scales*
 November 2002 Siegfried D. Schubert, Randall Dole, Huang van den Dool, Max J. Suarez, and Duane Waliser
- Volume 24** *Temperature Data Assimilation with Salinity Corrections: Validation for the NSIPP Ocean Data Assimilation System in the Tropical Pacific Ocean, 1993–1998*
 July 2003 Alberto Troccoli, Michele M. Rienecker, Christian L. Keppenne, and Gregory C. Johnson
- Volume 25** *Modeling, Simulation, and Forecasting of Subseasonal Variability*
 December 2003 Duane Waliser, Siegfried D. Schubert, Arun Kumar, Klaus Weickmann, and Randall Dole
- Volume 26** *Documentation and Validation of the Goddard Earth Observing System (GEOS) Data Assimilation System – Version 4*
 April 2005 Senior Authors: S. Bloom, A. da Silva and D. Dee
 Contributing Authors: M. Bosilovich, J-D. Chern, S. Pawson, S. Schubert, M. Sienkiewicz, I. Stajner, W-W. Tan, and M-L. Wu
- Volume 27** *The GEOS-5 Data Assimilation System - Documentation of Versions 5.0.1, 5.1.0, and 5.2.0.*
 December 2008 M.M. Rienecker, M.J. Suarez, R. Todling, J. Bacmeister, L. Takacs, H.-C. Liu, W. Gu, M. Sienkiewicz, R.D. Koster, R. Gelaro, I. Stajner, and J.E. Nielsen

- Volume 28**
April 2012
The GEOS-5 Atmospheric General Circulation Model: Mean Climate and Development from MERRA to Fortuna
Andrea Molod, Lawrence Takacs, Max Suarez, Julio Bacmeister, In-Sun Song, and Andrew Eichmann
- Volume 29**
June 2012
Atmospheric Reanalyses – Recent Progress and Prospects for the Future. A Report from a Technical Workshop, April 2010
Michele M. Rienecker, Dick Dee, Jack Woollen, Gilbert P. Compo, Kazutoshi Onogi, Ron Gelaro, Michael G. Bosilovich, Arlindo da Silva, Steven Pawson, Siegfried Schubert, Max Suarez, Dale Barker, Hirotaka Kamahori, Robert Kistler, and Suranjana Saha
- Volume 30**
December 2012
The GEOS-iODAS: Description and Evaluation
Guillaume Vernieres, Michele M. Rienecker, Robin Kovach and Christian L. Keppenne
- Volume 31**
March 2013
Global Surface Ocean Carbon Estimates in a Model Forced by MERRA
Watson W. Gregg, Nancy W. Casey and Cécile S. Rousseaux
- Volume 32**
March 2014
Estimates of AOD Trends (2002-2012) over the World's Major Cities based on the MERRA Aerosol Reanalysis
Simon Provençal, Pavel Kishcha, Emily Elhacham, Arlindo M. da Silva, and Pinhas Alpert
- Volume 33**
August 2014
The Effects of Chlorophyll Assimilation on Carbon Fluxes in a Global Biogeochemical Model
Cécile S. Rousseaux and Watson W. Gregg
- Volume 34**
September 2014
Background Error Covariance Estimation using Information from a Single Model Trajectory with Application to Ocean Data Assimilation into the GEOS-5 Coupled Model
Christian L. Keppenne, Michele M. Rienecker, Robin M. Kovach, and Guillaume Vernieres
- Volume 35**
December 2014
Observation-Corrected Precipitation Estimates in GEOS-5
Rolf H. Reichle and Qing Liu

- Volume 36** *Evaluation of the 7-km GEOS-5 Nature Run*
 March 2015 Ronald Gelaro, William M. Putman, Steven Pawson, Clara Draper, Andrea Molod, Peter M. Norris, Lesley Ott, Nikki Prive, Oreste Reale, Deepthi Achuthavarier, Michael Bosilovich, Virginie Buchard, Winston Chao, Lawrence Coy, Richard Cullather, Arlindo da Silva, Anton Darnenov, Ronald M. Errico, Marangelly Fuentes, Min-Jeong Kim, Randal Koster, Will McCarty, Jyothi Nattala, Gary Partyka, Siegfried Schubert, Guillaume Vernieres, Yuri Vikhliav, and Krzysztof Wargan
- Volume 37** *Maintaining Atmospheric Mass and Water Balance within Reanalysis*
 March 2015 Lawrence L. Takacs, Max Suarez, and Ricardo Todling
- Volume 38** *The Quick Fire Emissions Dataset (QFED) – Documentation of versions 2.1, 2.2 and 2.4*
 September 2015 Anton S. Darnenov and Arlindo da Silva
- Volume 39** *Land Boundary Conditions for the Goddard Earth Observing System Model Version 5 (GEOS-5) Climate Modeling System - Recent Updates and Data File Descriptions*
 September 2015 Sarith Mahanama, Randal Koster, Gregory Walker, Lawrence Takacs, Rolf Reichle, Gabrielle De Lannoy, Qing Liu, Bin Zhao, and Max Suarez
- Volume 40** *Soil Moisture Active Passive (SMAP) Project Assessment Report for the Beta-Release L4_SM Data Product*
 October 2015 Rolf H. Reichle, Gabrielle J. M. De Lannoy, Qing Liu, Andreas Colliander, Austin Conaty, Thomas Jackson, John Kimball, and Randal D. Koster
- Volume 41** *GDIS Workshop Report*
 October 2015 Siegfried Schubert, Will Pozzi, Kingtse Mo, Eric Wood, Kerstin Stahl, Mike Hayes, Juergen Vogt, Sonia Seneviratne, Ron Stewart, Roger Pulwarty, and Robert Stefanski
- Volume 42** *Soil Moisture Active Passive (SMAP) Project Calibration and Validation for the L4_C Beta-Release Data Product*
 November 2015 John Kimball, Lucas Jones, Joseph Glassy, E. Natasha Stavros, Nima Madani, Rolf Reichle, Thomas Jackson, and Andreas Colliander

- Volume 43** *MERRA-2: Initial Evaluation of the Climate*
September 2015 Michael G. Bosilovich, Santha Akella, Lawrence Coy, Richard Cullather, Clara Draper, Ronald Gelaro, Robin Kovach, Qing Liu, Andrea Molod, Peter Norris, Krzysztof Wargan, Winston Chao, Rolf Reichle, Lawrence Takacs, Yury Vikhliayev, Steve Bloom, Allison Collow, Stacey Firth, Gordon Labow, Gary Partyka, Steven Pawson, Oreste Reale, Siegfried Schubert, and Max Suarez
- Volume 44** *Estimation of the Ocean Skin Temperature using the NASA GEOS Atmospheric Data Assimilation System*
February 2016 Santha Akella, Ricardo Todling, Max Suarez
- Volume 45** *The MERRA-2 Aerosol Assimilation*
October 2016 C. A. Randles, A. M. da Silva, V. Buchard, A. Darmenov, P. R. Colarco, V. Aquila, H. Bian, E. P. Nowottnick, X. Pan, A. Smirnov, H. Yu, and R. Govindaraju
- Volume 46** *The MERRA-2 Input Observations: Summary and Assessment*
October 2016 Will McCarty, Lawrence Coy, Ronald Gelaro, Albert Huang, Dagmar Merkova, Edmond B. Smith, Meta Sienkiewicz, and Krzysztof Wargan
- Volume 47** *An Evaluation of Teleconnections Over the United States in an Ensemble of AMIP Simulations with the MERRA-2 Configuration of the GEOS Atmospheric Model.*
May 2017 Allison B. Marquardt Collow, Sarith P. Mahanama, Michael G. Bosilovich, Randal D. Koster, and Siegfried D. Schubert
- Volume 48** *Description of the GMAO OSSE for Weather Analysis Software Package: Version 3*
July 2017 Ronald M. Errico, Nikki C. Prive, David Carvalho, Meta Sienkiewicz, Amal El Akkraoui, Jing Guo, Ricardo Todling, Will McCarty, William M. Putman, Arlindo da Silva, Ronald Gelaro, and Isaac Moradi
- Volume 49** *Preliminary Evaluation of Influence of Aerosols on the Simulation of Brightness Temperature in the NASA Goddard Earth Observing System Atmospheric Data Assimilation System*
March 2018 Jong Kim, Santha Akella, Will McCarty, Ricardo Todling, and Arlindo M. da Silva

- Volume 50**
March 2018
The GMAO Hybrid Ensemble-Variational Atmospheric Data Assimilation System: Version 2.0
Ricardo Todling and Amal El Akkraoui
- Volume 51**
July 2018
The Atmosphere-Ocean Interface Layer of the NASA Goddard Earth Observing System Model and Data Assimilation System
Santha Akella and Max Suarez
- Volume 52**
July 2018
Soil Moisture Active Passive (SMAP) Project Assessment Report for Version 4 of the L4_SM Data Product
Rolf H. Reichle, Qing Liu, Randal D. Koster, Joe Ardizzone, Andreas Colliander, Wade Crow, Gabrielle J. M. De Lannoy, and John Kimball
- Volume 53**
October 2019
Ensemble Generation Strategies Employed in the GMAO GEOS-S2S Forecast System
Siegfried Schubert, Anna Borovikov, Young-Kwon Lim, and Andrea Molod
- Volume 54**
August 2020
Position Estimation of Atmospheric Motion Vectors for Observation System Simulation Experiments
David Carvalho and Will McCarty
- Volume 55**
February 2021
A Phenomenon-Based Decomposition of Model-Based Estimates of Boreal Winter ENSO Variability
Siegfried Schubert, Young-Kwon Lim, Andrea Molod, and Allison Collow
- Volume 56**
June 2021
Validation Assessment for the Soil Moisture Active Passive (SMAP) Level 4 Carbon (L4_C) Data Product Version 5
John S. Kimball, K. Arthur Endsley, Tobias Kundig, Joseph Glassy, Rolf H. Reichle, and Joseph V. Ardizzone
- Volume 57**
July 2021
Tendency Bias Correction in the GEOS AGCM
Yehui Chang, Siegfried Schubert, Randal Koster, and Andrea Molod

Volume 58
August 2021

*Soil Moisture Active Passive (SMAP) Project Assessment Report for
Version 5 of the L4_SM Data Product*

Rolf H. Reichle, Qing Liu, Randal D. Koster, Joseph V. Ardizzone,
Andreas Colliander, Wade Crow, Gabrielle J. M. De Lannoy, and John S.
Kimball

Volume 59
November 2021

*Observation-Corrected Land Surface Precipitation for the SMAP Level 4
Soil Moisture (Version 6) Product and the GEOS R21C Reanalysis*

Rolf H. Reichle and Qing Liu